

Phosphine on Venus Cannot be Explained by Conventional Processes

*William Bains^{1, #, *}, Janusz J. Petkowski^{1, #, *}, Sara Seager^{1, 2, 3}, Sukrit Ranjan^{1a}, Clara Sousa-Silva^{1, 2}, Paul B. Rimmer⁴, Zhuchang Zhan¹, Jane S. Greaves⁵, Anita M. S. Richards⁶*

¹Dept. of Earth, Atmospheric, and Planetary Sciences, Massachusetts Institute of Technology, 77 Mass. Ave., Cambridge, MA, 02139, USA.

²Dept. of Physics, Massachusetts Institute of Technology, 77 Mass. Ave., Cambridge, MA, 02139, USA.

³Dept. of Aeronautics and Astronautics, Massachusetts Institute of Technology, 77 Mass. Ave., Cambridge, MA, 02139, USA.

⁴Department of Earth Sciences, University of Cambridge, Downing Street, Cambridge CB2 3EQ, UK.

⁵School of Physics and Astronomy, Cardiff University, Cardiff CF24 3AA, UK.

⁶Jodrell Bank Centre for Astrophysics, Department of Physics and Astronomy, The University of Manchester, Alan Turing Building, Oxford Road, Manchester, M13 9PL, UK.

^a SCOL Postdoctoral Fellow

These authors contributed equally to this work, and are listed alphabetically.

* Correspondence to: bains@mit.edu, jjpetkow@mit.edu.

Keywords: Phosphine, Venus, Thermodynamics, Photochemistry, Biosignature gas, Life

Abstract

The recent candidate detection of ~20 ppb of phosphine in the middle atmosphere of Venus is so unexpected that it requires an exhaustive search for explanations of its origin. Phosphorus-containing species have not been modelled for Venus' atmosphere before and our work represents the first attempt to model phosphorus species in Venusian atmosphere. We thoroughly explore the potential pathways of formation of phosphine in a Venusian environment, including in the planet's atmosphere, cloud and haze layers, surface, and subsurface. We investigate gas reactions, geochemical reactions, photochemistry, and other non-equilibrium processes. None of these potential phosphine production pathways are sufficient to explain the presence of ppb phosphine levels on Venus. The presence of PH₃, therefore, must be the result of a process not previously considered plausible for Venusian conditions. The process could be unknown geochemistry, photochemistry, or even aerial microbial life, given that on Earth phosphine is exclusively associated with anthropogenic and biological sources. The detection of phosphine adds to the complexity of chemical processes in the Venusian environment and motivates *in situ* follow up sampling missions to Venus.

Introduction

Venus is about the same size and mass as Earth, and is sometimes called Earth's sister planet. Venus' atmospheric chemistry and surface conditions, however, are quite different from Earth's. The interior chemical composition of Venus is poorly known. It is assumed to be similar in chemical composition to the Earth's crust and mantle, mainly because of the similarity between Earth's and Venus' size and overall bulk density (Smrekar *et al.* 2014).

Unlike the bulk planet composition, the atmospheres of Earth and Venus are very different. Our understanding of the chemistry of the Venusian atmosphere and clouds is incomplete, especially when it comes to the experimentally-derived concentrations of chemical species, like phosphoric acid, that are central to the calculations presented in this paper. Nevertheless, the Venusian clouds and hazes are known to have a complex vertical atmospheric profile with several distinct layers. The main cloud layer (~48 km – ~70 km) is composed of droplets, which are believed to be made primarily of photochemically-produced sulfuric acid (Oschlisniok *et al.* 2012). Haze extends from below the clouds through the cloud layer to at least 100 km, may be composed of elemental sulfur as well as sulfuric acid (Taylor *et al.* 2018; Titov *et al.* 2018) (Fig. 1). The main sulfuric acid cloud decks also contain an unidentified UV-absorbing species. The UV absorber is very dynamic, with variable distribution in space and time within clouds (Haus *et al.* 2016; Lee *et al.* 2019) (reviewed in (Marcq *et al.* 2018; Taylor *et al.* 2018; Titov *et al.* 2018)).

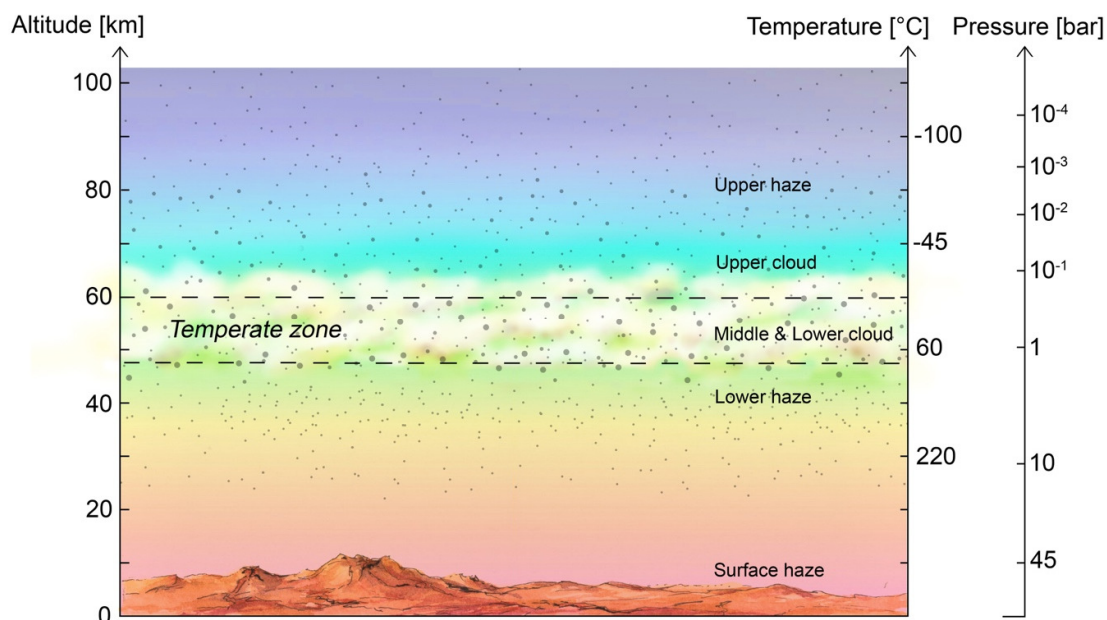


Fig. 1. A simplified schematic representation of the vertical structure of the main atmospheric layers on Venus (figure modified from (Seager *et al.* 2021)).

The recent candidate phosphine detection in the Venus' cloud decks adds further questions to the already complex picture of the chemical composition of the atmosphere of Venus

(Greaves *et al.* 2020). The detection was based on a single millimeter wavelength absorption line, and requires confirmation by the detection of additional phosphine spectral features. However, if correct, the presence of phosphine in Venus' atmosphere is highly unexpected, and requires explanation. This paper is the first step in providing such an explanation. We start the introduction with a short summary of the recent detection of phosphine in the atmosphere of Venus and put it in the context of similar detections on other Solar System planets. Next, we review the chemistry and biology of phosphine gas, focusing on its unique production by life here on Earth (Section 1.1). We conclude the introduction with the motivation for the work presented in this paper (Section 1.2), the overall approach (Section 1.3), and the outline of the employed methods and the obtained results (Section 1.4).

1. 1. Phosphine in Solar Systems Bodies

1. 1. 1. Detection of Phosphine on Venus and Other Planets

The recent candidate detection of ppb amounts of phosphine in the atmosphere of Venus is a highly unexpected discovery. Millimetre-waveband spectra of Venus from both ALMA and the JCMT telescopes at 266.9445 GHz show a PH₃ absorption-line profile against the thermal background from deeper, hotter layers of the atmosphere indicating ~20 ppb abundance. Uncertainties arise primarily from uncertainties in pressure-broadening coefficients and noise in the JCMT signal. Throughout this paper we will describe the predicted abundance as ~20 ppb unless otherwise stated. The thermal emission has a peak emission at 56 km with the FWHM spans approximately 53 to 61 km (Greaves *et al.* 2020). Phosphine is therefore present above ~55 km: whether it is present below this altitude is not determined by these observations. The upper limit on phosphine occurrence is not defined by the observations, but is set by the half-life of phosphine at <80 km, as discussed below.

Phosphine is a reduced, reactive gaseous phosphorus species, which is not expected to be present in the oxidized, hydrogen-poor Venusian atmosphere, surface, or interior. Phosphine is detected in the atmospheres of three other solar system planets: Jupiter, Saturn, and Earth. Phosphine is present in the giant planet atmospheres of Jupiter and Saturn, as identified by ground-based telescope observations at submillimeter and infrared wavelengths (Bregman *et al.* 1975; Larson *et al.* 1977; Tarrago *et al.* 1992; Weisstein and Serabyn 1996). In giant planets, PH₃ is expected to contain the entirety of the atmospheres' phosphorus in the deep atmosphere layers (Visscher *et al.* 2006), where the pressure, temperature and the concentration of H₂ are sufficiently high for PH₃ formation to be thermodynamically favored. In the upper atmosphere, phosphine is present at concentrations several orders of magnitude higher than predicted by thermodynamic equilibrium (Fletcher *et al.* 2009). Phosphine in the upper layers is dredged up by convection after its formation deeper in the atmosphere, at depths greater than 600 km (Noll and Marley 1997).

An analogous process of forming phosphine under high H₂ pressure and high temperature followed by dredge-up to the observable atmosphere cannot happen on worlds like Venus or Earth for two reasons. First, hydrogen is a trace species in rocky planet atmospheres, so the formation of phosphine is not favored as it is in the deep atmospheres of the H₂-dominated

giant planets. On Earth H_2 reaches 0.55 ppm levels (Novelli *et al.* 1999), on Venus it is much lower at ~ 4 ppb (Gruchola *et al.* 2019; Krasnopolsky 2010). Second, rocky planet atmospheres do not extend to a depth where, even if their atmosphere were composed primarily of hydrogen, phosphine formation would be favored (the possibility that phosphine can be formed below the surface and then being erupted out of volcanoes is addressed separately in Section 3.2.2 and Section 3.2.3, but is also highly unlikely).

Despite such unfavorable conditions for phosphine production, Earth is known to have PH_3 in its atmosphere at ppq to ppt levels (see e.g. (Gassmann *et al.* 1996; Glindemann *et al.* 2003; Pasek *et al.* 2014) and reviewed in (Sousa-Silva *et al.* 2020)) PH_3 's persistence in the Earth atmosphere is a result of the presence of microbial life on the Earth's surface (as discussed in Section 1.1.2 below), and of human industrial activity.

Neither the deep formation of phosphine and subsequent dredging to the surface nor its biological synthesis has hitherto been considered a plausible process to occur on Venus.

1. 1. 2. Phosphine is Exclusively Associated with Life on Earth

On Earth phosphine is a gas exclusively associated with life and is not made by any other natural atmospheric or geological chemical process (see e.g. (Gassmann and Glindemann 1993; Glindemann *et al.* 2003; Glindemann *et al.* 2005a; Glindemann *et al.* 1996)) and reviewed in (Bains *et al.* 2019a; Bains *et al.* 2019b; Sousa-Silva *et al.* 2020)). Terrestrial phosphine fulfils the criteria for being a biosignature gas, a gas whose detection indicates the presence of life (Catling *et al.* 2018; Seager and Bains 2015; Seager *et al.* 2016; Sousa-Silva *et al.* 2020; Walker *et al.* 2018). Previous work predicted that, if detected on a temperate rocky planet, phosphine is a robust biosignature gas due to spectroscopic potential and limited false positives in such environments, although detection is extremely challenging (Sousa-Silva *et al.* 2020). Since phosphine is mostly studied in the context of industrial chemistry, agriculture and laboratory chemical synthesis, its biology is not widely known. This warrants a brief introduction on the chemistry and biology of phosphine in the context of its biosignature potential on rocky planets.

On Earth, biological PH_3 production is associated with microbial activity in environments that are strictly anoxic (lacking oxygen) and highly reduced. The majority of reports of biological PH_3 production come from the studies of environments with anaerobic niches such as wetlands, sewage and animal intestinal tracts, flatus, and feces (reviewed in (Sousa-Silva *et al.* 2020)). Several studies have also reported the production of PH_3 from mixed bacterial cultures in the lab (Jenkins *et al.* 2000; Rutishauser and Bachofen 1999). Despite the fact that the exact metabolic pathway leading to PH_3 production in anaerobic bacteria is still unknown, it is clear that phosphine is a biosignature gas on Earth, albeit strictly associated with the anaerobic biosphere. On Earth phosphine could be made directly by microbial reduction of more oxidized phosphorus species or indirectly by microbial production of reduced phosphorus compounds, such as hypophosphite, and their subsequent disproportionation to

PH₃ (Gassmann and Glindemann 1993; Glindemann *et al.* 1999; Glindemann *et al.* 2005a; Glindemann *et al.* 1996). In either case however the presence of phosphine is an indicator of the presence of life. For more information on phosphine in the context of terrestrial biology see recent studies by (Bains *et al.* 2019a; Bains *et al.* 2019b; Sousa-Silva *et al.* 2020).

1. 2. Motivation

Detection of phosphine in the atmosphere of Venus is completely unexpected. If the detection is confirmed by further observations, the presence of phosphine in Venus' atmosphere suggests that our understanding of Venusian atmospheric chemistry is at least incomplete, and that the source of that phosphine needs to be identified. In light of the exclusively biological production of phosphine on Earth, the only rocky planet hitherto known to have phosphine in its atmosphere, the question arises whether the detection of phosphine on Venus could indicate the presence of life. For such a claim to even be entertained, all other possible sources of phosphine must be identified and eliminated. We emphasize that, even if the detection of phosphine is confirmed in the atmosphere of Venus, this can only be considered as evidence of the presence of life if *all* other sources of phosphine can be ruled out (Catling *et al.* 2018). This paper is a first step in that undertaking, considering possible non-biological mechanisms for making phosphine in the atmosphere, surface or subsurface of Venus.

1. 3. Approach: Photochemistry, Kinetics, and Thermodynamics

The ideal approach to identify the possible source of any gas in a planet's atmosphere would be to exhaustively model the rate of all possible reactions that could create and destroy that gas. Presently this is impossible. Exhaustive modelling requires knowledge of all the components of the atmosphere, surface, and subsurface of the planet. While some components of Venus' atmosphere are well known, many, including gases relevant to phosphine reactivity, remain unknown. In addition, exhaustive modelling requires accurate knowledge of the rates of all possible reactions between component molecules under all relevant conditions. Many reaction rates for known species in the Venusian environment have not been measured.

We therefore break the modelling problem into two parts. 1] We construct a photochemical model accounting for the formation and destruction of phosphine based on previous photochemical models of Venus' atmosphere. 2] We separately and complementarily use a thermodynamic approach to model formation pathways for phosphine. While the thermodynamic modelling is not intended to substitute for the full kinetic modelling of chemical reactions, it plays a useful and necessary role to rule out chemical reactions that could produce phosphine.

Together the two modelling units provide qualitative upper bounds on Venusian phosphine production.

1. 4. Paper Outline

In this paper, we apply chemical modelling to attempt to explain the production of the highly unexpected discovery of the trace gas phosphine in the atmosphere of Venus (Greaves *et al.* 2020).

The main body of the paper is divided into two sections, modelling the photochemistry and kinetics of phosphine in the atmosphere (Section 2) and thermodynamics in the atmosphere, surface, and subsurface (Section 3). Detailed methods for these sections are provided in online supplementary material (Supplementary Section 1.1, Supplementary Section 1.2 and Supplementary Section 1.3).

In Section 4 we summarize other processes, including lightning and exotic physical and chemical phenomena that could in principle lead to the formation of phosphine on Venus.

In the Discussion Section (Section 5) we explore several unconventional explanations for the phosphine on Venus, including exotic geochemistry, photochemistry and biologically-driven formation of phosphine. A range of chemical reactions can produce phosphine under Venus conditions, but all of these require reactants that are themselves extremely unlikely to form on Venus, a problem we term “displaced improbability”. We conclude the paper by arguing that the source of phosphine on Venus cannot be explained by our current knowledge of the planet. All potential sources fall short by many orders of magnitude. We argue that further aggressive observations of Venus and its atmosphere, as well as the development of astrobiology-focused space missions, should get the highest priority and would be crucial for an unambiguous explanation for the source of phosphine in the Venusian atmosphere.

2. Photochemistry and Kinetics of Phosphine in the Atmosphere of Venus

The overall goal of our photochemical calculations is to determine if photochemically-driven mechanisms can maintain the detected ~20 ppb of PH₃ at any altitude. This is not yet possible within a self-consistent model because synthesis rates of PH₃ from oxidized species are largely unknown. To account for the limitations caused by missing PH₃ kinetics, we make the complex chemistry of phosphine in the Venusian atmosphere tractable by modelling phosphine photochemical destruction and synthesis networks separately.

We proceed by first calculating the destruction rates for PH₃, for which reaction kinetics are relatively well known. We do so by (1) using a photochemical model to estimate the vertical radical concentration profiles in the Venusian atmosphere, and (2) using the radical profiles to estimate PH₃ lifetimes (and hence destruction rates) throughout the atmosphere. Separating the photochemical model calculations and lifetime estimates enables us to repeat our lifetime calculations with radical profiles derived from a different model (Bierson and Zhang 2019), permitting us to test the sensitivity of our conclusions to the choice of photochemical model (Ranjan *et al.* 2020). Second, we explore the photochemical pathways for the synthesis of PH₃ and determine whether the PH₃ synthesis network can compensate for the known PH₃

destruction mechanisms and sustain a ~20 ppb concentration of phosphine at any altitude in the Venusian atmosphere.

We show that photochemical synthesis of PH₃ is unable to explain the observed PH₃ concentration. Although the major source of uncertainty in this calculation is the extremely poor knowledge of the PH₃ synthesis pathways, our approach is conservative such that these uncertainties do not affect our main conclusions

2. 1. Introduction to Photochemistry and Kinetics Analysis

In this section, we summarize the photochemical models used in this work (Section 2.2.1. and Section 2.2.2.), including the addition of PH₃ to the photochemical network, and estimate the lifetime of phosphine in the Venusian atmosphere (see Supplementary Section 1.1. and its subsections in Supplementary Information). We discuss in detail all the known processes that affect the lifetime of phosphine, including destruction of phosphine by atmospheric radicals, direct UV photolysis and vertical transport in the atmosphere of Venus. We also discuss significant limitations and uncertainties of phosphine lifetime calculations.

The estimation of the lifetime of phosphine on Venus is key for determining production rates that are required to maintain the detected tens of ppb concentration in the Venusian atmosphere. We compare the photochemical destruction rates from our photochemical model with the predicted maximum possible photochemical production rate of phosphine, to assess the possibility of its photochemically-driven formation (Section 2.2.1. and 2.2.2.). We explain why our predicted phosphine photochemical production is many orders of magnitude lower than that needed to explain the observed abundance of phosphine.

(Greaves *et al.* 2020) provided a preliminary description of a photochemistry model for the Venusian atmosphere that includes phosphorus species. Here we provide a more complete description of that model, and apply it to phosphine chemistry on Venus. The model uses the ARGO 1D photochemistry-diffusion code (Rimmer and Helling 2016) to solve the atmospheric transport equation for the steady-state vertical composition profile. ARGO is a Lagrangian photochemistry/diffusion code. The code follows a single parcel of gas as it moves from the bottom to the top of the atmosphere, as determined by a prescribed temperature profile. The code updates temperature, pressure, and actinic ultraviolet flux at each height in the atmosphere. In this reference frame, bulk diffusion terms are accounted for by time-dependence of the chemical production, P_i (cm³ s⁻¹), and loss, L_i (s⁻¹), and so below the homopause, the chemical equation being solved is effectively:

$$\frac{\partial n_i}{\partial t} = P_i[t(z, v_v)] - L_i[t(z, v_z)]n_i, \quad (1)$$

where n_i (cm⁻³) is the number density of species i , t (s) is time, z [cm] is atmospheric height, and $v_z = K_{zz}/H_0$ (cm/s) is the effective vertical velocity due to Eddy diffusion, from the Eddy diffusion coefficient K_{zz} (cm² s⁻¹). The model is run until the abundance of every major and significant minor species (any with $n_i > 10^5$ cm⁻³) does not change by more than 1% between two global iterations.

The handful of known reactions of PH_3 with the major reactive Venusian species O, Cl, OH, and H were combined with previously published Venus atmospheric networks of (Krasnopolsky 2012; Krasnopolsky 2013) and (Zhang *et al.* 2012), and the network of STAND2019 of (Rimmer and Rugheimer 2019), which includes H/C/N/O species. This model and its results are the same as those presented in (Greaves *et al.* 2020). Details of the reaction networks, initial conditions and modelling are provided in Supplementary Section 1.1. and its subsections in Supplementary Information.

This whole-atmosphere model allows us to assess the lifetime of PH_3 throughout the atmosphere self-consistently. The model accounts for photochemistry, thermochemistry and chemical diffusion. UV transport calculation was modified in two ways. First, we ignore the UV absorption of SO_2 for the first three global iterations, and include it afterwards. This seems to help the model to converge. After the first three global iterations, we include UV absorption by SO_2 and by the ‘mysterious absorber’ with properties described by (Krasnopolsky 2007) (see Supplementary Section 1.1.1. in Supplementary Information).

With these conditions, using the photochemical network described below, convergence required 33 global iterations of the model.

The counterbalance of photochemical destruction of phosphine is the possibility that phosphine is photochemically generated in gas or droplet phases. The possibility of gas phase production was considered as follows. A network of reactions that could generate PH_3 from H_3PO_4 was constructed; H_3PO_4 was selected as the starting molecule because H_3PO_4 is predicted to be the most abundant phosphorus species in Venus’ atmosphere at cloud level and above, and because H_3PO_4 is the only phosphorus species for which gas phase kinetic data is available. The maximum possible rate of phosphine production was calculated as the flux through this network assuming no back reactions. More detail on the network, its construction and estimation of the reaction rates is provided in Supplementary Information, Supplementary Section 1.2. The possibility of photochemical production of phosphine in cloud droplets is discussed briefly in Section 5.2.

2. 2. Results of the Photochemistry and Kinetics Analysis

2. 2. 1. Lifetime and Necessary Production Rate of PH_3 in the Venusian Atmosphere

The abundance of phosphine on Venus is a result of a balance between its production and destruction. Estimating Venusian PH_3 destruction rate (and hence its lifetime) as a function of altitude is key for understanding the PH_3 production rates required to maintain a ~20 ppb atmospheric concentration. Figure 2 presents our estimates of PH_3 destruction rate and lifetime as a function of altitude, broken down by specific destruction mechanisms.

We begin by commenting broadly on PH_3 photochemical destruction rates in the Venusian atmosphere. Attack by O is the main loss mechanism in the high atmosphere (>60-80 km), attack by Cl the main loss mechanism in the middle atmosphere, and thermolysis the main loss mechanism at the planet surface; this is consistent with calculations performed with radical profiles derived from other models of Venus, albeit ones that do not consider PH_3 (Bierson and Zhang 2019). Direct photolysis is included, but is found not to be the dominant

loss mechanism at any height in the atmosphere for any of the models considered. The presence of PH₃ suppresses radical concentrations in the lower atmosphere. The concentrations of radicals are low in the lower atmosphere, and so even in small abundances, PH₃ becomes a significant scavenger; consequently models that exclude PH₃ (e.g., (Bierson and Zhang 2019)) may overestimate photochemical destruction rates in the deep atmosphere.

We next discuss the chemistry of atomic chlorine, which determines the profile of PH₃ in the mid atmosphere. Atomic Cl is predicted to occur well below the limit of detection, with mixing ratios of $<10^{-17}$ beneath the clouds according to all the atmospheric models we consider. Even at these mixing ratios, Cl significantly affects the lifetime of PH₃ below the clouds of Venus. In our model the vertical profile of Cl atoms is complex. In brief, ClS₂ is produced by thermal reactions between sulfur species, CO and HCl below 5km, and is efficiently broken down to Cl atoms by 327 - 485 nm photons that penetrate below 35 km. Above 30 km Cl is removed by reaction with chemical products of SO₃ which itself is produced by thermal dissociation of H₂SO₄. Cl abundance is predicted to be $<1 \text{ cm}^{-3}$ near the surface (the Cl is produced thermochemically near the surface, and then locked into ClS₂), $>100 \text{ cm}^{-3}$ at 25 - 35 km (from ClS₂ photolysis), and above 50 km, $<1 \text{ cm}^{-3}$ between 42 and 54 km (due to reactions with chemical products of SO₃), and then increases from 1 cm^{-3} to 10^8 cm^{-3} between 58 and 100 km due to HCl photolysis (See SI Section 1.1.5.3 for further details on Cl chemistry in our model).

However other models using different networks show different Cl atom abundances. The atomic and radical profiles from Bierson (Bierson and Zhang 2019), Krasnopolsky (Krasnopolsky 2007) and our profiles disagree with each other by over almost five orders of magnitude, which means that the predicted chemical lifetimes for PH₃ due to destruction by these atoms and radicals differs by several orders of magnitude

If destruction by atoms and radicals were the only way to remove PH₃, then the lifetime of PH₃ would be very poorly constrained. It would depend on abundances of species that cannot be measured, and which can vary over almost five orders of magnitude between networks. However, the thermal decomposition, diffusion timescale and photochemical destruction of PH₃ are robust to differences in chemical networks and provide us with a confident upper limit to the lifetime of PH₃ in the atmosphere of Venus. We therefore move on to the role of transport.

PH₃ has a lifetime of $< 10^4$ seconds in the high atmosphere ($>60 - 80$ km) due to high levels of UV radiation and its concomitant radicals. In the deep atmosphere (<50 km), which is UV-shielded, PH₃ lifetime to photochemical destruction may be much longer (up to 10^{11} seconds). Vertical transport of PH₃ to high altitudes ultimately limits the PH₃ lifetime in much of the lower atmosphere. However, transport in the lower atmosphere of Venus is slow: consequently, PH₃ lifetimes may be as high as ~ 300 years in parts of the lower atmosphere. If we instead estimate the lifetime using the radical concentration profiles of (Bierson and

Zhang 2019), we predict lifetimes of ≤ 700 years in the deep atmosphere, because the PH_3 must diffuse to a higher z_0^1 (up to 80 km), compared to our model (60 km).

The comparatively long lifetime of PH_3 predicted for parts of the deep atmosphere (~100s of years) motivates us to consider the possibility that low photochemical or abiotic production of PH_3 could result in accumulation of phosphine over time and diffuse upwards explain the ~20 ppb PH_3 abundance observed by (Greaves *et al.* 2020). This scenario requires an efficient unknown phosphine formation mechanism deep in the atmosphere, and/or efficient transport to the detection altitudes of 53-61 km but not the destruction altitude (>60-80 km). Our calculations suggest there is no such transport pattern for the Venusian atmosphere.

The rate of destruction of PH_3 (at the cloud level or below) is much slower than on Earth, because of the much lower concentration of OH radicals in the Venusian atmosphere. A much smaller production rate is therefore needed to generate a 20 ppb concentration in the atmosphere than would be true on Earth. We calculated the total, planet-wide outgassing flux necessary to maintain an atmospheric concentration of 20 ppb in the atmosphere of Venus at the detection altitudes of 53-61 km. We find that a flux of $\sim 10^6 - 10^7$ phosphine molecules $\text{cm}^{-2} \text{s}^{-1}$ (averaged across the whole planet) is needed to reproduce the observed phosphine mixing ratio of 20 ppb above 55 km (Greaves *et al.* 2020). This is equivalent to $\sim 8 \times 10^3 - 8 \times 10^4$ tonnes year^{-1} . For comparison, methane is produced at a rate of $\sim 340 \times 10^6$ tonnes/ year from non-anthropogenic sources on Earth, $\sim 14 \times 10^6$ tonnes of which are geological (i.e. not dependent on life) (Saunio *et al.* 2016).

In the remainder of this paper, we explore the possibility of an efficient abiotic phosphine formation mechanism in the Venusian atmosphere.

¹ Altitude at which the photochemical lifetime of PH_3 becomes short ($\leq 10^4$ s), i.e. where the radical population become high; see Supplementary Section 1.1.1.

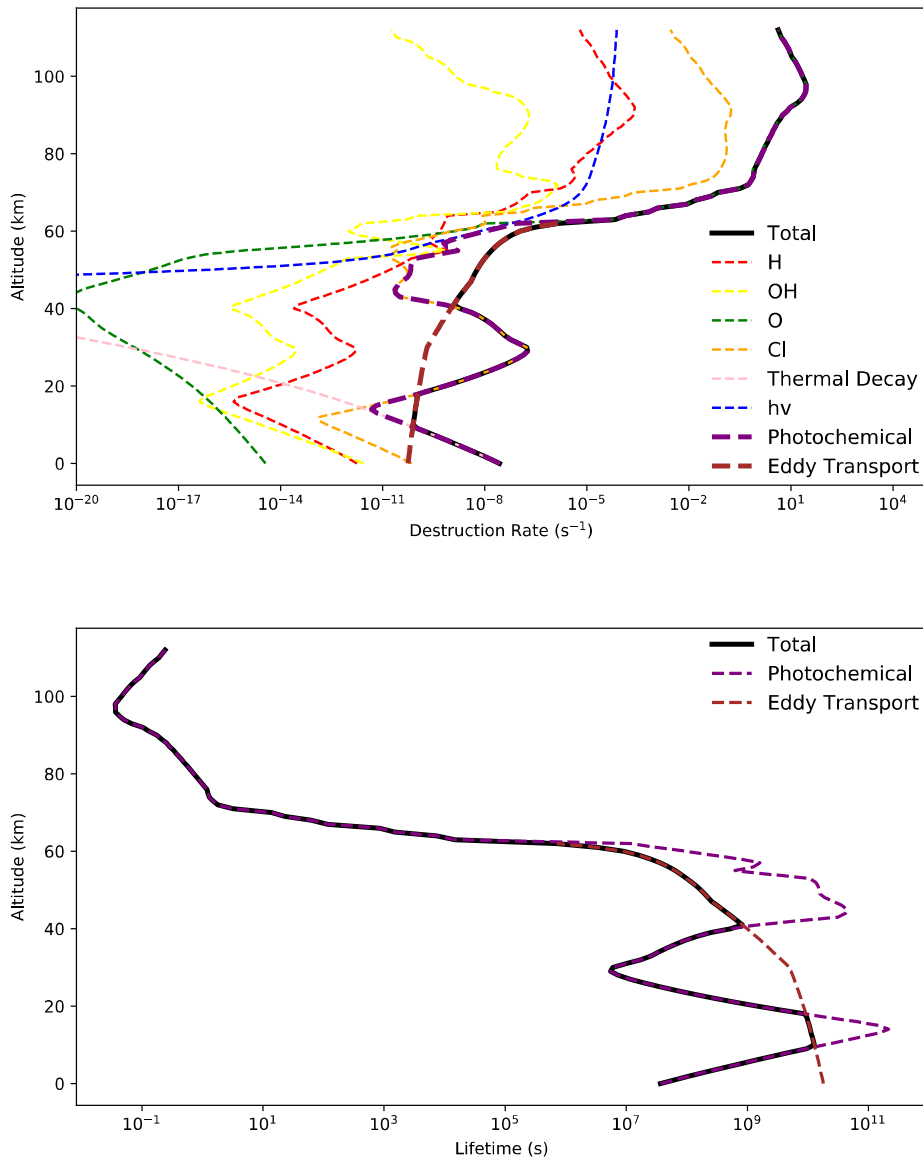


Fig. 2. The lifetime of phosphine in Venusian atmosphere. *Top panel:* Removal rates for PH_3 in the Venusian atmosphere, as a function of altitude. x axis: Destruction rate (s^{-1}), y axis: Altitude (km). Individual photochemical loss processes are shown in thin dashed lines. Also shown is the loss rate due to diffusion to the upper atmosphere, calculated by inverting the diffusion timescale. Thick black line presents overall loss rate, which is the minimum of the photochemical and diffusion loss rates. *Bottom panel:* Photochemical, diffusion, and overall lifetimes of PH_3 in the Venusian atmosphere, calculated by inverting the corresponding loss rates. x axis: Lifetime (s), y axis: Altitude (km). Overall, the photochemical lifetime of PH_3 is long in the lower atmosphere but short in the upper atmosphere, meaning that transport to the upper atmosphere ultimately limits PH_3 lifetime in much of the lower atmosphere. Even so, PH_3 lifetimes of order centuries are possible in the lower atmosphere.

2. 2. 2. Photochemical Synthesis of Phosphine Cannot Explain the Observed PH_3 Abundance in the Atmosphere of Venus

Photochemical synthesis of phosphine, by reduction of oxidized phosphorus species by atmospheric radicals, could in principle lead to the formation of phosphine. We argue however that photochemically driven reactions in Venus' atmosphere cannot produce PH_3 in

sufficient amounts to explain the detection of ~20 ppb. We find that the reactions involving atmospheric radicals capable of reducing oxidized phosphorus species (e.g., hydrogen radicals) are too slow, and the required forward reaction rates are too low, by factors of 10^3 to 10^6 (see Figure 3 and Table 1 in Section 5.1). We present our reasoning in detail below.

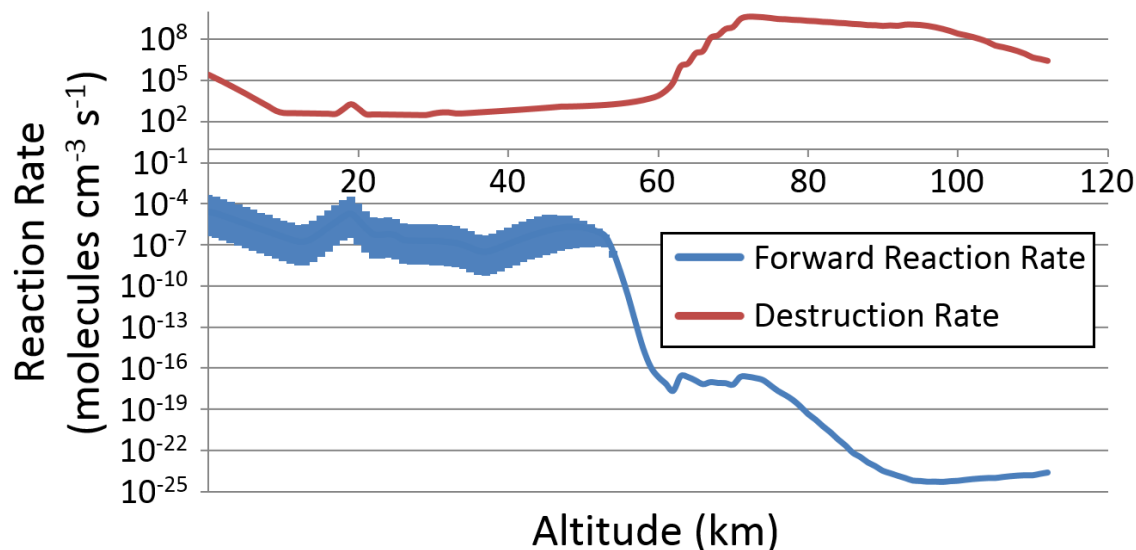


Fig. 3. The photochemical production and destruction rates of phosphine. x axis: Altitude (km), y axis: Reaction rate (molecules $\text{cm}^{-3} \text{s}^{-1}$). Maximum rate of forward reaction through the kinetic network as a function of altitude (blue line) compared with the photochemical destruction rate (red line). The base of the clouds is assumed to be at any altitude between 45 km and 55 km, which gives a range of forward rates reflecting a range of phosphorus species concentrations, themselves depending on the lower boundary of the cloud layer as described in Supplementary Information, Supplementary Section 1.3.2.2. Under no conditions the rate of the photochemical formation of phosphine is sufficient to balance the photochemical destruction rate, therefore making the photochemical production of phosphine unlikely.

Figure 3 shows that there is no altitude at which the maximum possible forward reaction rate is sufficient to counter the destruction rate: the minimum ratio of destruction/synthesis rates is 2.7×10^4 . Figure 4 analyses which reactions in the network are responsible for the slow production of phosphine. The main ‘blockage’ in the network (Figure 4) for PH_3 synthesis is the series of reactions that can lead from $\text{P}=\text{O}$ to PH or PH_2 . The conversion of phosphoric acid (H_3PO_4) to the $\text{P}^{(+3)}$ radical H_2PO_3 is also a rate-limiting process, supporting the idea that the spontaneous production of phosphite or phosphorous acid is not favored (discussed further below in Section 3.2.1.2; note that phosphorous acid itself – H_3PO_3 – is not stable in gas phase.)

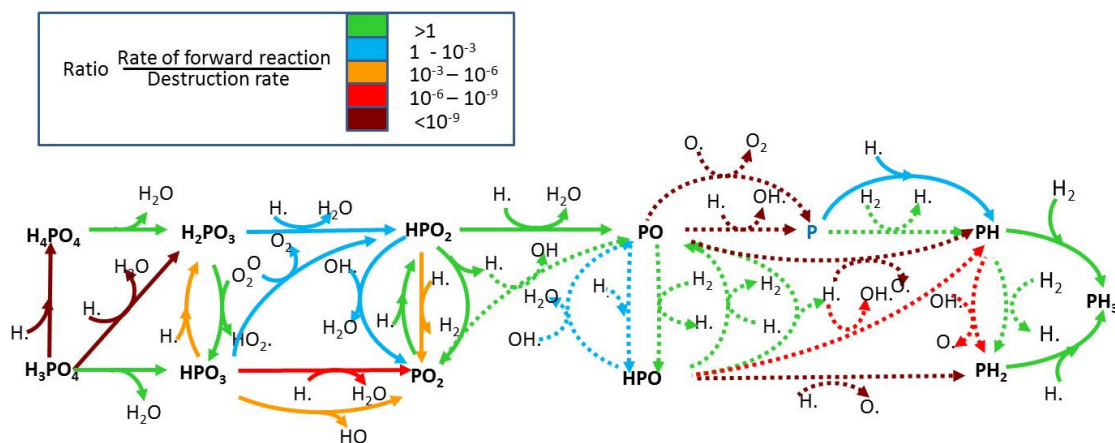


Fig. 4. Exploration of the potential photochemical pathways for the synthesis of PH₃. The reaction network was constructed as described in Supplementary Information, Supplementary Section 1.2. The destruction rate of phosphine was calculated from the photochemical model (Supplementary Information, Supplementary Section 1.1.1). Maximum possible forward reaction rates were calculated as described in Supplementary Information, Supplementary Section 1.2. For each altitude, the ratio R = reaction rate/destruction rate was calculated for each reaction. The reactions are colored by the *maximum* R for any altitude for that reaction. There is no path to PH₃ synthesis through the network that does not cross at least one reaction that has an $R < 10^{-9}$, i.e. is at least nine orders of magnitude too slow to account for the observed levels of phosphine. Therefore, there is no reaction path that can efficiently produce phosphine photochemically. The transformation of P=O to PH or PH₂ is the main bottleneck of the network. The forward kinetic network is constructed as a function of altitude. Reactions are colored for the assumption that the cloud base occurs at 48 km. Figure modified from (Greaves *et al.* 2020).

We note in summary that that our analysis is very conservative because it is purposely highly biased towards predicting the production of phosphine, for two reasons:

1. We assume that *all* of the atmospheric phosphorus is concentrated into one species, the species that is reacting in each reaction. Such scenario is highly improbable. In reality phosphorus species would predominantly be present as H₃PO₄ or P₄O₁₀ (see Section 3.2.1.1), and all other species would be trace gases.
2. We assume that only forward (reducing) reactions occur. If back (oxidizing) reactions were also considered, they would reduce the calculated net rate of reduction, and lower the overall production rate of phosphine.

Therefore, our network provides the maximum possible phosphine production rate from known photochemical processes. The maximum rate predicted is more than four orders of magnitude too low to account for the presence of ~20 ppb PH₃ in Venus' atmosphere. In reality back reactions would significantly lower the efficiency of the formation of PH₃. Several such back reactions could occur, the net result of forward and back reactions occurring at the same time is the phosphorus-catalyzed recombination of H, O and OH into H₂O instead of the production of reduced phosphorus species. The precedent for such phosphorus-catalyzed recombination chemistry is known in terrestrial flame chemistry (Twarowski 1993; Twarowski 1995; Twarowski 1996). We note however that this hypothesis needs more detailed modelling and experimental studies to be confirmed.

Our forward PH₃ production reaction network contains no provision for reactions of oxidized phosphorus species with sulfur or oxidized chlorine species like ClO, which play a substantial role in Venusian atmospheric chemistry (Marcq *et al.* 2018; Sandor and Clancy 2018; Taylor

and Hunten 2014). No reaction kinetics are reported for reaction of oxidized phosphorus species with reactive, oxidizing S or Cl species. It is unknown if such hypothetical photochemical processes involving sulfur or chlorine species can lead to the reduction of oxidized phosphorus species and, as a result, to the production of phosphine. We discuss such unknown chemical processes as a potential source of phosphine on Venus in Section 5.2.

Our approach suggests that phosphorus monoxide (PO) could be a significant component of the reaction chemistry of phosphorus in Venus' atmosphere. PO has not been observed or modelled as an atmospheric species on Venus to date. PO's presence could be confirmed by directed observation, as it was done in the past for PO (Tenenbaum *et al.* 2007) and phosphorus oxoacids (Turner *et al.* 2018) in the interstellar medium. We emphasize however that we are postulating the existence of PO as a transient intermediate species, not a major component of the Venusian atmosphere.

2. 3. Summary and Conclusion of the Photochemistry and Kinetic Analysis

We have carried out a detailed analysis of photochemical and other endergonic chemistry that could produce phosphine under Venus conditions. Our models provide the destruction rate and lifetime for phosphine in Venus' atmosphere, and hence a flux rate necessary to maintain ~20 ppb phosphine stably in the atmosphere. Our analysis confirms that none of the modelled kinetic pathways can explain the levels of phosphine observed, falling short by many orders of magnitude, even using the most conservative assessments available.

We note that these are all calculations of gas phase photochemistry. Solid phase photochemistry is not relevant, as no significant UV penetrates to the ground on Venus. We address the question of the UV photochemistry of the cloud droplets in Section 5.2.

3. Thermodynamic Analysis of Potential Phosphine-Producing Reactions

3. 1. Introduction to Thermodynamics of Phosphine Production

In the absence of the kinetic data for chemical reactions that could lead to phosphine formation we employ a thermodynamic approach to investigate the plausibility of phosphine production on Venus. If no combination of conditions (different temperatures, pressures, reducing agents and concentrations), from any observation or model, can result in the production of phosphine, then a spontaneous reaction can be confidently ruled out as a source of phosphine on Venus.

A thermodynamic analysis cannot substitute for the full kinetic modelling of chemical reactions, but it is a useful tool to rule out possible chemical pathways for phosphine production, if the kinetic data is not available.

We approach the calculation of the thermodynamics of chemical reactions in the Venusian environment by calculating the free energy (ΔG) of any reaction involving stable chemical species detected or modelled in Venus' atmosphere that could generate phosphine, both in

the atmosphere and on the surface. We tested hundreds of partial pressure and cloud altitude combinations, for a total of thousands of conditions for each of the dozens of reactions.

We also explore the thermodynamics of the subsurface formation of phosphine by employing the concept of oxygen fugacity of crustal and mantle rocks.

Calculation of the free energy of reaction was performed using standard methods (see Supplementary Information, Supplementary Section 1.3.1.). Non-ideality of gases was calculated using Berthelot's equation (Rock 1969). Solids were assumed to be in their ideal state, i.e. as pure materials. Reactions were chosen as follows. To produce phosphine, a reaction must have 1) a source of phosphorus, 2) a source of hydrogen and 3) a reducing agent. The relative abundance of the sources of phosphorus in the atmosphere were calculated as described below (see Supplementary Information, Supplementary Section 1.3.2.). All reducing gases, potential reducing solids, and gaseous sources of hydrogen that have been measured or modelled were used to construct all possible hypothetical reducing reactions with all sources of phosphorus. The vertical concentration profiles of gases were taken from the photochemical model described above in Section 2 and in Supplementary Information, Supplementary Section 1.1. The thermodynamics of the production of phosphine and of phosphite (which could disproportionate to form phosphine) were also modelled (see Supplementary Information, Supplementary Section 1.3.2. for further details). Detailed modelling of the Venusian subsurface chemistry is not practical, as the rock compositions are not known, and a very large number of different minerals could be present. We therefore modelled the oxygen fugacity (f_{O_2}), for a range of temperatures (700 – 1600 K), of subsurface rocks needed to generate phosphine in the subsurface Venusian environment, as described in more detail below in Section 3.2.2. and in Supplementary Information, Supplementary Section 1.3.3.

3. 2. Results of the Thermodynamic Analysis of Potential Phosphine-Producing Reactions

3. 2. 1. Surface and Atmospheric Thermodynamics of Phosphine Production

3. 2. 1. 1. Identification of Dominant Atmospheric Phosphorus Species

Phosphine, a reduced form of phosphorus, is not a dominant species in the oxidized Venusian environment. The oxidized Venusian conditions favor the formation of oxidized phosphorus compounds. To identify the dominant atmospheric phosphorus species, we have modelled the relative abundance of oxidized phosphorus species under Venus' atmosphere conditions.

Both P(+3) and P(+5) oxidized phosphorus species can be present as oxyacids or as acid anhydrides. The thermodynamic model shows that P_4O_6 is thermodynamically preferred over P_4O_{10} in Venus' lower atmosphere (<35 km) (Fig. 5). In the lower atmosphere, dehydrated forms of phosphorus dominate over hydrated forms, due to the combination of high temperature and low water concentration.

P_4O_6 as a dominant phosphorus species on Venus may be surprising, but it is in agreement with previous studies on brown dwarfs and gas giants done by (Visscher *et al.* 2006). At temperature and pressure regimes of higher altitudes we find H_3PO_4 dominates. Visscher *et al.* find the most stable form of phosphorus in analogous regimes in brown dwarfs is $NH_4H_2PO_4$ (i.e. ammonium dihydrogenphosphate). This species would not form on Venus, where the concentration of ammonia is essentially zero. Its free acid analogue, which would be formed by incubating $NH_4H_2PO_4$ in acid, is H_3PO_4 .

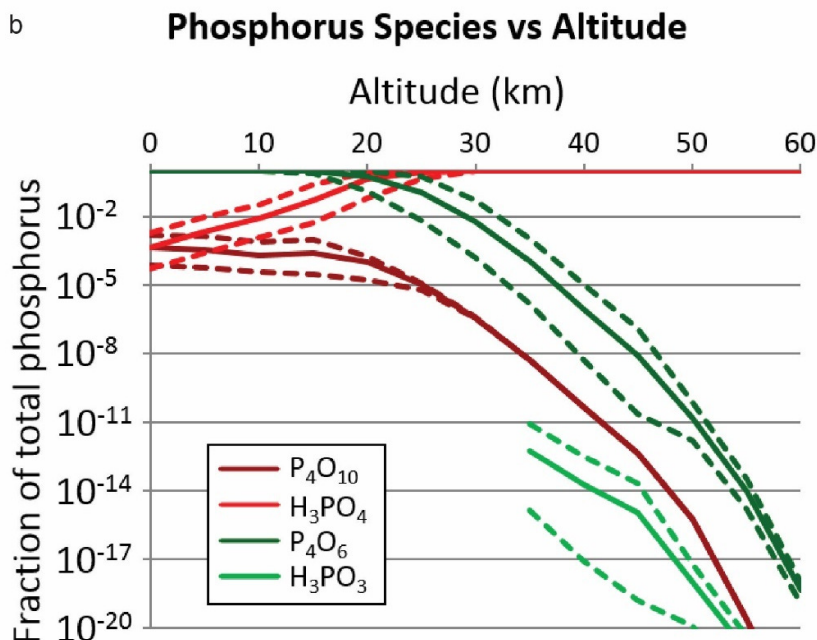


Fig. 5. Model of the relative abundance of phosphorus oxyacid species under Venus atmosphere conditions, as a function of altitude. x axis: Altitude (km), y axis: Fraction of total phosphorus. Solid lines show the dominant phosphorus species. Dashed lines show upper and lower limits for the relative fractions of each species, as modelled in different chemical environments (Supplementary Information, Supplementary Section 1.3.2.2.). P_4O_6 and H_3PO_4 are the thermodynamically dominant phosphorus species in the lower (<35 km) and the upper (>35 km) atmosphere of Venus, respectively. Note that phosphorous acid (H_3PO_3) is not stable to evaporation, and so only exists in the cloud layer.

The model predicts that by far the dominant species in the cloud layer is phosphoric acid (H_3PO_4). The principle uncertainties in the model are the abundance of water in the atmosphere (which influences the ratio of oxide to oxyacid) and the abundance of reducing agents. We discuss the abundance of reducing agents in the next section. The abundance of water would have to be many orders of magnitude higher than that modelled or measured for H_3PO_4 not to be the dominant species above 40 km.

We note that our model is incomplete. In reality highly concentrated H_3PO_4 consists of a mixture of 'pure' H_3PO_4 , $H_3PO_4 \cdot H_2O$ co-crystals, and many dehydration products (e.g., $H_4P_2O_7$, $H_5P_3O_{10}$ etc.). However detailed thermodynamic data for such minor phosphorus species under Venus conditions is not available, therefore our model serves as a best possible approximation.

3. 2. 1. 2. *Formation of Phosphine in the Venusian Atmosphere-Surface Environment Cannot Proceed Spontaneously*

Our calculations show that formation of phosphine in the Venusian atmosphere and on the surface cannot proceed spontaneously. None of the tested reactions in thousands of considered conditions makes phosphine or phosphorous acid formation thermodynamically favorable. All chemical reactions that can produce phosphine in the Venusian environment are on average 100 kJ/mol too energetically costly (10 - 400 kJ/mol) to proceed spontaneously (see Figure 6, Supplementary Figure S9 and Supplementary Figure S10).

The reduction of oxidized phosphorus species by surface minerals is ruled out. The only common reduced surface minerals are likely to be iron minerals. Iron(II) sulfide and iron(II) chloride are not stable under Venus surface conditions (Fegley 1997)(Supplementary Figure S8) and reduced iron oxides cannot reduce P_4O_6 to PH_3 (Supplementary Figure S9).

The reduction of mineral phosphate by reduced atmospheric species to produce PH_3 is also ruled out thermodynamically (Supplementary Figure S10). We considered five model minerals, calcium phosphate (whitlockite) $Ca_3(PO_4)_2$, calcium fluorophosphate (fluorapatite) $Ca_5(PO_4)_3F$, magnesium phosphate $Mg_3(PO_4)_2$, aluminum phosphate (berlinite) $AlPO_4$, potassium phosphate K_3PO_4 , and their reduction by the reducing atmosphere species: H_2 , OCS , H_2S , CO , elemental sulfur (S_8 or S_2). We note that, although chemical reactions occurring below 30 km are unlikely to be the source of the observed phosphine, there remains the possibility that surface minerals could be transported above 30 km as dust, and so we considered mineral reduction as a source of phosphorus at all altitudes up to 60 km.

We summarize the results in Figure 6, where we show the distribution of number of reactions that make phosphine as a function of their free energy and of altitude (Figure 6).

As an example of the thermodynamic calculations, we expand on the possible formation of P(+3) species, and specifically phosphorous acid. Phosphorous acid can spontaneously disproportionate to phosphine on heating to 200 °C (Gokhale *et al.* 1967). Phosphorous acid only exists in liquid or solution phase, and hence cannot be formed below the cloud decks. If phosphorous acid were formed in the clouds, then it could ‘rain out’ to hotter regions of the atmosphere and disproportionate there, providing a source of phosphine. However thermodynamic calculation shows that this is an improbable source of phosphine. The amount of phosphorous acid present in the clouds in thermodynamic equilibrium with other phosphorus species can be calculated from the relative abundance ratio shown in Figure 5. (We note that at the high acid concentrations of cloud droplets, phosphite ions would be fully protonated to form phosphorous acid, so the same argument applies to phosphites.) H_3PO_3 is a vanishingly small fraction of the total phosphorus inventory; if the cloud droplets contain 1 molar H_3PO_4 , then the concentration of H_3PO_3 would be $\sim 6 \cdot 10^{-17}$ molar at the cloud base (47 km) and at $\sim 10^{-21}$ molar at the altitude above which PH_3 was detected (~ 55 km). If we assume that the total volume of cloud material is $\sim 1 \cdot 10^{10}$ m³ (calculated from the droplet sizes and abundances as a function of altitude as listed in (Esposito *et al.* 1983)), the clouds about 47 km would contain ~ 44 milligrams of H_3PO_3 in the whole Venusian atmosphere. Reduction

of phosphate to phosphite by atmospheric components and subsequent disproportionation of phosphite to phosphine is therefore extremely unlikely to be the mechanism responsible for Venus's phosphine.

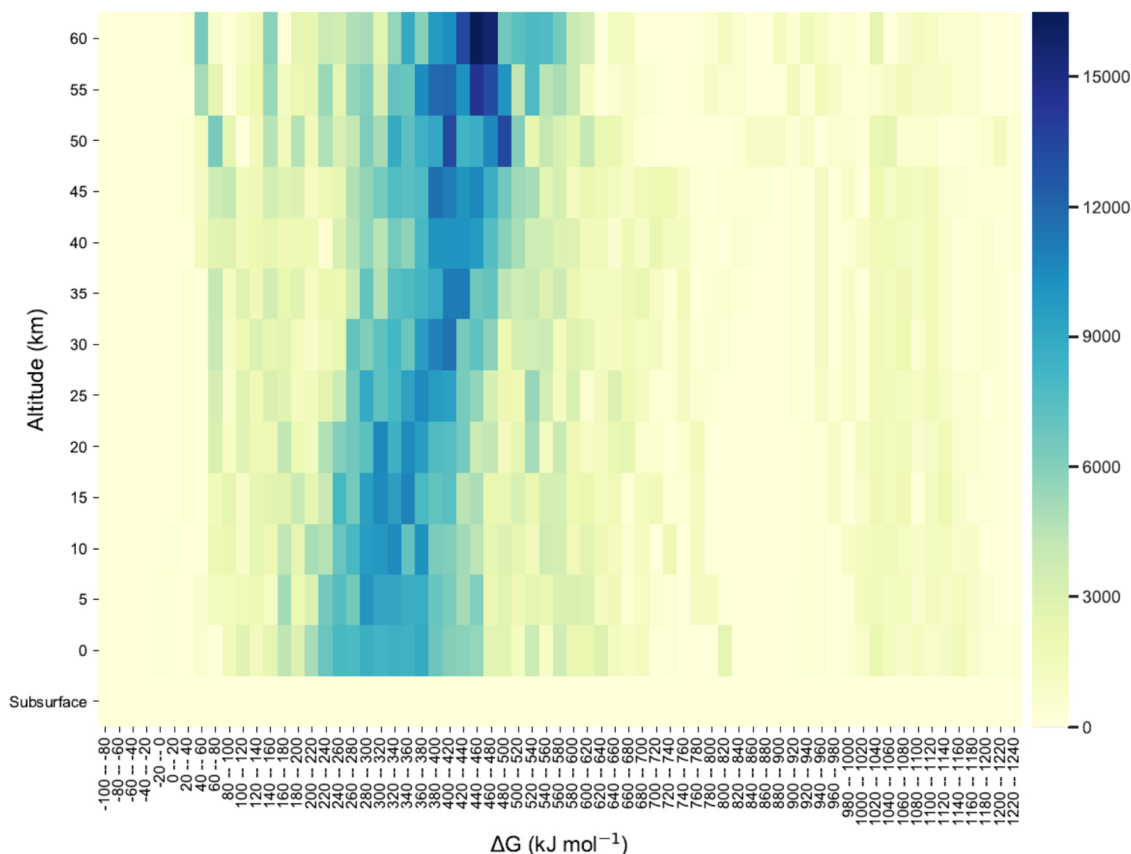
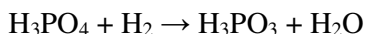


Fig. 6. The infeasibility of phosphine production in the Venusian atmosphere, surface and subsurface. The y axis shows altitude above the surface and each column (x axis) is a bin of data in a range of Gibbs Free Energy (ΔG). The darker the color of a cell the more reactions/conditions fall within a given ΔG range. The Gibbs Free Energies are from reactions of subsurface, surface and atmospheric phosphorus species with gaseous or solid reducing agents. Reactions with gases were calculated with a high or a low gas concentration, derived from published data (Table S5), in all combinations. Reactions of P_4O_6 , P_4O_{10} , H_3PO_4 and H_3PO_3 were considered (the last of these only in solution phase in the clouds), as well as surface reduction of phosphate minerals. Subsurface thermodynamics were based on fugacity calculations under a wide range of conditions (see Section 3.2.2). None of the conditions give a negative free energy, which would indicate a reaction that spontaneously produced phosphine. Thermodynamics was only followed to the altitude of the cloud tops, after which phosphorus species and water are expected to freeze out making reactions of stable phosphorus compounds implausible. Phosphine production is not thermodynamically favored under the conditions of the Venusian atmosphere, surface and subsurface conditions. Figure modified from (Greaves *et al.* 2020).

We could argue that the complex atmosphere of Venus is not fully characterized, and specifically that the clouds may be more reduced than we think, and that the more reduced character of the Venusian atmosphere might explain the presence of phosphine. We can show quantitatively how much more reduced the atmosphere of Venus would have to be to favor the production of phosphorous acid (H_3PO_3) (or phosphine).

The standard free energy of reaction:



varies from 47 kJ/mol at 260 K to 59 kJ/mol at 590 K. The reverse reaction is therefore highly favored. To drive the forward reaction, there would have to be a large excess of H₂ over H₂O. Taking the standard reference Venus atmosphere abundance for H₂O, we can calculate how much hydrogen as a model reductant would have to be present in the Venusian atmosphere to make phosphorous acid production plausible. To achieve equilibrium between H₃PO₃ and H₃PO₄ would require a pressure of ~200,000 bars of H₂ at 60 km altitude, reduced to only ~20 bars at 20 km altitude. These are the conditions deep inside gas giant planets where phosphorus is indeed present primarily in reduced states, mostly phosphine.

While the Venusian atmosphere certainly still holds some surprises, we are confident that it is significantly more oxidized than the atmosphere of Jupiter.

Moreover, we note that the sensitivity analysis to the concentrations of gases in the Venusian atmosphere shows that only very substantial systematic errors (at least 10⁴-fold difference) in gas abundance measurements or modelling could account for the production of phosphine. Such dramatic differences from current expectation are therefore highly unlikely (see Supplementary Section 2.1. and Figure S11).

If an unknown, non-volatile material that was a less powerful reducing agent than hydrogen was present in the clouds, could it reduce phosphoric acid to phosphorous acid? (If it were more powerful than hydrogen then it would split water and generate hydrogen, as discussed above.) This cannot be definitively ruled out in the absence of specifics, but two arguments suggest that it could not. Firstly, if hydrogen cannot reduce phosphoric acid to phosphorous acid, then a less powerful reducing agent is unlikely to be able to do so. Secondly, the closest parallel to such chemistry that we know has been tested is the autoclaving of phosphate-containing agar media (agar is a polysaccharide and hence a weak reducing agent). Autoclaving phosphate-containing agar is found to produce hydrogen peroxide (an oxidizing agent) and not phosphite (a reducing agent) (Tanaka *et al.* 2014). If any phosphite was produced, the hydrogen peroxide would oxidize it again.

3. 2. 2. Subsurface Thermodynamics of Phosphine Production

3. 2. 2. 1. Formation of Phosphine in the Venusian Subsurface Environment Cannot Proceed Spontaneously

In principle, chemistry occurring below the surface in crust or mantle rocks might be considered a source of phosphine. It is impractical to perform calculations of the thermodynamics of specific reactions in the subsurface of Venus, because the composition of the rocks is not known and the thermodynamics of individual reactions are not known. We therefore simplify the problem of calculating whether subsurface chemistry could generate phosphine by using the concept of oxygen fugacity. Oxygen fugacity is the notional concentration of free oxygen in a mineral at thermodynamic equilibrium; the higher the concentration, the more oxidizing the rock is. (See (Frost 1991) and Supplementary Section 1.3.3. for more details on f_{O_2} and its calculation). A higher oxygen fugacity (concentration of free oxygen in the crustal rocks) means a more oxidized rock and a lower probability of

reduction of phosphates. We find that the oxygen fugacity of plausible crust and mantle rocks is 8 - 15 orders of magnitude too high to support reduction of phosphate. It is therefore not possible that subsurface activity on Venus, including volcanism, would produce substantial amounts of phosphine.

We present our reasoning as follows. We compared the fugacity of the phosphate/phosphine equilibrium to the fugacity of standard mineral buffers representative of terrestrial rocks. The results are shown in Figure 7.

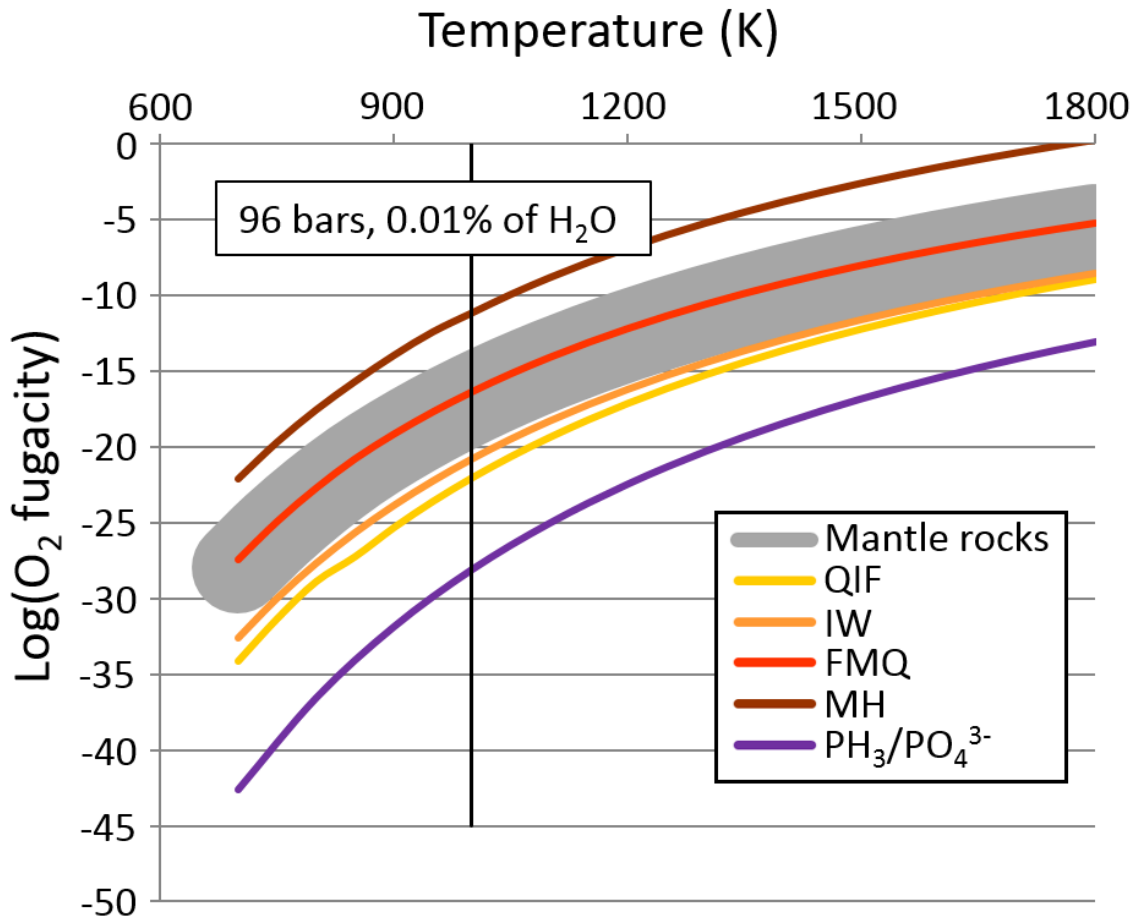


Fig. 7. Comparison of the fugacity of the phosphate/phosphine equilibrium to the fugacity of the standard mineral buffers of terrestrial rocks. x axis: log O₂ fugacity, y axis: Temperature (K). Fugacity of the production of phosphine from phosphate minerals is calculated for 96 bars and 0.01% water in the rocks. The fugacity of the phosphate/phosphine equilibrium is shown as a purple line. The other curves are O₂ fugacities of standard rock buffers. The phosphate/phosphine fO₂ curve lies below the QIF buffer line (the most reduced rock of the buffers shown) which falls below the typical fO₂ of terrestrial mantle or crustal rocks (grey band region). Therefore, typical terrestrial rocks are too oxidized to produce PH₃ from phosphates and the formation of phosphine is highly unlikely under Venusian subsurface conditions.

To interpret any fO₂ curve, any point above a fugacity line will mean that the oxidized member of a reaction will be favored, anything below a fugacity line means that the reduced member is favored.

The phosphate/phosphine fO₂ curves lie substantially below the QIF buffer line, which itself falls well below the typical fO₂ of mantle or crustal rocks. Rare cases of very reduced rocks

are found in some locations, e.g. (Ulff-Møller 1985), with an fO_2 of \sim QIF-1. However, such rocks are unlikely to contain any water, because it would react with the metallic iron in the rock. The fO_2 of Lunar and asteroidal olivines and plagioclase is usually around IW-2 to IW+2 (Karner *et al.* 2004). All of them are too oxidized to produce PH_3 from phosphate. This means that in crustal and mantle rocks, phosphorus will overwhelmingly be present as phosphate.

The results of our fugacity calculations are also supported by observations that PH_3 is not known to be made by volcanoes on Earth, although in principle reduced phosphorus species could be produced in ocean-floor hydrothermal systems through serpentinization reactions (Pasek *et al.* 2020) (an environment with no analogue on Venus). Estimation of the production of PH_3 through volcanism on a simulated anoxic early Earth concluded that only trace amounts of volcanic phosphine can be produced through this process. The predicted maximum production rate of phosphine on the early Earth is only \sim 100 tons per year (Holland 1984), even assuming a highly reduced planet with abundant water. The volcanic production of phosphine in more oxidized, dehydrated planetary scenarios is even more unlikely.

The redox state of the crustal rocks on Venus is unknown. The relatively reduced QIF buffer is an Fe(II)/Fe(0) buffer: to have a substantially more reducing rock, a more electropositive metal than iron would need to be present in significant amounts as elemental metal, which itself would imply that all the iron (and nickel) in the rock would have to be reduced to elemental metal as well. This is a possible but implausible scenario.

We validate our approach by calculation of the fugacity of the terrestrial H_2S/SO_2 equilibrium. The results from the computed SO_2/H_2S line (Figure S12) are qualitatively consistent with field observations on Earth and modelling on Mars (see Supplementary Section 2.2.1.).

Another way to demonstrate that subsurface chemistry cannot generate atmospheric phosphine is to consider the amount of volcanism that would be necessary to generate the observed amount of phosphine in the atmosphere. We find that to maintain \sim 20 ppb of PH_3 on Venus a volcanic flux many orders of magnitude greater than that on Earth is required. We modelled volcanic outgassing as follows.

The thermodynamics inherent in Figure 7 does not state that phosphine cannot be made by geochemistry, just that the ratio of phosphine to phosphate would be extremely small. We estimate the amount of volcanism that would be needed to maintain an atmospheric abundance of \sim 20 ppb as follows. We calculated the ratio of phosphate to phosphine (formally of P(+5):P(-3)) that would be produced by volcanic rocks using the $f(O_2)$ approach described above, based on the $f(O_2)$ values of six redox buffers with redox states between IW (Iron/Wustit: Fe/FeO) and MH (Magnetite/Haematite: Fe_3O_4/Fe_2O_3) buffers, including the IW and MH buffers themselves, and for a range of temperatures, pressures and rock water content that reflect the extreme ranges plausible for Venus' crust. From this, the amount of phosphorus that would have to be erupted to provide the flux of 4.16 kg/second (needed to

maintain an abundance of ~20 ppb in the atmosphere) can be calculated. These fluxes are shown in Figure 8. (See Supplementary Information Section 2.2.3 for details of the data sources and calculations).

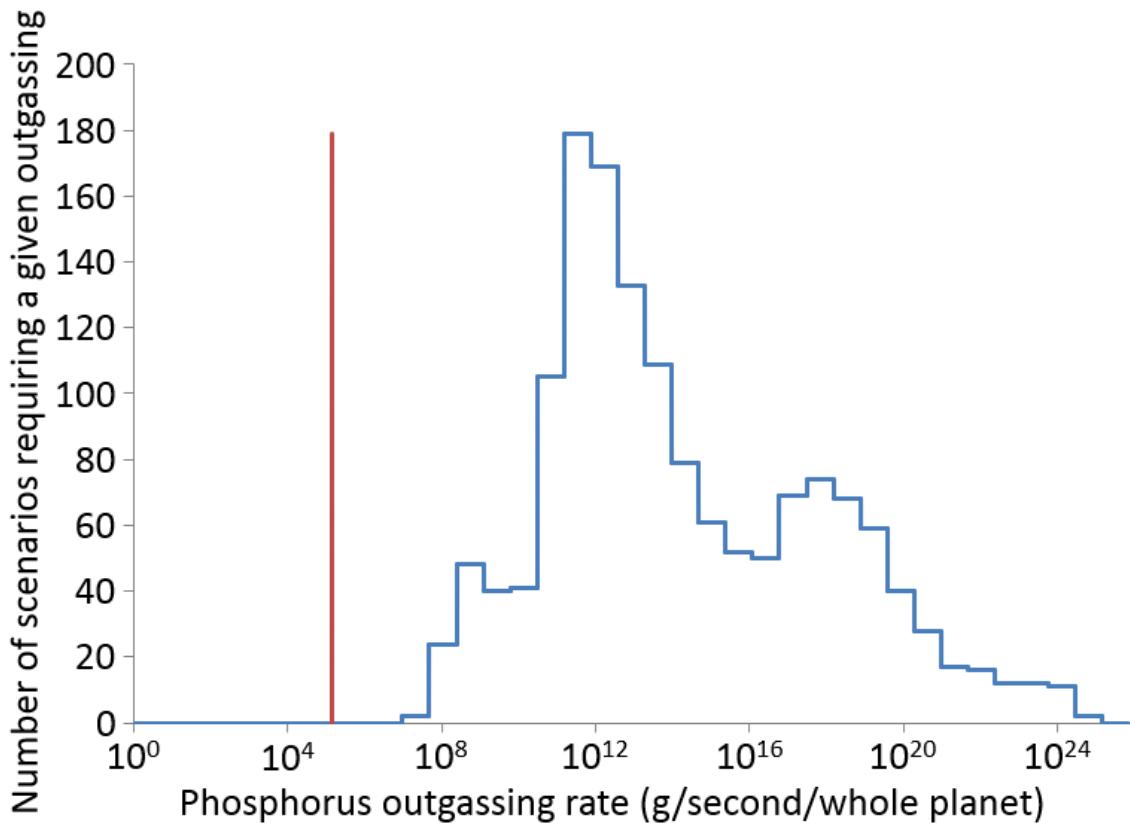


Fig. 8. The assessment of the volcanic production of phosphine. x axis: total phosphorus outgassing rate in grams of phosphorus per second across the whole planet, binned in log(5) bins. y axis: number of combinations of f(O₂) buffer, temperature, pressure and water content for which that outgassing rate provided 1.43 kg/second phosphine flux. Blue line – model output. Red line – estimated terrestrial phosphorus outgassing flux (See Supplementary Section 2.2.3 for details). To explain the observed abundance of phosphine at least many hundred times more volcanism on Venus than on Earth is required.

Few conditions require a total flux of less than 10⁹ grams of phosphorus per second. For comparison, the flux of phosphorus from modern day Earth volcanism (of all sorts) is ~ 143 kg/second (shown as a vertical red line of Figure 8 – see Supplementary Section 2.2.3 for details). This is 220 times lower than the most extreme rate predicted for Venus, representing outgassing at 90 bar and 1600 K, from rocks containing 1.5% water (a high value even for Earth) and with a fugacity of the Iron/Wustite buffer (at the bottom range of plausibility for mantle rocks). More realistic values of f(O₂), water content, temperature and pressure require tens of thousands of times more volcanism on Venus than on Earth to produce the amount of phosphine required. We note that the Venusian crust (and by inference the upper mantle, due to the resurfacing event) seems more oxidized than Earth (Wordsworth 2016), and that Venus probably lacks the global tectonic activity seen on Earth (i.e. plate tectonics) (Byrne *et al.* 2018). Orbiter topographical studies suggest there are not many large, active, volcanic hotspots on Venus (Shalygin *et al.* 2015; Treiman 2017) and it is postulated that the overall volcanic flux is much lower than that on Earth (Mikhail and Heap 2017). Very recent studies

identified only 37 possibly active volcanic structures on Venus (Gülcher *et al.* 2020). We therefore consider it highly unlikely that Venus has more than 200 times the volcanic activity of Earth needed to explain the presence of phosphine in its atmosphere.

Fugacity is dependent on pressure, temperature and water concentration. We probed the sensitivity of our conclusions to variation in all three parameters (see Supplementary Section 2.2.2. and Figure S13). No realistic values of pressure (up to 10,000 bar), water content (up to 5%) or temperature (up to 1800 K) can support phosphine production (Figure S13). We note that phosphorous acid and phosphites cannot be produced by volcanoes, as they break down at temperatures $> \sim 450$ K.

3. 2. 3. Phosphides from Crustal and Mantle Minerals or Meteorites as a Source of Phosphine

3. 2. 3. 1. Phosphides from Crustal and Mantle Minerals as a Source of Phosphine

The presence of phosphides in surface or mantle minerals, if they exist, cannot explain the observed amounts of atmospheric phosphine.

One might argue that mineral phosphides could form in the deep mantle and survive volcanic eruption in a very dry Venusian crust and subsequent injection into the atmosphere, where they are hydrolyzed by the $\text{H}_2\text{SO}_4/\text{H}_2\text{O}$ mix to form phosphine.

Phosphides are stable to extremely high temperatures and pressures (Japel *et al.* 2002), and so could be formed deep in the mantle and brought to the surface through plume volcanism, if such volcanism occurs on Venus. Mineral phosphides are hydrolyzed by acid solutions in water to form phosphine (Pasek and Lauretta 2005; Pasek *et al.* 2014), although the kinetics and thermodynamics of their hydrolysis by low partial pressures of water vapor have not been explored.

However, the amount of phosphides released into the atmosphere, and scale and frequency of such volcanic eruptions needed for this scenario of phosphine production to be possible, makes it seem very unlikely. Mineral phosphides are known on Earth, where they are rare but widely distributed. A mineral fulgurite - a glass resulting from lightning strikes was proposed as a potential source that could in principle contain reduced phosphorus species (Pasek and Block 2009). It is estimated that fulgurites probably contain $< 0.5\%$ phosphorus (Gailliot 1980), and are widely stated as being 'rare' (e.g. (Glover 1979; Petty 1936; Pye 1982)). Phosphides can also originate in pyrometamorphic rocks. Pyrometamorphic rocks form as a result of fossil fuel fires, a process that is probably not relevant to Venus (Britvin *et al.* 2019). In principle, phosphides could be produced volcanically, but the amount needed to provide sufficient phosphine to explain a phosphine abundance of ~ 20 ppb in the atmosphere is implausible. At least 3×10^{11} grams of phosphides (300,000 tons) would need to be erupted from the deep mantle every year and be efficiently converted to phosphine for this to explain the presence of ~ 20 ppb phosphine in the atmosphere. For context, the Siberian and Deccan traps, vast volcanic flood plains that represent the most extensive volcanism in the

Phanerozoic on Earth, were probably created by massive plume eruptions that at their peak produced 1 km^3 of basalt/year, which would deliver $\sim 10^{12}$ g of phosphorus to the surface, per year, the large majority as phosphate. (Renne and Basu 1991; Sen 2001). Thus, for present-day phosphide eruption to explain the presence of ~ 20 ppb phosphine in Venus' atmosphere, the planet would have to be as volcanically active today as the most active volcanic eruption on Earth in the last 500 million years. As discussed above, no evidence for such recent catastrophic volcanism exists on Venus.

3. 2. 3. 2. *Phosphide-Containing Meteorites as a Source of Phosphine*

We also exclude exogenous meteoritic delivery of phosphides to Venus as a potential source of observed amounts of phosphine.

Iron-nickel meteorites are known to contain reduced species of phosphorus, mostly as phosphides (Geist *et al.* 2005). Such metal-rich meteorites could also be a source of phosphide and hence, upon its hydrolysis, of phosphine. For example, reduced phosphorus species can be found in the meteoritic mineral schreibersite $(\text{Fe,Ni})_3\text{P}$, the most common mineral containing reduced phosphorus (Pech *et al.* 2011), and in other minerals (Buseck 1969; Ma *et al.* 2014; Pratesi *et al.* 2006; Zolensky *et al.* 2008). It has been suggested that schreibersite was a source of reduced phosphorus species on early Earth (Baross *et al.* 2007), and could in principle continue to be a trace source of reduced phosphorus species today.

The accretion rate of meteoritic material to the Earth today is of the order of 20-70 kilotons/year (Peucker-Ehrenbrink 1996). $\sim 6\%$ of this material is iron/nickel meteorites (Emiliani 1992) which contain phosphides at a level of an average of 0.25% phosphorus by weight (Geist *et al.* 2005). If we rely on the extremely conservative assumption that hydrolysis of $(\text{Fe,Ni})_3\text{P}$ phosphides to phosphine is 100% efficient, that would deliver a maximum of ~ 10 tons of phosphine to the Earth every year, or about 110 milligrams/second, which is a negligible amount globally (Greaves *et al.* 2020; Sousa-Silva *et al.* 2020). This estimated maximal yearly meteoritic delivery of phosphine on Venus is ~ 8 orders of magnitude too low to explain detected amounts.

Our calculations are also in agreement with previous estimates of the phosphine production through meteoritic delivery, which were also found to be negligible (Holland 1984) and with very recent work by Carrillo-Sánchez who show that the great majority of meteoritic phosphorus species is oxidized (even though the severe conditions of atmospheric entry do create trace amounts of elemental P, this elemental P gets readily oxidized as well) (Carrillo-Sánchez *et al.* 2020).

3.3. Conclusions of the Thermodynamic Analysis of Potential Phosphine-Producing Reactions

We show with our thermodynamic analyses that none of the **known** possible routes for production of PH₃ on Venus can explain the presence of ~20 ppb phosphine. All fall short, often by many orders of magnitude (Table 1).

The thermodynamics of known reactions between chemical species in the atmosphere and on the surface of Venus are too energetically costly and cannot be responsible for the spontaneous formation of phosphine.

Similarly, the formation of phosphine in the subsurface is not favored. Oxygen fugacity of the crustal and mantle rocks is many orders of magnitude too high to reduce mineral phosphates to phosphine.

Finally, we show that the hydrolysis of phosphide minerals, both from crustal and mantle rocks, as well as delivered by meteorites, cannot provide sufficient amounts of phosphine.

4. Other Potential Processes of Phosphine Formation

4.1. Potential Endergonic Processes of Phosphine Formation

Several potential sources of energy that could drive the formation of PH₃ should be mentioned briefly for completeness, although we argue that none of them could be responsible for the observed abundance of phosphine on Venus.

Lightning strikes cannot create sufficient amounts of phosphine to explain the observed ~20 ppb amounts of phosphine in the atmosphere of Venus. Lightning may be capable of producing a plethora of molecules that are thermodynamically disfavored. However, our calculations suggest that lightning's production of PH₃ is at most ~7 orders of magnitude too low to explain detected amounts (Sousa-Silva *et al.* 2020). We estimate that the maximum amount of phosphine produced by lightning in one Venusian year is 3.38×10^8 grams. This would generate a partial pressure of phosphine of 0.76 parts per quadrillion if lightning-produced phosphine accumulated for a full (Venusian) year with no destruction. 0.76ppq is 7 orders of magnitude lower than observed by (Greaves *et al.* 2020), and destruction rates much faster than a year are expected as discussed above (see Supplementary Section 2.3.1. for details on the estimation of phosphine production by lightning).

We note that our predicted value of phosphine production through lightning is an upper bound and, in reality, the lightning-induced production of reduced phosphorus species in Venusian atmosphere is likely to be much less efficient. The well-studied formation of analogous N species by lightning strikes on Earth favors formation of nitrates and nitrites, and not the thermally less stable reduced forms of N like ammonia (Ardaseva *et al.* 2017; Mancinelli and McKay 1988; Rakov and Uman 2003).

Moreover, the above calculations agree with several studies on the formation of reduced phosphorus species, including PH₃, by laboratory-simulated lightning. Such experiments can produce traces of phosphine from discharges onto phosphate salt solutions, but at very low efficiency (Glindemann *et al.* 1999; Glindemann *et al.* 2004).

Mechanochemically-driven reduction of phosphate to phosphine in rocks, by tribochemical weathering at quartz and calcite or marble inclusions, was postulated as a potential abiotic source of phosphine (Glindemann *et al.* 2005b). However scaling the results presented in (Glindemann *et al.* 2005b) to plausible global earthquake activity (even under very optimistic assumptions that all the rock moved during an Earthquake-induced landslide can be the substrate for this chemistry) suggests that the flux of phosphine produced would be at least two orders of magnitude too small to account for the observed abundance of phosphine in Venus' atmosphere. In addition, tribochemical production of phosphine in crustal rocks requires a local fluid to provide hydrogen atoms, which is very unlikely to be present in Venus' crust. The crustal rocks are above the critical temperature of water and under an atmosphere with $\sim 3 \cdot 10^{-5}$ partial pressure of water; they are therefore expected to be extremely desiccated with no local hydrogen source. (see Supplementary Section 2.3.3 for more details on tribochemical production of phosphine).

A very large comet or asteroid impact could theoretically generate a highly reduced atmosphere for millions of years that could lead to formation of conditions that are more favorable for phosphine production (Kasting 1990). We note however that a scale of such impact has to be comparable to the hypothetical impact that is postulated to have created a transient H₂-rich atmosphere on early Earth ~ 4.48 billion years ago (Benner *et al.* 2019; Service 2019). Even the Chicxulub impactor, which resulted in a crater 150 km wide and contributed to the extinction of the dinosaurs did not manage to significantly change the redox state of Earth's atmosphere (although it had dramatic effects on radiative balance, and hence climate (Brugger *et al.* 2017; Toon *et al.* 2016)). An impact as large as Chicxulub occurs every 50-100 million years. It is statistically highly unlikely that an even larger cataclysm of this sort happened in recent Venusian history. The radar mapping of the surface of Venus does not show sufficiently large recent craters on the surface of Venus and therefore does not support the recent large impact scenario (Ivanov and Head 2011; Kreslavsky *et al.* 2015). Smaller impacts could only generate phosphine through delivery of meteoritic phosphide, which is insufficient to account for phosphine production as discussed above in Section 3.2.3.2. and in (Greaves *et al.* 2020).

Lastly, solar X-rays and solar wind protons carry substantial energy, but are absorbed at high altitudes, and so could not penetrate to the clouds where phosphorus species might be found and where phosphine is detected, and hence cannot drive the formation of phosphine.

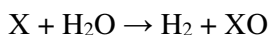
4. 2. Other Potential Exergonic Processes as Sources of Phosphine

In principle some exotic chemistry on Venus, not considered before, could be responsible for the formation of phosphine. In this section we address a few potential examples, including formation of phosphine from elemental phosphorus or production of phosphine with reducing

agents more powerful than molecular hydrogen. We argue that all such scenarios just replace the implausibility of making phosphine with another, equally implausible set of conditions which could then produce phosphine (i.e. a “displaced improbability”).

For example, if elemental phosphorus could be erupted from Venusian volcanoes, it could be reduced by atmospheric gases to phosphine. However, the production of elemental phosphorus from phosphate rocks under Venus’ conditions is itself extremely improbable on thermodynamic grounds (see Supplementary Section 2.3.2.2. and Supplementary Section 2.3.2.3. for details on the possibility of formation of elemental phosphorus on Venus). Invoking elemental phosphorus as a source of phosphine therefore just begs the question of where the elemental phosphorus can come from.

Other reducing agents could exist on the surface of Venus, and be more powerful reducing agents than hydrogen. Previous suggestions for rare Venusian surface minerals include lead or bismuth sulfide, elemental metals or other materials (Schaefer and Fegley Jr 2004; Treiman *et al.* 2016). Some Venusian mountaintops show ‘snowcaps’ of a highly radar-reflective material. The chemical composition of these deposits is unknown (Taylor *et al.* 2018), and could conceivably be a source of exotic chemistry. However, we know that water is present (as gas) in Venus’ atmosphere. If a more powerful reducing agent than hydrogen is present on the surface, then the reaction:



would happen spontaneously, oxidizing that reducing agent and reducing water to hydrogen. To invoke a more powerful reducing agent than hydrogen one therefore has to explain both what it is *and* why it does not react with water present in the atmosphere.

5. Summary and Discussion

5.1. Summary

Phosphorus-containing species have not been modelled for Venus’ atmosphere prior to Greaves *et al.* (2020). This work represents the first full description of a model of phosphorus species on Venus. We have explored every plausible chemical and physical process (and a number of implausible but possible ones) that could lead to the formation of phosphine on Venus, making conservative estimates where exact values were not known. We have ruled out all conventional explanations of phosphine production that can explain the recent detection ~20 ppb of phosphine in the Venusian atmosphere (Greaves *et al.* 2020). Specifically, we have explored photochemical production (at least 4 orders of magnitude below the rate required to explain the observed ~20ppb levels), atmospheric equilibrium thermodynamics (on average 100kJ/mol too energetically costly), surface and subsurface chemistry (8 – 15 orders of magnitude too low), and a range of other processes. We conclude that phosphine on Venus must be produced by a physical or chemical process that is not expected to occur on terrestrial rocky planets.

5. 2. Unknown Chemistry as an Explanation for the Presence of PH₃

If no conventional chemical processes can produce phosphine, is there a not yet considered process or set of processes that could be responsible for its formation?

One of the possibilities is that chemical species exist in the crust, or in the atmosphere of Venus, that we have not considered. Perhaps an unknown atmospheric chemical drives phosphine formation, especially considering that the photochemistry of Venus' atmosphere is not fully understood. Such a mechanism would have to be compatible with what we do know about Venus; for example, a powerful reductant would have to be compatible with the observed presence of water in Venus' atmosphere, as discussed in Section 4.2.

A specific example of such a mechanism would be photochemistry in the cloud droplets. The photochemistry of phosphorus species in sulfuric acid droplets is completely unknown, and so in principle phosphine could be produced photochemically in the sulfuric acid droplets of the cloud layer. However, we consider this unlikely, not least because it is known that phosphine is rapidly oxidized by sulfuric acid to phosphoric acid. Phosphorous acid is also oxidized. Even if a photochemical process did produce phosphine in sulfuric acid, it seems unlikely that it would escape oxidation back to phosphoric acid. In fact, we expect the sulfuric acid cloud layer to be a sink for phosphine (one which we have not incorporated into the models above for lack of kinetic data.). See Supplementary Section 2.3.2.1. for more on cloud droplet chemistry, and the chemistry of phosphine in sulfuric acid.

A second possibility is that reactions we have not considered possible sources of phosphine could actually be occurring. For example, the reduction of calcium phosphate to phosphine by carbon monoxide is thermodynamically possible under conditions prevailing above altitudes of 120 km. But there is no mechanism that can transport calcium phosphate dust to such high altitudes, and the reaction of calcium phosphate with CO would take millions of years to produce detectable phosphine at 170 K. Furthermore, phosphine produced at 120 km altitude would be destroyed in fractions of a second by solar UV (see Supplementary Section 2.3.3.4), making such a scenario for the formation of PH₃ highly unlikely.

Other, completely unknown chemistry could be a source of phosphine, but in the absence of suggestions as to what that chemistry might be, such speculation cannot be considered a hypothesis to be tested.

5. 3. Phosphine as a Venus Cloud Biosignature Gas

Could living organisms in the temperate clouds of Venus produce phosphine? For decades many have speculated that the Venusian clouds are a suitable habitat for life (Cockell 1999; Grinspoon 1997; Grinspoon and Bullock 2007; Morowitz and Sagan 1967; Schulze-Makuch *et al.* 2004; Schulze-Makuch and Irwin 2002; Schulze-Makuch and Irwin 2006). The anomalous UV absorber in Venus' atmosphere has been proposed as a biosignature (Limaye *et al.* 2018; Seager *et al.* 2021), though chemical processes may be the source (Wu *et al.* 2018). Unknown chemical species in the clouds absorb more than half of the UV flux that the planet receives, an absorption which is not constant across the planet but has unexplained

temporal and spatial differences and constraints (Lee *et al.* 2019; Marcq *et al.* 2019). Recent work has developed the case for phosphine as a biosignature gas in anoxic environments (Bains *et al.* 2019a; Bains *et al.* 2019b; Sousa-Silva *et al.* 2020). We emphasize that a biosignature is a sign that life is present. It may or may not be produced directly by life. While we do not know whether life on Earth produces phosphine itself, or produces reduced phosphorus species such as phosphite or hypophosphite that subsequently disproportionate to phosphine, the association of phosphine with biology (and in recent centuries with human technology) is clear (Bains *et al.* 2019a; Gassmann and Glindemann 1993; Glindemann *et al.* 1999; Glindemann *et al.* 2005a; Glindemann *et al.* 1996; Sousa-Silva *et al.* 2020). We therefore explored the possibility that the Venusian PH₃ is produced by life.

We emphasize that the presence of phosphine in Venus' atmosphere does not prove the presence of life. Any explanation for the unexpected finding of PH₃ in Venus' atmosphere must be tested, and to be tested it must be articulated. Here we articulate what the conjecture does and does not explain.

On Earth PH₃ is exclusively associated with biological activity (reviewed in (Bains *et al.* 2019a; Bains *et al.* 2019b; Sousa-Silva *et al.* 2020)). Specifically, we previously proposed that PH₃ production on Earth is associated with a strictly oxygen-free, highly reduced, hot, moderately acid ecosystems (pH<5, 80 °C) or cooler, very acid conditions (pH <2, 20 °C) (Bains *et al.* 2019a; Bains *et al.* 2019b; Sousa-Silva *et al.* 2020). The Venusian clouds have some apparent parallels to these environments on Earth where life produces PH₃, although obviously the Venusian clouds are not reduced. Could PH₃ on Venus also be associated with biological activity? We have argued above that producing phosphine in the Venusian atmosphere requires energy. A unique feature of life is that it captures chemical energy and uses it to drive chemical reactions that would not happen spontaneously in the environment (such as production of O₂ via photosynthesis on Earth). One widely accepted criterion for a biosignature is a gas completely out of equilibrium with its environment (Krissansen-Totton *et al.* 2016; Lovelock 1975), as phosphine is on Venus.

Could life make phosphine using biochemical mechanisms known from Earth? We tested a specific model of PH₃ production, through metabolic reactions analogous to those that could occur in Earth life (Bains *et al.* 2019a; Bains *et al.* 2019b; Sousa-Silva *et al.* 2020).

The redox reactions involving phosphorus species that could be of biochemical origin are of the general form of:

- 1) $XH + H^+ + H_2PO_4^- \rightarrow H_2PO_3^- + H_2O + X^+$
- 2) $4XH + 4H^+ + H_2PO_4^- \rightarrow PH_3 + 3H_2O + OH^- + 4X^+$
- 3) $3XH + 3H^+ + H_2PO_3^- \rightarrow PH_3 + 2H_2O + OH^- + 3X^+$

Where XH and X⁺ are the reduced and oxidized form of a biological reducing agent respectively. Reactions are assumed to occur at pH=7.

We calculated the free energy needed to reduce phosphorus species to phosphine with the following assumptions. We assume that a cell living in a cloud droplet is composed mainly of water (Figure 9).

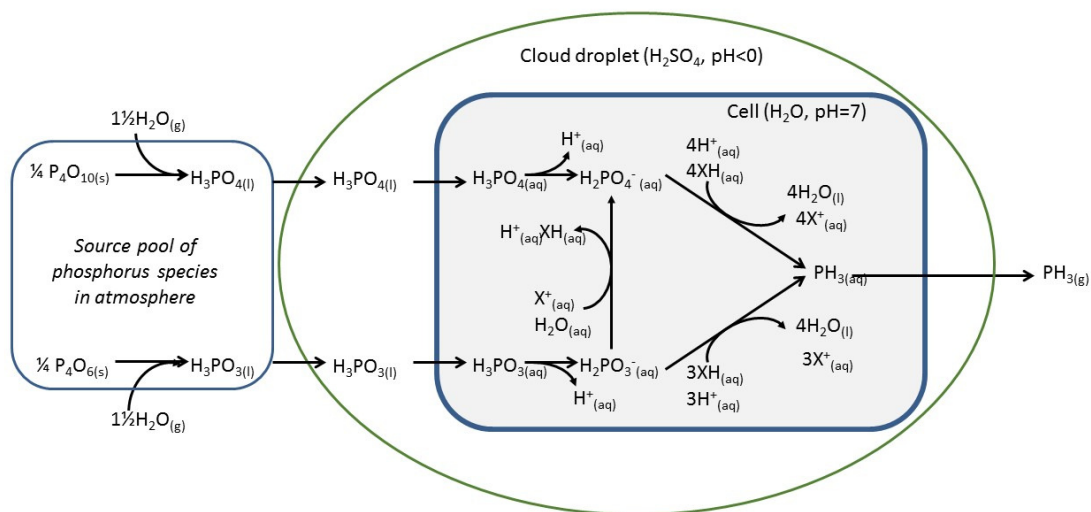


Fig. 9. A model for biological production of phosphine on Venus. The favored path for reduction of atmospheric phosphorus species to phosphine is reduction of phosphoric acid to phosphine (upper reaction pathway on the schematic above). Correspondingly, the reduction of phosphite to phosphine is disfavored, because of the low concentration of the phosphite reactant (lower reaction pathway on the schematic above). If the concentration of phosphite is allowed to rise in the cell, then reduction of phosphate to phosphite becomes less energetically favorable, and reduction of phosphite to phosphine correspondingly more favorable. It is plausible to suggest, though it is speculative, that phosphite would accumulate in cells to a level where its reduction to phosphine was thermodynamically neutral, allowing a multi-step reduction pathway for phosphate. HX: biological reducing agent, such as NADH.

Phosphorus species were assumed to be present in the extracellular droplet phase as oxyacids at 1 molal concentration (see Supplementary Section 1.3.2.2). We have assumed that, like terrestrial acidophiles, the putative Venusian organisms keep their interior at $pH > 5$, as do Earth organisms, even those living at environments of $pH = 0$ or $pH = 12$ (Baker-Austin and Dopson 2007; Horikoshi 2016). Indeed, the electrochemistry of the reducing agents discussed here probably has no meaning at low pH , as compounds such as NADH and Fe/S proteins will be rapidly destroyed at $pH = 0$. An internal $pH = 7$ was assumed here. The energy implicit in converting phosphate from the external pH ($pH = 0$) to the intracellular pH ($pH = 7$) was calculated as discussed extensively in (Bains *et al.* 2019a), and Supplementary Section 2.4. If the free energy needed to convert extracellular phosphorus to intracellular singly ionized forms at 1 mM was calculated as positive, it was assumed that the cell could not import phosphorus and no phosphine production could occur (i.e. the phosphorus was assumed to enter the cell by passive diffusion). The ratio of $H_2PO_3^-/H_2PO_4^-$ inside the cell immediately after transport was assumed to be the same as the ratio of H_3PO_3/H_3PO_4 outside the cell (but see below).

We estimated the thermodynamics of reduction of phosphorus species to phosphine *assuming* life in the clouds of Venus had a metabolism that included reducing agents functionally similar to those used universally by terrestrial life. We chose NADH, FADH₂, ubiquinone and two iron-sulfur proteins as model agents to illustrate the range of reducing power of different biological reducing agents in terrestrial biochemistry. We do not expect these specific chemicals to be present in putative Venusian life; we use them solely for illustration. Our result shows that biological production of PH₃ is thermodynamically possible if the Venusian organism had a reducing metabolite with a redox potential similar to NADH or to iron-sulfur (Fe-S) proteins, but not if its internal redox carrier has a redox potential similar to ubiquinone or FADH₂ (Figure 10).

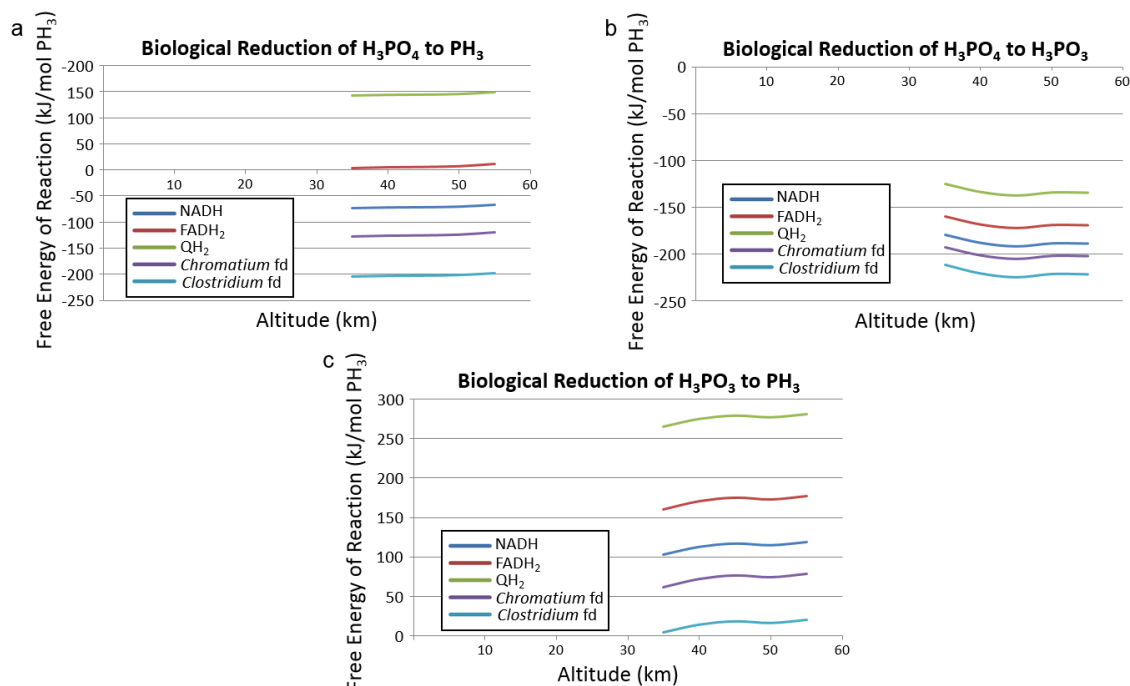


Fig. 10. A biochemical system could exergonically produce phosphine under Venus cloud conditions by reduction of phosphate, assuming passive import processes. The y axes show free energy of reduction of phosphate to phosphine while the x axes show altitude in the Venus atmosphere. Biological reduction of oxidized phosphorus species is assumed to only take place in the clouds at altitudes 35-55 km as any hypothetical organisms are presumed to only live in the cloud, and hence no calculations are performed below 35 km altitude. The different color curves represent the free energy for reduction by an example different biological reducing agents. The curves show that three (NADH and two Fe-S clusters) out of the five biological agents are thermodynamically favored for the reduction of phosphate to phosphine (i.e., have negative values of free energy). Reduction of phosphite to PH₃ is disfavored under all conditions (unless the concentration of phosphite is allowed to rise in the cell – as shown in Figure 9). (a) Biological reduction of phosphate to phosphine (b) Biological reduction of phosphate to phosphite (c) Biological reduction of phosphite to phosphine. The biological reducing agents assumed are redox equivalents of: NADH: nicotinamide adenine dinucleotide; FADH₂: Flavin adenine dinucleotide; QH₂: ubiquinone (Co-enzyme Q); *Chromatium* ferredoxin (fd): Iron-sulfur protein from *Chromatium vinosum*; *Clostridium* ferredoxin (fd): Iron-sulfur protein from *Clostridium thermoaceticum*.

In particular, iron-sulfur proteins have sufficient reducing power to reduce phosphorus to phosphine under the proposed Venusian conditions. We note that iron-sulfur proteins are considered ‘primitive’ in Earth life, both in the sense of being chemically simpler than

complex, derived molecules such as NADH and in terms of probably being one of, if not the one, original redox active agent in metabolism (Beinert *et al.* 1997). Fe-S clusters can be accommodated by many chemical contexts and do not require existence of terrestrial biochemistry or proteins. NADH is a much more complex and biochemistry specific reductant. Others have also suggested life based on an iron-sulfur based redox metabolism in the clouds of Venus (Limaye *et al.* 2018).

How can biology reduce H_3PO_4 to PH_3 if the chemistry of their environment cannot? PH_3 production can be thermodynamically favored because living organisms can generate more powerful reducing agents than H_2 (Bains *et al.* 2019a). The overall process of reducing phosphate in a Venusian environment remains energy-consuming, i.e. the putative organisms must gain energy from somewhere to generate the reducing agents that can then make phosphine. However, we note that life on Earth produces many compounds from common chemicals in the environment, sometimes in large amounts, that require substantial energy investment to make (Seager *et al.* 2012). In itself the expenditure of energy for the biosynthesis of PH_3 is not a criterion for ruling out a biological source for phosphine.

The total, planet-wide outgassing flux necessary to maintain an atmospheric concentration of ~ 20 ppb in the atmosphere of Venus is $\sim 10^6 - 10^7$ phosphine molecules $\text{cm}^{-2} \text{s}^{-1}$. Only microbes living in highly anoxic, reducing, acidic ecological niches produce phosphine on Earth (Bains *et al.* 2019a) and such niches can produce phosphine at a rate of $10^7 - 10^8$ phosphine molecules $\text{cm}^{-2} \text{s}^{-1}$ (reviewed in (Sousa-Silva *et al.* 2020)). Such a production rate is substantially above the rate required of hypothetical Venusian life, which suggests that droplets in the 10 km thick cloud layer could be quite sparsely populated, as compared to the terrestrial phosphine producing ecological niches. We also note that terrestrial phosphine-producing organisms are probably phosphorus-limited, because feeding them more phosphorus increases the rate at which they make phosphine. If the Vega descent data is accurate, then the Venusian cloud layers particles contain much more phosphorus than any terrestrial ecosystem.

We conclude that it is thermodynamically possible that biochemical reactions similar to those seen in terrestrial biochemistry could produce phosphine in the clouds of Venus. However, there remain major problems with the concept of life in the clouds of Venus. The clouds are often described as being 'habitable' because of their moderate pressure (~ 1 bar) and temperature (~ 60 °C). However, moderate temperature and pressure do not necessarily make the clouds habitable (Seager *et al.* 2021) (and in any case pressure is irrelevant - terrestrial life can grow at any pressure from >1000 bar (Nunoura *et al.* 2018) to <1 millibar (Pavlov *et al.* 2010)). To survive in the clouds, organisms would have to survive in an extremely chemically aggressive environment, one that is highly acidic and with an extremely low concentration of water (highly dehydrating and very low water activity). Sulfuric acid is a notoriously aggressive reagent towards sugars and aldehydes, reducing dry sucrose to charcoal in seconds. In principle life could exist in an aqueous droplet inside the sulfuric acid cloud drop (as drawn in Figure 9 above), but this poses formidable problems in itself. No biological membrane could remain intact against such a chemical gradient, and the energy required to counteract leakage of water out of the cell (or sulfuric acid into it) will be orders

of magnitude greater than the energy used by terrestrial halophiles to maintain their internal environment.

We conclude that, while we cannot rule out life as a source of the phosphine on Venus, the hypothesis that the phosphine is produced by life cannot *a priori* be favored over the hypothesis of unknown photochemistry or unknown atmospheric chemistry. All seem equally unlikely, and hence all call for further investigation. We note, after (Catling *et al.* 2018), that the extraordinary claim of life should be the hypothesis of last resort only after all conceivable abiotic alternatives are exhausted.

5. 4. Future Work on Identifying the Source of Phosphine on Venus

Our analysis argues that no conventional source can explain the presence of ~20 ppb phosphine on Venus. If the presence of phosphine in the atmosphere of Venus is confirmed, it calls for further investigation. Such an investigation would likely require a combination of a remote observation campaigns combined with orbiter and lander missions, supported by laboratory work on Earth.

Phosphine may be made by an unknown abiotic surface or cloud chemical processes. Knowledge of those processes will rely at least in part on more detailed knowledge of the Venusian atmosphere and geology. Missions focused on planetary geology, including landers, could help with *in situ* assessment of the possibility of geochemical production of phosphine on the surface of Venus and confirm or refute our conclusions that the geochemical processes on rocky planets are incapable of efficient phosphine production. Phosphine might also be made by organisms in the cloud layer. Instrument design for missions should bear this possibility in mind.

The first priority should be to confirm the presence of phosphine in the atmosphere of Venus with observations of additional spectral features, in the microwave or infrared where phosphine is a strong absorber (Sousa-Silva *et al.* 2014; Sousa-Silva *et al.* 2020; Sousa-Silva *et al.* 2013). Subsequently, observations should focus on constraining the distribution and abundances of phosphine throughout the Venusian clouds. Ultimately, long-term *in situ* observations of the clouds of Venus should also be carried out. Such long-term missions capable of detailed studies of clouds, aerosols, hazes and their spectral, physical and chemical properties (including mapping any changes over extended time periods) were proposed before (e.g. EnVision mission (Ghail *et al.* 2016), Aerobot aerial platforms (van den Berg *et al.* 2006) and the Venus Atmospheric Mobile Platform, developed by Northrop Grumman Aerospace (Lee *et al.* 2015)). Simultaneous observation of atmospheric features, such as UV absorber and phosphine distribution, would be more valuable than either alone. Some concepts of the aerial platforms are considered for the upcoming VENERA-D mission by ROSCOSMOS and NASA (Zasova *et al.* 2017).

The data that are especially lacking relate to reliable chemistry measurements and detailed models of Venusian clouds. Such models and measurements should extend their focus beyond sulfur chemistry and focus on phosphorus as well. For example, studies aimed at

detection of P-H bonds (strong absorbers around 4.3 and 10 microns (Sousa-Silva *et al.* 2019)) in any Venusian environment would be critical to further confirm the extent of propensity of the reduced phosphorus species on Venus. Such studies would require high resolution spectroscopy to distinguish PH₃ from overlapping CO₂ absorption; the necessary resolution should be within the capabilities of CRIRES+(VLT). Detection of P=O bonds would also be a valuable goal, because our kinetic model suggests that production and reduction of phosphorus monoxide (PO) is a rate-limiting factor in the pathway to atmospheric, abiotic phosphine production.

Neither the detailed chemistry nor the photochemistry of any of the potential phosphorus components of Venus' atmosphere are known, but could be investigated on Earth as a preliminary step for remote measurements and *in situ* observations. Progress towards identification of the source of phosphine on Venus can be made by laboratory experimentation here on Earth, especially regarding the properties of phosphorus species under Venus atmosphere and cloud conditions, including studies of chemical reactivity and solubility of phosphorus species in concentrated sulfuric acid and high CO₂.

A sample return missions would be required for any detailed biochemical characterization of a putative Venusian aerial biosphere.

Last but not least, our investigation presented in this paper is a useful template for the future investigations of biosignature gases, when these are detected on an exoplanet. Currently, a major focus in exoplanet astronomy is the near-future detection of the presence of life on exoplanets through detection of gases in exoplanet atmospheres that may be attributed to biological activity (Catling *et al.* 2018; Schwieterman *et al.* 2018; Seager and Bains 2015; Seager *et al.* 2016). A wide range of gases have been suggested, and a smaller number studied, as candidate biosignatures (Seager *et al.* 2012). However, detection is only the first step. Evaluation of the chemical context of the gas in a given planetary scenario is central to ruling life out or supporting the hypothesis that life is a source for that gas. This requires detailed analysis of possible formation and destruction pathways, local geology, atmospheric composition, all with inadequate knowledge (Catling *et al.* 2018; Schwieterman *et al.* 2018; Walker *et al.* 2018). We believe that the discovery of the Venusian phosphine and the analysis that is presented in this work can form the basis of a template approach that should be applied to any biosignature gas detection to determine if it is a 'false positive', i.e. a gas that could be produced by abiotic processes. We note that the step of assessing of false positive scenarios for any biosignature gas is highly planet-specific. The task of replicating our approach here with other, less well-characterized worlds will not be easy, but will be essential for the attribution of any gas to a biological origin.

6. Conclusions

(Greaves *et al.* 2020) have reported the candidate spectral signature of phosphine at altitudes >~57 km in the clouds of Venus, corresponding to an abundance of tens of ppb. It was previously predicted that any detectable abundance of PH₃ in the atmosphere of a rocky planet would be an indicator of biological activity (Sousa-Silva *et al.* 2020). In this paper we

show in detail that no abiotic mechanism based on our current understanding of Venus can explain the presence of ~20 ppb phosphine in Venus' clouds. If the detection is correct, then this means that our current understanding of Venus is significantly incomplete.

If phosphine is not a biological product, then it must be produced by planetary geo- or atmospheric chemistry. In either case our understanding, not only of Venus but of all terrestrial planets and exoplanets, needs a major paradigm shift. Because the source of phosphine is not known, we call for further aggressive observations of Venus and its atmosphere, laboratory studies of phosphorous chemistry in the context of the Venusian environment and the development of Venus space missions to study its atmosphere and search for signs of life.

7. Acknowledgements

We thank Joanna Petkowska-Hankel for the translation of the original Russian Vega and Venera papers and the preparation of Figure 1. We thank Carver J. Bierson and Xi Zhang for insightful discussions about the atmosphere of Venus, and for sharing a preprint of their article and the vertical radical profiles derived therein. We are grateful to Bob and Anna Damms for Russian translations. We thank the Heising-Simons Foundation and the Change Happens Foundation for funding. SR acknowledges the funding from the Simons Foundation (495062). Clara Sousa-Silva acknowledges the 51 Pegasi b Fellowship and the Heising-Simons Foundation.

8. References

- Ardaseva A., Rimmer P. B., Waldmann I., Rocchetto M., Yurchenko S. N., Helling C., and Tennyson J. (2017) Lightning chemistry on Earth-like exoplanets. *Monthly Notices of the Royal Astronomical Society*, 470: 187-196.
- Bains W., Petkowski J. J., Sousa-Silva C., and Seager S. (2019a) New environmental model for thermodynamic ecology of biological phosphine production. *Science of The Total Environment*, 658: 521-536.
- Bains W., Petkowski J. J., Sousa-Silva C., and Seager S. (2019b) Trivalent Phosphorus and Phosphines as Components of Biochemistry in Anoxic Environments. *Astrobiology*, 19: 885-902.
- Baker-Austin C., and Dopson M. (2007) Life in acid: pH homeostasis in acidophiles. *Trends in Microbiology*, 15: 165-171.
- Baross J., Benner S. A., Cody G. D., Copley S. D., Pace N. R., Scott J. H., Shapiro R., Sogin M. L., Stein J. L., Summons R. and others. (2007) The limits of organic life in planetary systems. National Academies Press.
- Beinert H., Holm R. H., and Münck E. (1997) Iron-Sulfur Clusters: Nature's Modular, Multipurpose Structures. *Science*, 277: 653.
- Benner S. A., Bell E. A., Biondi E., Brassler R., Carell T., Kim H.-J., Mojzsis S. J., Omran A., Pasek M. A., and Trail D. (2019) When did Life Likely Emerge on Earth in an RNA-First Process? *arXiv preprint arXiv:1908.11327*.
- Bierson C. J., and Zhang X. (2019) Chemical cycling in the Venusian atmosphere: A full photochemical model from the surface to 110 km. *Journal of Geophysical Research: Planets*, e2019JE006159.

- Bregman J. D., Lester D. F., and Rank D. M. (1975) Observation of the nu-squared band of PH₃ in the atmosphere of Saturn. *Astrophysical Journal*, 202: L55-L56.
- Britvin S. N., Murashko M. N., Vapnik Y., Polekhovskiy Y. S., Krivovichev S. V., Vereshchagin O. S., Vlasenko N. S., Shilovskikh V. V., and Zaitsev A. N. (2019) Zuktamrurite, FeP₂, a new mineral, the phosphide analogue of löllingite, FeAs₂. *Physics and Chemistry of Minerals*, 46: 361-369.
- Brugger J., Feulner G., and Petri S. (2017) Baby, it's cold outside: climate model simulations of the effects of the asteroid impact at the end of the Cretaceous. *Geophysical Research Letters*, 44: 419-427.
- Buseck P. R. (1969) Phosphide from meteorites: barringerite, a new iron-nickel mineral. *Science*, 165: 169-171.
- Byrne P. K., Ghail R. C., Sengör A. M. C., Klimczak C., Hahn R. M., James P. B., and Solomon S. C. (2018) The Lithosphere of Venus Has Been Broken and, in Places, Mobile.
- Carrillo-Sánchez J. D., Bones D. L., Douglas K. M., Flynn G. J., Wirick S., Fegley B., Araki T., Kaulich B., and Plane J. M. C. (2020) Injection of meteoric phosphorus into planetary atmospheres. *Planetary and Space Science*: 104926.
- Catling D. C., Krissansen-Totton J., Kiang N. Y., Crisp D., Robinson T. D., DasSarma S., Rushby A. J., Del Genio A., Bains W., and Domagal-Goldman S. (2018) Exoplanet biosignatures: a framework for their assessment. *Astrobiology*, 18: 709-738.
- Cockell C. S. (1999) Life on venus. *Planetary and Space Science*, 47: 1487-1501.
- Emiliani C. (1992) Planet Earth: Cosmology, Geology, and the Evolution of Life and Environment. Cambridge University Press.
- Esposito L. W., Knollenberg R. G., Marov M. Y. A., Toon O. B., and Turco R. R. (1983) 16. The Clouds and Hazes of Venus. *Venus*: 484.
- Fegley B. (1997) Why Pyrite Is Unstable on the Surface of Venus. *Icarus*, 128: 474-479.
- Fletcher L. N., Orton G. S., Teanby N. A., and Irwin P. G. J. (2009) Phosphine on Jupiter and Saturn from Cassini/CIRS. *Icarus*, 202: 543-564.
- Frost B. R. (1991) Introduction to oxygen fugacity and its petrologic significance. In: *Reviews in mineralogy vol 25. Oxide minerals: petrologic and magnetic significance*. edited by DH Lindsleys, Mineralogical Society of America, Washington, DC, USA.
- Gailliot M. P. (1980) "Petrified Lightning" A Discussion of Sand Fulgurites. *Rocks & Minerals*, 55: 13-17.
- Gassmann G., and Glindemann D. (1993) Phosphane (PH₃) in the Biosphere. *Angewandte Chemie International Edition in English*, 32: 761-763.
- Gassmann G., Van Beusekom J. E. E., and Glindemann D. (1996) Offshore atmospheric phosphine. *Naturwissenschaften*, 83: 129-131.
- Geist V., Wagner G., Nolze G., and Moretzki O. (2005) Investigations of the meteoritic mineral (Fe,Ni)₃P. *Crystal Research and Technology*, 40: 52-64.
- Ghail R., Wilson C. F., and Widemann T. (2016) Envision M5 venus orbiter proposal: Opportunities and challenges. AAS/Division for Planetary Sciences Meeting Abstracts# 48.
- Glindemann D., de Graaf R. M., and Schwartz A. W. (1999) Chemical Reduction of Phosphate on the Primitive Earth. *Origins of life and evolution of the biosphere*, 29: 555-561.
- Glindemann D., Edwards M., and Kusch P. (2003) Phosphine gas in the upper troposphere. *Atmospheric Environment*, 37: 2429-2433.
- Glindemann D., Edwards M., Liu J.-a., and Kusch P. (2005a) Phosphine in soils, sludges, biogases and atmospheric implications—a review. *Ecological Engineering*, 24: 457-463.

- Glindemann D., Edwards M., and Morgenstern P. (2005b) Phosphine from Rocks: Mechanically Driven Phosphate Reduction? *Environmental Science & Technology*, 39: 8295-8299.
- Glindemann D., Edwards M., and Schrems O. (2004) Phosphine and methylphosphine production by simulated lightning—a study for the volatile phosphorus cycle and cloud formation in the earth atmosphere. *Atmospheric Environment*, 38: 6867-6874.
- Glindemann D., Stottmeister U., and Bergmann A. (1996) Free phosphine from the anaerobic biosphere. *Environmental Science and Pollution Research*, 3: 17-19.
- Glover J. E. (1979) Formation and distribution of sand fulgurites. *Australian Geographer*, 14: 172-175.
- Gokhale S. D., Jolly W. L., Thomas S., and Britton D. (1967) Phosphine. In: *Inorganic Syntheses*. edited by SY Tyrees, McGraw Hill, pp 56-58
- Greaves J. S., Richards A. M. S., Bains W., Rimmer P. B., Sagawa H., Clements D. L., Seager S., Petkowski J. J., Sousa-Silva C., Ranjan S. and others. (2020) Phosphine Gas in the Cloud Decks of Venus. *Nature Astronomy*, in press.
- Grinspoon D. H. (1997) Venus revealed: a new look below the clouds of our mysterious twin planet.
- Grinspoon D. H., and Bullock M. A. (2007) Astrobiology and Venus exploration. *Geophysical Monograph - American Geophysical Union*, 176: 191.
- Gruchola S., Galli A., Vorbürger A., and Wurz P. (2019) The upper atmosphere of Venus: Model predictions for mass spectrometry measurements. *Planetary and space science*, 170: 29-41.
- Gülcher A. J. P., Gerya T. V., Montési L. G. J., and Munch J. (2020) Corona structures driven by plume–lithosphere interactions and evidence for ongoing plume activity on Venus. *Nature Geoscience*: 1-8.
- Haus R., Kappel D., Tellmann S., Arnold G., Piccioni G., Drossart P., and Häusler B. (2016) Radiative energy balance of Venus based on improved models of the middle and lower atmosphere. *Icarus*, 272: 178-205.
- Holland H. D. (1984) The chemical evolution of the atmosphere and oceans. Princeton University Press.
- Horikoshi K. (2016) Alkaliphiles. In: *Extremophiles: Where It All Began*, Springer Japan, Tokyo, pp 53-78.
- Ivanov M. A., and Head J. W. (2011) Global geological map of Venus. *Planetary and Space Science*, 59: 1559-1600.
- Japel S., Prewitt C., Boctor N., and Veblen D. (2002) Iron-nickel phosphides at high pressures and temperatures. AGU Fall Meeting Abstracts.
- Jenkins R. O., Morris T. A., Craig P. J., Ritchie A. W., and Ostah N. (2000) Phosphine generation by mixed-and mono-septic-cultures of anaerobic bacteria. *Science of the Total Environment*, 250: 73-81.
- Karner J., Papike J., and Shearer C. (2004) Plagioclase from planetary basalts: Chemical signatures that reflect planetary volatile budgets, oxygen fugacity, and styles of igneous differentiation. *American Mineralogist*, 89: 1101-1109.
- Kasting J. F. (1990) Bolide impacts and the oxidation state of carbon in the Earth's early atmosphere. *Origins of Life and Evolution of the Biosphere*, 20: 199-231.
- Krasnopolsky V. A. (2007) Chemical kinetic model for the lower atmosphere of Venus. *Icarus*, 191: 25-37.
- Krasnopolsky V. A. (2010) Venus night airglow: Ground-based detection of OH, observations of O₂ emissions, and photochemical model. *Icarus*, 207: 17-27.
- Krasnopolsky V. A. (2012) A photochemical model for the Venus atmosphere at 47–112 km. *Icarus*, 218: 230-246.

- Krasnopolsky V. A. (2013) S3 and S4 abundances and improved chemical kinetic model for the lower atmosphere of Venus. *Icarus*, 225: 570-580.
- Kreslavsky M. A., Ivanov M. A., and Head J. W. (2015) The resurfacing history of Venus: Constraints from buffered crater densities. *Icarus*, 250: 438-450.
- Krissansen-Totton J., Bergsman D. S., and Catling D. C. (2016) On detecting biospheres from chemical thermodynamic disequilibrium in planetary atmospheres. *Astrobiology*, 16: 39-67.
- Larson H. P., Treffers R. R., and Fink U. (1977) Phosphine in Jupiter's atmosphere-The evidence from high-altitude observations at 5 micrometers. *The Astrophysical Journal*, 211: 972-979.
- Lee G., Polidan R. S., and Ross F. (2015) Venus Atmospheric Maneuverable Platform (VAMP)-A Low Cost Venus Exploration Concept. AGU Fall Meeting Abstracts.
- Lee Y. J., Jessup K.-L., Perez-Hoyos S., Titov D. V., Lebonnois S., Peralta J., Horinouchi T., Imamura T., Limaye S., and Marcq E. (2019) Long-term Variations of Venus's 365 nm Albedo Observed by Venus Express, Akatsuki, MESSENGER, and the Hubble Space Telescope. *The Astronomical Journal*, 158: 126.
- Limaye S. S., Mogul R., Smith D. J., Ansari A. H., Słowik G. P., and Vaishampayan P. (2018) Venus' Spectral Signatures and the Potential for Life in the Clouds. *Astrobiology*, 18: 1181-1198.
- Lovelock J. E. (1975) Thermodynamics and the recognition of alien biospheres. *Proceedings of the Royal Society of London. Series B. Biological Sciences*, 189: 167-181.
- Ma C., Beckett J. R., and Rossman G. R. (2014) Monipite, MoNiP, a new phosphide mineral in a Ca-Al-rich inclusion from the Allende meteorite. *American Mineralogist*, 99: 198-205.
- Mancinelli R. L., and McKay C. P. (1988) The evolution of nitrogen cycling. *Origins of Life and Evolution of the Biosphere*, 18: 311-325.
- Marcq E., Lea Jessup K., Baggio L., Encrenaz T., Joo Lee Y., Montmessin F., Belyaev D., Korablev O., and Bertaux J.-L. (2019) Climatology of SO₂ and UV absorber at Venus' cloud top from SPICAV-UV nadir dataset. *Icarus*.
- Marcq E., Mills F. P., Parkinson C. D., and Vandaele A. C. (2018) Composition and chemistry of the neutral atmosphere of Venus. *Space Science Reviews*, 214: 10.
- Mikhail S., and Heap M. J. (2017) Hot climate inhibits volcanism on Venus: Constraints from rock deformation experiments and argon isotope geochemistry. *Physics of the Earth and Planetary Interiors*, 268: 18-34.
- Morowitz H., and Sagan C. (1967) Life in the Clouds of Venus? *Nature*, 215: 1259.
- Noll K. S., and Marley M. S. (1997) Detectability of CO, PH₃, AsH₃, and GeH₄ in the atmosphere of GL 229B. In: *ASP Conference Series Planets Beyond the Solar System and the Next Generation of Space Missions*.
- Novelli P. C., Lang P. M., Masarie K. A., Hurst D. F., Myers R., and Elkins J. W. (1999) Molecular hydrogen in the troposphere: Global distribution and budget. *Journal of Geophysical Research: Atmospheres*, 104: 30427-30444.
- Nunoura T., Nishizawa M., Hirai M., Shimamura S., Harnvoravongchai P., Koide O., Morono Y., Fukui T., Inagaki F., and Miyazaki J. (2018) Microbial diversity in sediments from the bottom of the Challenger Deep, the Mariana Trench. *Microbes and environments*: ME17194.
- Oschlisniok J., Häusler B., Pätzold M., Tyler G. L., Bird M. K., Tellmann S., Remus S., and Andert T. (2012) Microwave absorptivity by sulfuric acid in the Venus atmosphere: First results from the Venus Express Radio Science experiment VeRa. *Icarus*, 221: 940-948.

- Pasek M., and Block K. (2009) Lightning-induced reduction of phosphorus oxidation state. *Nature Geoscience*, 2: 553.
- Pasek M., Omran A., Lang C., Gull M., Abbatiello J., Feng T., and Garong L. A.-L., Heather (2020) Serpentinization as a route to liberating phosphorus on habitable worlds. *Preprint*.
- Pasek M. A., and Lauretta D. S. (2005) Aqueous Corrosion of Phosphide Minerals from Iron Meteorites: A Highly Reactive Source of Prebiotic Phosphorus on the Surface of the Early Earth. *Astrobiology*, 5: 515-535.
- Pasek M. A., Sampson J. M., and Atlas Z. (2014) Redox chemistry in the phosphorus biogeochemical cycle. *Proceedings of the National Academy of Sciences*, 111: 15468-15473.
- Pavlov A. K., Shelegedin V. N., Vdovina M. A., and Pavlov A. A. (2010) Growth of microorganisms in martian-like shallow subsurface conditions: laboratory modelling. *International Journal of Astrobiology*, 9: 51-58.
- Pech H., Vazquez M. G., Van Buren J., Foster K. L., Shi L., Salmassi T. M., Ivey M. M., and Pasek M. A. (2011) Elucidating the Redox Cycle of Environmental Phosphorus Using Ion Chromatography. *Journal of Chromatographic Science*, 49: 573-581.
- Petty J. J. (1936) The origin and occurrence of fulgurites in the Atlantic coastal plain. *American Journal of Science*, 31: 1-18.
- Peucker-Ehrenbrink B. (1996) Accretion of extraterrestrial matter during the last 80 million years and its effect on the marine osmium isotope record. *Geochimica et Cosmochimica Acta*, 60: 3187-3196.
- Pratesi G., Bindi L., and Moggi-Cecchi V. (2006) Icosahedral coordination of phosphorus in the crystal structure of melliniite, a new phosphide mineral from the Northwest Africa 1054 acapulcoite. *American Mineralogist*, 91: 451-454.
- Pye K. (1982) SEM observations on some sand fulgurites from northern Australia. *Journal of Sedimentary Research*, 52: 991-998.
- Rakov V. A., and Uman M. A. (2003) Lightning: physics and effects. Cambridge University Press.
- Ranjan S., Schwieterman E. W., Harman C., Fateev A., Sousa-Silva C., Seager S., and Hu R. (2020) Photochemistry of Anoxic Abiotic Habitable Planet Atmospheres: Impact of New H₂O Cross Sections. *The Astrophysical Journal*, 896: 148.
- Renne P. R., and Basu A. R. (1991) Rapid eruption of the Siberian Traps flood basalts at the Permo-Triassic boundary. *Science*, 253: 176-179.
- Rimmer P. B., and Helling C. (2016) A chemical kinetics network for lightning and life in planetary atmospheres. *The Astrophysical Journal Supplement Series*, 224: 9.
- Rimmer P. B., and Rugheimer S. (2019) Hydrogen cyanide in nitrogen-rich atmospheres of rocky exoplanets. *Icarus*, 329: 124-131.
- Rock P. A. (1969) Chemical thermodynamics: principles and applications. The Macmillan Company, London, UK.
- Rutishauser B. V., and Bachofen R. (1999) Phosphine formation from sewage sludge cultures. *Anaerobe*, 5: 525-531.
- Sandor B. J., and Clancy R. T. (2018) First measurements of ClO in the Venus atmosphere—altitude dependence and temporal variation. *Icarus*, 313: 15-24.
- Saunoy M., Bousquet P., Poulter B., Peregon A., Ciais P., Canadell J. G., Dlugokencky E. J., Etiope G., Bastviken D., and Houweling S. (2016) The global methane budget 2000–2012. *Earth System Science Data*, 8: 697-751.
- Schaefer L., and Fegley Jr B. (2004) Heavy metal frost on Venus. *Icarus*, 168: 215-219.

- Schulze-Makuch D., Grinspoon D. H., Abbas O., Irwin L. N., and Bullock M. A. (2004) A sulfur-based survival strategy for putative phototrophic life in the Venusian atmosphere. *Astrobiology*, 4: 11-18.
- Schulze-Makuch D., and Irwin L. N. (2002) Reassessing the possibility of life on Venus: proposal for an astrobiology mission. *Astrobiology*, 2: 197-202.
- Schulze-Makuch D., and Irwin L. N. (2006) The prospect of alien life in exotic forms on other worlds. *Naturwissenschaften*, 93: 155-172.
- Schwieterman E. W., Kiang N. Y., Parenteau M. N., Harman C. E., DasSarma S., Fisher T. M., Arney G. N., Hartnett H. E., Reinhard C. T., Olson S. L. and others. (2018) Exoplanet Biosignatures: A Review of Remotely Detectable Signs of Life. *Astrobiology*, 18: 663-708.
- Seager S., and Bains W. (2015) The search for signs of life on exoplanets at the interface of chemistry and planetary science. *Sci Adv*, 1: e1500047.
- Seager S., Bains W., and Petkowski J. J. (2016) Toward a List of Molecules as Potential Biosignature Gases for the Search for Life on Exoplanets and Applications to Terrestrial Biochemistry. *Astrobiology*, 16: 465-485.
- Seager S., Petkowski J. J., Gao P., Bains W., Bryan N. C., Ranjan S., and Greaves J. (2021) The Venusian Lower Atmosphere Haze: A Depot for Desiccated Life Particles for the Persistence of the Hypothetical Venusian Aerial Biosphere *Astrobiology*, 21.
- Seager S., Schrenk M., and Bains W. (2012) An Astrophysical View of Earth-Based Metabolic Biosignature Gases. *Astrobiology*, 12: 61-82.
- Sen G. (2001) Generation of Deccan trap magmas. *Journal of Earth System Science*, 110: 409-431.
- Service R. F. (2019) Seeing the dawn. *Science*, 363: 116.
- Shalygin E. V., Markiewicz W. J., Basilevsky A. T., Titov D. V., Ignatiev N. I., and Head J. W. (2015) Active volcanism on Venus in the Ganiki Chasma rift zone. *Geophysical Research Letters*, 42: 4762-4769.
- Smrekar S. E., Stofan E. R., and Mueller N. (2014) Venus: surface and interior. In: *Encyclopedia of the Solar System*, Elsevier, pp 323-341.
- Sousa-Silva C., Al-Refaie A. F., Tennyson J., and Yurchenko S. N. (2014) ExoMol line lists–VII. The rotation–vibration spectrum of phosphine up to 1500 K. *Monthly Notices of the Royal Astronomical Society*, 446: 2337-2347.
- Sousa-Silva C., Petkowski J. J., and Seager S. (2019) Molecular simulations for the spectroscopic detection of atmospheric gases. *Physical Chemistry Chemical Physics*, 21: 18970-18987.
- Sousa-Silva C., Seager S., Ranjan S., Petkowski J. J., Hu R., Zhan Z., and Bains W. (2020) Phosphine as a Biosignature Gas in Exoplanet Atmospheres. *Astrobiology*, 20: 235-268.
- Sousa-Silva C., Yurchenko S. N., and Tennyson J. (2013) A computed room temperature line list for phosphine. *Journal of Molecular Spectroscopy*, 288: 28-37.
- Tanaka T., Kawasaki K., Daimon S., Kitagawa W., Yamamoto K., Tamaki H., Tanaka M., Nakatsu C. H., and Kamagata Y. (2014) A hidden pitfall in the preparation of agar media undermines microorganism cultivability. *Applied and environmental microbiology*, 80: 7659-7666.
- Tarrago G., Lacombe N., Lévy A., Guelachvili G., Bézard B., and Drossart P. (1992) Phosphine spectrum at 4–5 μm : Analysis and line-by-line simulation of $2v_2$, $v_2 + v_4$, $2v_4$, v_1 , and v_3 bands. *Journal of Molecular Spectroscopy*, 154: 30-42.
- Taylor F. W., and Hunten D. M. (2014) Venus: Atmosphere. In: *Encyclopedia of the Solar System*, Elsevier, pp 305-322.

- Taylor F. W., Svedhem H., and Head J. W. (2018) Venus: the atmosphere, climate, surface, interior and near-space environment of an Earth-like planet. *Space Science Reviews*, 214: 35.
- Tenenbaum E. D., Woolf N. J., and Ziurys L. M. (2007) Identification of Phosphorus Monoxide (X 2Pir) in VY Canis Majoris: Detection of the First PO Bond in Space. *The Astrophysical Journal Letters*, 666: L29.
- Titov D. V., Ignatiev N. I., McGouldrick K., Wilquet V., and Wilson C. F. (2018) Clouds and hazes of Venus. *Space Sci. Rec.*, 214: 126 doi.org/10.1007/s11214-018-0552-z.
- Toon O. B., Bardeen C., and Garcia R. (2016) Designing global climate and atmospheric chemistry simulations for 1 and 10 km diameter asteroid impacts using the properties of ejecta from the K-Pg impact. *Atmospheric Chemistry and Physics*, 16: 13185-13212.
- Treiman A., Harrington E., and Sharpton V. (2016) Venus' radar-bright highlands: Different signatures and materials on Ovda Regio and on Maxwell Montes. *Icarus*, 280: 172-182.
- Treiman A. H. (2017) Recent Volcanism on Venus: A Possible Volcanic Plume Deposit on Nissaba Corona, Eistla Regio.
- Turner A. M., Bergantini A., Abplanalp M. J., Zhu C., Góbi S., Sun B.-J., Chao K.-H., Chang A. H. H., Meinert C., and Kaiser R. I. (2018) An interstellar synthesis of phosphorus oxoacids. *Nature communications*, 9: 3851.
- Twarowski A. (1993) The influence of phosphorus oxides and acids on the rate of H + OH recombination. *Combustion and Flame*, 94: 91-107.
- Twarowski A. (1995) Reduction of a phosphorus oxide and acid reaction set. *Combustion and Flame*, 102: 41-54.
- Twarowski A. (1996) The temperature dependence of H + OH recombination in phosphorus oxide containing post-combustion gases. *Combustion and Flame*, 105: 407-413.
- Ulf-Møller F. (1985) Solidification history of the Kitdlit Lens: immiscible metal and sulphide liquids from a basaltic dyke on Disko, central West Greenland. *Journal of Petrology*, 26: 64-91.
- van den Berg M. L., Falkner P., Atzei A. C., and Peacock A. (2006) Venus microsat explorer programme, an ESA technology reference study. *Acta Astronautica*, 59: 593-597.
- Visscher C., Lodders K., and Fegley B. (2006) Atmospheric Chemistry in Giant Planets, Brown Dwarfs, and Low-Mass Dwarf Stars. II. Sulfur and Phosphorus. *The Astrophysical Journal*, 648: 1181.
- Walker S. I., Bains W., Cronin L., DasSarma S., Danielache S., Domagal-Goldman S., Kacar B., Kiang N. Y., Lenardic A., Reinhard C. T. and others. (2018) Exoplanet Biosignatures: Future Directions. *Astrobiology*, 18: 779-824.
- Weisstein E. W., and Serabyn E. (1996) Submillimeter line search in Jupiter and Saturn. *Icarus*, 123: 23-36.
- Wordsworth R. D. (2016) Atmospheric nitrogen evolution on Earth and Venus. *Earth and Planetary Science Letters*, 447: 103-111.
- Wu Z., Wan H., Xu J., Lu B., Lu Y., Eckhardt A. K., Schreiner P. R., Xie C., Guo H., and Zeng X. (2018) The near-UV absorber OSSO and its isomers. *Chemical Communications*, 54: 4517-4520.
- Zasova L., Ignatiev N., Korablev O., Eismont N., Gerasimov M., Khatuntsev I., Jessup K. L., and Economou T. (2017) Venera-D: Expanding our Horizon of Terrestrial Planet Climate and Geology through the Comprehensive Exploration of Venus.
- Zhang X., Liang M. C., Mills F. P., Belyaev D. A., and Yung Y. L. (2012) Sulfur chemistry in the middle atmosphere of Venus. *Icarus*, 217: 714-739.

Zolensky M., Gounelle M., Mikouchi T., Ohsumi K., Le L., Hagiya K., and Tachikawa O.
(2008) Andreyivanovite: A second new phosphide from the Kaidun meteorite.
American Mineralogist, 93: 1295-1299.

Phosphine on Venus Cannot be Explained by Conventional Processes: Supplementary Information

1. Supplementary Approach and Methods:

1. 1. Methods Used in Photochemistry and Kinetics Analysis

1. 1. 1. Photochemical Model of the Venusian Atmosphere

To estimate the vertical radical concentration profiles relevant to PH₃ photochemistry, we use the photochemical model of the Venusian atmosphere previously reported in (Greaves *et al.* 2020). This photochemical model of Venus's atmosphere accounts for photochemistry, thermochemistry, and chemical diffusion.

1. 1. 1. 1. Modelling Framework

To solve for a self-consistent set of atmospheric constituent concentrations we employ a 1D photochemistry-diffusion code, called ARGO (Rimmer and Helling 2016), which solves the continuity-transport equation. ARGO is a Lagrangian photochemistry/diffusion code that follows a single parcel as it moves from the bottom to the top of the atmosphere, determined by a prescribed temperature profile. The temperature, pressure, and actinic ultraviolet flux are updated at each height in the atmosphere. In this reference frame, bulk diffusion terms are accounted for by time-dependence of the chemical production, P_i (cm³ s⁻¹), and loss, L_i (s⁻¹) rates. Below the homopause, molecular diffusion can be neglected, and the equation to be solved is:

$$\frac{\partial n_i}{\partial t} = P_i[t(z, v_z)] - L_i[t(z, v_z)]n_i, \quad (1)$$

where n_i (cm⁻³) is the number density of species i , t (s) is time, z [cm] is atmospheric height above the surface, and $v_z = K_{zz}/H_0$ (cm/s) is the effective vertical velocity due to Eddy diffusion, from the Eddy diffusion coefficient K_{zz} (cm² s⁻¹). Molecular diffusion into and out of the parcel is accounted for by production and loss 'reactions' that remove specific species as the parcel moves upwards, adding them back as the parcel moves downwards, at a rate determined by molecular diffusion (Rimmer and Helling 2016; Rimmer and Helling 2019). The mixing ratios are saved at a given height before the parcel proceeds to the next height, constructing atmospheric profiles for all species included in the accompanying chemical network.

1. 1. 1. 2. Photochemistry

Photochemistry is solved for the depth-dependent actinic flux in the standard way using a 2-stream δ -Eddington approximation (Toon *et al.* 1989), using the atmospheric profiles, and then transport a parcel through the atmosphere again with these updated depth-dependent actinic fluxes. Each time this is accomplished is a single global iteration for the model, and the model is run until every major and significant minor species (any with $n_i > 10^5$ cm⁻³) agrees between

two global iterations to within 1%. We modify the standard actinic flux calculation in two ways. First, we ignore the absorption of SO₂ for the first three global iterations, and include it afterwards. This seems to help the model to converge. In addition, we have included a ‘mysterious absorber’ with properties (Krasnopolsky 2012):

$$\frac{d\tau}{dz} = 0.056/km e^{-(z-67 \text{ km})/3 \text{ km}} e^{-(\lambda-3600 \text{ \AA})/1000 \text{ \AA}}, z > 67 \text{ km}; \quad (2)$$

$$\frac{d\tau}{dz} = 0.056/km e^{-(\lambda-3600 \text{ \AA})/1000 \text{ \AA}}, 58 \text{ km} \leq z \leq 67 \text{ km}; \quad (3)$$

$$\frac{d\tau}{dz} = 0, z \leq 58 \text{ km}; \quad (4)$$

1. 1. 1. 3. Photochemical Network

Chemical networks for Venus are limited and prior work often specializes on one part of the atmosphere over another. A variety of sources were therefore used to assemble a whole atmosphere photochemical network. The chemical network is based on STAND2019 (Rimmer and Rugheimer 2019), which includes H/C/N/O species. (Greaves *et al.* 2020) extended this network by adding a limited S/Cl/P network relevant for the Venusian atmosphere. This network is a copy of the low altitude atmospheric network of Krasnopolsky (Krasnopolsky 2007; Krasnopolsky 2013) and the middle atmosphere network of Zhang (Zhang *et al.* 2012). The network is further modified by removing any reverse reactions explicitly included in (Krasnopolsky 2007; Krasnopolsky 2013), and instead by self-consistently calculating reverse reactions throughout the atmosphere.

For our chemical network, we use STAND2019 (Rimmer and Rugheimer 2019), which includes H/C/N/O species. We have also added a limited S/Cl/P network relevant for the Venusian atmosphere by copying the low atmospheric network of Krasnopolsky (Krasnopolsky 2007; Krasnopolsky 2013) and the middle atmosphere network of Zhang (Zhang *et al.* 2012). For network reactions that do not involve PH₃, we use the networks of Krasnopolsky (Krasnopolsky 2007) and Zhang (Zhang *et al.* 2012), modified as follows. The network of Krasnopolsky include specific reverse reaction rates. We excluded these, and instead used the forward reactions and the thermochemical constants from Burcat (Burcat and Ruscic 2005) for calculating the reverse reactions for those species already included in STAND2019, as well as reactions that include the species S, S₂, S₃, S₄, S₅, S₆, S₇, S₈, HS, SO, ClO, ClS, Cl₂, H₂S, OCS, SO₂, SO₃, S₂O, HOCl, ClCO, Cl₂S, Cl₂S₂, HSO₃, H₂SO₄ as described by (Rimmer and Helling 2016; Visscher and Moses 2011). We added reverse reactions for the reactions from the (Zhang *et al.* 2012) middle atmosphere network wherever possible. We supplemented this network with the following reactions:

R1: $\text{H} + \text{PH}_3 \rightarrow \text{H}_2 + \text{PH}_2$: Arrhenius parameters used were $A=7.22 \times 10^{-11} \text{ cm}^3 \text{ s}^{-1}$ and $E=7.37 \text{ kJ mol}^{-1}$ (Arthur and Cooper 1997). These authors state that these parameters are valid over 200-

500 K; we confirm that they are consistent with the theoretical calculations of (Yu *et al.* 1999) at higher temperatures to within a factor of 2.

R2: $\text{OH} + \text{PH}_3 \rightarrow \text{H}_2\text{O} + \text{PH}_2$: Arrhenius parameters used were i.e. $A=2.71 \times 10^{-11} \text{ cm}^3 \text{ s}^{-1}$ and $E=1.29 \text{ kJ mol}^{-1}$, from (Fritz *et al.* 1982), based on measurements from 250-450 K.

R3: $\text{O} + \text{PH}_3 \rightarrow \text{H}_2\text{PO} + \text{H}$: Rate parameter used was $k = 4.75 \times 10^{-11} \text{ cm}^3 \text{ s}^{-1}$ (Nava and Stief 1989) based on measurement from 208-408 K, with value. The addition reaction probably dominates for $T < 1000 \text{ K}$; The abstraction reaction $\text{O} + \text{PH}_3 \rightarrow \text{OH} + \text{PH}_2$ should become significant above 1000 K. As temperatures never exceed 750 K in the Venusian atmosphere, the abstraction reaction will not be significant on Venus. H_2PO formed will be oxidized further to H_3PO_4 as a stable end product.

R4: $\text{Cl} + \text{PH}_3 \rightarrow \text{HCl} + \text{PH}_2$: Rate parameter used was $k = 2.4 \times 10^{-10} \text{ cm}^3 \text{ s}^{-1}$, from (Iyer *et al.* 1983). Iyer et al only study this reaction at 298 K; we are not aware of studies at any other temperature. We therefore adopt this reaction rate throughout the atmosphere, which will formally under-estimate the rate of destruction at higher temperatures.

The rate constant for thermolytic breakdown of PH_3 via $\text{PH}_3 + \text{M} \rightarrow \text{PH}_2 + \text{H} + \text{M}$ was calculated as described below.

We include the reverse reactions for these phosphine reactions using the same approach as above, using Burcat polynomials (Burcat and Ruscic 2005).

The reaction of N radical with PH_3 has not been observed; an upper limit for this reaction near Earth-ambient conditions is $4 \times 10^{-14} \text{ cm}^3 \text{ s}^{-1}$, which is 2-3 orders of magnitude lower than attack by O, OH, and H radicals (Hamilton and Murrells 1985). As N radicals are predicted to be present only at very low concentrations in the regions of the Venusian atmosphere relevant to this study ($< 80 \text{ km}$; (Krasnopolsky 2012)), we therefore neglect loss due to attack by N. Formally this will further under-estimate the PH_3 loss rate, but by a trivial amount.

We neglect the possibility that the products of PH_3 destruction can recombine to restore PH_3 , except for the reaction $\text{PH}_2 + \text{H} + \text{M} \rightarrow \text{PH}_3 + \text{M}$, which is included as the reverse reaction for thermolytic decay of PH_3 (see below). This formally overestimates PH_3 destruction rates. The products of PH_3 destruction are rare even in the H_2 -rich atmospheres of Jupiter and Saturn, and recombination correspondingly unlikely. In Venus' H-poor atmosphere the products will be even rarer, making the rate of recombination of phosphine from its breakdown products negligible (Sousa-Silva *et al.* 2020). This assumption can be tested experimentally by searching for PH_3 products (e.g. diphosphine (P_2H_4)) in the Venusian atmosphere.

We also include condensation of S_n species (Lyons 2008) and sulfuric acid H_2SO_4 (Kulmala and Laaksonen 1990), as functions of the vapor pressures (p_{vap} , bar) which are calculated as follows:

$$\log_{10} p_{\text{vap}} (\text{S}_2) = 7.024 - \frac{6091 \text{ K}}{T} \quad (5)$$

$$\log_{10} p_{\text{vap}} (\text{S}_3) = 6.343 - \frac{6202 \text{ K}}{T} \quad (6)$$

$$\log_{10} p_{\text{vap}} (\text{S}_4) = 6.003 - \frac{6048 \text{ K}}{T} \quad (7)$$

$$\log_{10} p_{\text{vap}} (\text{S}_5) = 5.061 - \frac{4715 \text{ K}}{T} \quad (8)$$

$$\log_{10} p_{\text{vap}} (\text{S}_6) = 4.804 - \frac{3814 \text{ K}}{T} \quad (9)$$

$$\log_{10} p_{\text{vap}} (\text{S}_7) = 5.213 - \frac{4114 \text{ K}}{T} \quad (10)$$

$$\log_{10} p_{\text{vap}} (\text{S}_8) = 4.188 - \frac{3269 \text{ K}}{T} \quad (11)$$

$$\log_{10} p_{\text{vap}} (\text{H}_2\text{SO}_4) = 4.4753 - \frac{3229 \text{ K}}{T+710920 \text{ K}} - \frac{3.1723 \times 10^6 \text{ K}^2}{T^2} + \frac{4.0832 \times 10^8 \text{ K}^3}{T^3} - \frac{2.0321 \times 10^{10} \text{ K}^4}{T^4} \quad (12)$$

SO_2 can be photochemically converted to H_2SO_4 and S_8 , which can condense and be removed to the clouds.

We add removal of SO_2 into the clouds in order to match the top boundary conditions from the lower atmosphere models (Krasnopolsky 2007) to the bottom boundary conditions for the middle atmosphere models. The former is orders of magnitude lower than the latter, implying strong depletion across the cloud layer (Zhang *et al.* 2012). Bierson *et al.* accomplished this by depleting SO_2 via oxidation to SO_3 and removal by reaction with H_2O to form sulfuric acid (Bierson and Zhang 2019). To achieve this Bierson *et al.* had to decrease K_{zz} within the cloud layer and fix H_2O to be equal to observed concentrations throughout the atmosphere, which implies an unknown source of H_2O in the clouds and yet undetermined chemical cycle that both provides sufficient H_2O reacting with SO_3 to deplete SO_2 by orders of magnitude and that maintains H_2O mixing ratios at more than an order of magnitude lower than SO_2 mixing ratios. We do not fix the H_2O concentrations, and so instead have depleted SO_2 by including rainout with a Henry's Law approximation modified as described by Sander (ref. (Sander 2015), their Section 2.7). Incorporating this loss term brings the SO_2 curve into better agreement with observation, and may instead be interpreted as approximating photochemical loss of SO_2 via a different mechanism or series of reactions.

1. 1. 1. 4. Thermolytic Decay of PH_3

The thermal decomposition of phosphine is important near the base of the atmosphere. Concentrations of radicals below the clouds of Venus are very uncertain, but even with the largest published predictions (Krasnopolsky 2007) for radical concentrations in the lower atmosphere of $\sim 1000 \text{ cm}^{-3}$, reaction of PH_3 with radicals will be extremely slow (order $>10^8$

seconds). In this environment, thermal decomposition dominates PH₃ destruction and therefore determines the lifetime of PH₃. The thermal decomposition of PH₃ has been considered theoretically (Cardelino *et al.* 2003). Theoretical values of k_{uni} (s⁻¹) and k_{∞} (s⁻¹) are given as (Cardelino *et al.* 2003):

$$k_{\text{uni}} = 3.55 \times 10^{14} \text{ s}^{-1} e^{-35644 \text{ K}/T} \quad (13)$$

$$k_{\infty} = 1.91 \times 10^{18} \text{ s}^{-1} e^{-40063 \text{ K}/T} \quad (14)$$

but no value for the rate constant at the low-pressure limit, k_0 (cm³ s⁻¹), is provided. This rate constant has to be determined to use the Lindemann expression to calculate the rate constant over a wide range of pressures:

$$k = \frac{k_{\infty}}{1 + k_{\infty}/(k_0[M])} \quad (15)$$

where [M] is the number density of the third body (in our case [M] = n , where n (cm⁻³) is the atmospheric number density). The rate constant at the low pressure limit can be estimated by considering that k_{uni} was calculated for 1300 bar and 900 K, so [M] = 1.07×10^{22} cm⁻³, and solving Equation (15) with $k = k_{\text{uni}}$. Doing so yields:

$$k_0 = 3.4 \times 10^{-8} \text{ cm}^3 \text{ s}^{-1} e^{-35644 \text{ K}/T} \quad (16)$$

An alternative way to estimate k_0 from k_{∞} is to perform a simple conversion of units, with $k_0 = kT/(1 \text{ bar}) k_{\infty}$, which gives:

$$k_0 = 2.6 \times 10^{-4} \text{ cm}^3 \text{ s}^{-1} \left(\frac{T}{300 \text{ K}} \right) e^{-40063 \text{ K}/T} \quad (17)$$

Finally, we can use the decomposition of NH₃ as an analogue of the decomposition of PH₃. The low-pressure thermal decomposition rate limit for NH₃ has been experimentally determined over a temperature range of 1740-3300 K (Davidson *et al.* 1990). We assume that the principle difference between the two gases is the activation energy for bond scission (i.e. the bond strength). The activation energy at the high pressure limit for PH₃ is of 40063 K (Cardelino *et al.* 2003), for NH₃ 48840 K (Cardelino *et al.* 2003). We assume this ratio is the same at the low pressure limit, where the measured activation energy for NH₃ is 39960 K (Davidson *et al.* 1990). We therefore find:

$$k_0 = 7.2 \times 10^{-9} \text{ cm}^3 \text{ s}^{-1} e^{-32778 \text{ K}/T} \quad (18)$$

The timescales for thermal decomposition derived from these rate constants, along with the timescale using only k_{∞} , are shown in (ref. (Greaves *et al.* 2020), their Figure S10). Since our first estimate, Equation (16), yields the longest timescale, and will therefore be most favorable for abiotic PH₃ scenarios, we use that value.

1. 1. 1. 5. UV Photolysis of Phosphine

PH₃ photolyzes via PH₃ + hv → PH₂ + H upon absorption of ≤ 230 nm UV (Kaye and Strobel 1984; Visconti 1981). We estimate the photolysis rate coefficient J_A by (Seager *et al.* 2013):

$$J_A = \int_{\lambda} q_{\lambda} I_{\lambda} e^{-\tau_{\lambda}} \sigma_{\lambda} d\lambda, \quad (19)$$

where I_{λ} is the solar intensity at the top of the atmosphere, τ_{λ} is the optical depth of the overlying atmosphere, σ_{λ} is the absorption cross-section of PH₃, and q_{λ} is the quantum yield of PH₃ photolysis. For I_{λ} , we use the solar instellation spectrum aggregated by (Hu *et al.* 2012) by concatenating the quiet-sun emission spectrum (from (Curdt *et al.* 2004); 110-119 nm) to the Air Mass Zero reference spectrum from the American Society for Testing and Materials (<http://irredc.nrel.gov/solar/spectra/am0/>) (>119.5 nm). We scale the insolation by cos(z)=0.5 to match the dayside mean cos(z) adopted by (Krasnopolsky 2012), by 0.5 to account for diurnal variation, and by 0.72⁻² to account for Venus's closer orbit to the Sun.

We take the absorption cross-sections of PH₃ from (Chen *et al.* 1991), reported at 295 K. We follow (Kaye and Strobel 1984) in taking the quantum yield of photolysis to be unity at wavelengths ≤ 230 nm.

In calculating τ_{λ} , we include absorption due to CO₂ and SO₂, following the insight of (Krasnopolsky 2006) that to first order every UV photon <218 nm is absorbed by one of these gases. For the absorption cross-sections of SO₂ and CO₂, we use the aggregation of (Ranjan and Sasselov 2017), who in these wavelength ranges draw primarily on (Huestis and Berkowitz 2010; Shemansky 1972), and (Manatt and Lane 1993). The UV profile of the Venusian atmosphere was modified to include the 'unknown UV absorber' with properties described by (Krasnopolsky 2007):

$$\frac{d\tau}{dz} = 0.056/km e^{-(z-67 \text{ km})/3 \text{ km}} e^{-(\lambda-3600 \text{ \AA})/1000 \text{ \AA}}, \quad z > 67 \text{ km}; \quad (20)$$

$$\frac{d\tau}{dz} = 0.056/km e^{-(\lambda-3600 \text{ \AA})/1000 \text{ \AA}}, \quad 58 \text{ km} \leq z \leq 67 \text{ km}; \quad (21)$$

$$\frac{d\tau}{dz} = 0, \quad z \leq 58 \text{ km}; \quad (22)$$

Our approach neglects scattering; this means UV radiation penetrates deeper into the atmosphere than we model here, meaning we overestimate photolysis rates. Even so, direct photolysis is not a dominant loss process for PH₃ in the Venusian atmosphere <100 km (Figure 2, in the main text).

1. 1. 1. 6. Model Input: Atmospheric Profile of Venus and Initial Boundary Conditions

We describe the details behind the selection of photochemical model inputs by (Greaves *et al.* 2020), and reproduce their atmospheric profile of Venus (Figure S1 and Figure S2). In short, we take fixed surface boundary conditions from (Krasnopolsky 2007) for the major atmospheric species, and with initial surface boundary conditions from (Krasnopolsky 2007) for minor species, radicals and atoms (these conditions are reproduced in Table S1). (Greaves *et al.* 2020) provide validation for this model by comparing with observed concentrations of CO, H₂O, HCl, H₂S, OCS, S₃, SO, SO₂ and PH₃.

Here and in (Greaves *et al.* 2020), we are comparing a 1D photochemistry model set up to approximate the global-average height-dependent chemistry of a three-dimensional and dynamic atmosphere. Measurements, on the other hand, often apply to particular latitudinal and longitudinal regions measured at a particular time. As such, the errors shown here estimate not only the error bars of individual measurements, but the variation between measurements taken at the same altitude, wherever possible.

(Krasnopolsky 2013) provides single measurements per height for S₃, and we use their error bars as variance. (Krasnopolsky 2013) also gives mixing ratios for CO and OCS, but provides no error bars, but rounds mixing ratios to the nearest multiple of 5, so an ± 5 error was applied to each datapoint. (Marcq *et al.* 2008) measure CO, CSO, H₂O and SO₂ mixing ratios at a variety of latitudes at a given altitude. The error bars were averaged for all data points, and the variance was estimated by taking the maximum datapoint plus this error, and the minimum datapoint minus this error. For the measurements of H₂O and HCl, we use the errors from (Bertaux *et al.* 2007) averaged over all datapoints within 10 km of the plotted datapoint. The observations and errors for HCl were plotted on a linear scale, and the 1- σ errors reach mixing ratios of zero in the upper atmosphere, which is why the error on log scale is so large. Finally, for the SO and SO₂ observations from (Belyaev *et al.* 2012), which show many dozens of datapoints at altitudes between 75 and ~100 km. Since the error bars were far smaller than the difference between datapoints at similar altitudes, the variance is estimated simply by using the maximum and minimum values for the mixing ratios within 10 km regions. The data and errors are shown in Table S2.

1. 1. 2. Photochemical Model Input: Atmospheric Profile of Venus

In modeling the Venusian atmosphere, we follow (Krasnopolsky 2007; Krasnopolsky 2012) in taking the temperature-pressure (TP) profile from the Venus International Reference Atmosphere (VIRA). Specifically, we use previously published TP profiles of (Seiff *et al.* 1985): for the deep atmosphere profile (0-32 km) and for the altitudes between 32-100 km, where we use the 45

degrees latitude profile. For the altitudes between 100-112 km we use the VIRA dayside profile from (Keating *et al.* 1985). Figure S1 shows the temperature-pressure profile adopted in this work. We similarly follow (Krasnopolsky 2007; Krasnopolsky 2012) in the Eddy diffusion profile, taking it to be constant at $2.2 \times 10^3 \text{ cm}^2 \text{ s}^{-1}$ for $z < 30 \text{ km}$, $1 \times 10^4 \text{ cm}^2 \text{ s}^{-1}$ for $z = 47\text{-}60 \text{ km}$, $1 \times 10^7 \text{ cm}^2 \text{ s}^{-1}$ for $z > 100 \text{ km}$, and connected exponentially at intermediate altitudes. Figure S2 shows the Eddy diffusion profile adopted in this work.

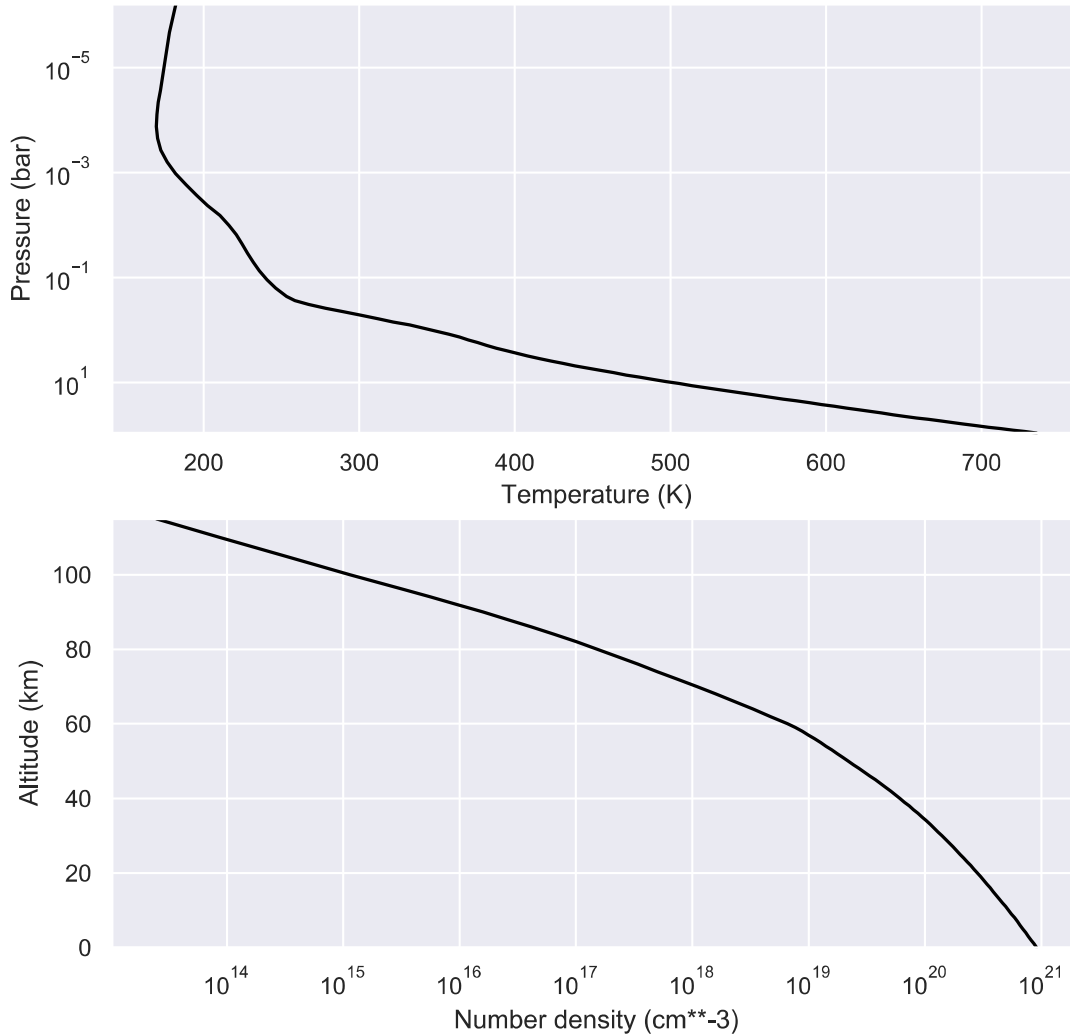


Fig. S1. Temperature-pressure profile used in photochemical modeling of the Venusian atmosphere, following (Krasnopolsky 2007; Krasnopolsky 2012). From (Greaves *et al.* 2020), their Fig. S7.

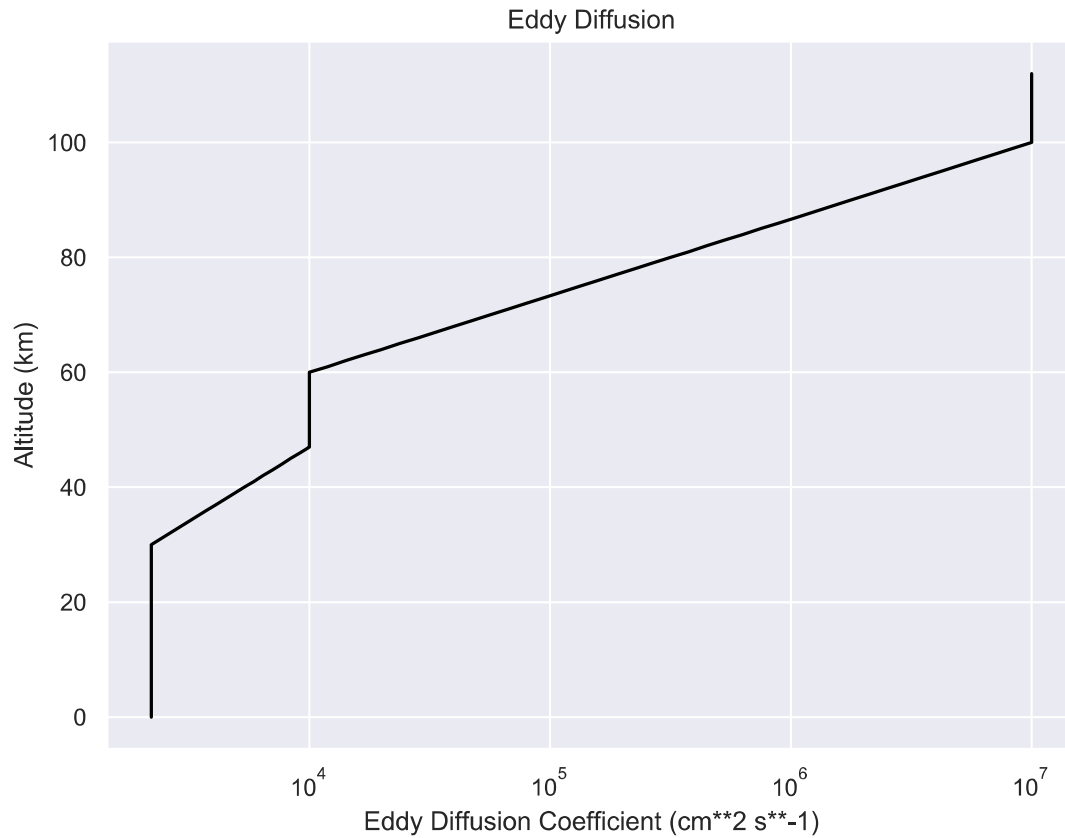


Fig. S2. Eddy diffusion profile used in the photochemical modelling of the Venusian atmosphere, following (Krasnopolsky 2007; Krasnopolsky 2012). From (Greaves *et al.* 2020), their Fig. S8.

1. 1. 3. Initial Chemical Boundary Conditions

We use the fixed surface boundary conditions, which are based on the surface abundances of (Krasnopolsky 2007) for the major atmospheric species, and with initial surface boundary conditions from (Krasnopolsky 2007) for minor species, radicals and atoms. The initial surface abundances for our model are shown in Table 1.

Species	Mixing Ratio
CO ₂	0.96
N ₂	0.03
SO ₂	1.5 x 10 ⁻⁴
H ₂ O	3.0 x 10 ⁻⁵
CO	2.0 x 10 ⁻⁵
OCS	5.0 x 10 ⁻⁶
S ₂	7.5 x 10 ⁻⁷

HCl	5.0×10^{-7}
S_n ($3 \leq n \leq 8$)	3.3×10^{-7}
NO	5.5×10^{-9}
H ₂	3.0×10^{-9}
H ₂ S	1.0×10^{-9}
SO	3.0×10^{-11}
ClSO ₂	3.0×10^{-11}
SO ₂ Cl ₂	1.0×10^{-11}
HS	8.0×10^{-13}
SNO	1.0×10^{-13}
SCI	6.7×10^{-15}
HSCI	2.8×10^{-15}
Cl ₂	1.0×10^{-16}
S	7.5×10^{-17}
H	7.3×10^{-19}
OH	7.3×10^{-19}

Table S1. Initial surface conditions for atmospheric chemistry. Table adapted from (Greaves *et al.* 2020), their Table S2.

We include a source of PH₃ in the clouds, with flux:

$$\Phi(z) = 0.5\Phi_0 \left[\tanh\left(\frac{z-45 \text{ km}}{2 \text{ km}}\right) \tanh\left(\frac{65 \text{ km}-z}{2 \text{ km}}\right) + 1 \right] \quad (23)$$

where $\Phi(z)$ ($\text{cm}^{-2} \text{ s}^{-1}$) is the PH₃ flux at height z (km), and $\Phi_0=10^7$ ($\text{cm}^{-2} \text{ s}^{-1}$) is assigned to reproduce a 10 ppb PH₃ concentration, which is the lower bound of the values inferred by (Greaves *et al.* 2020).

1. 1. 4. Photochemical Model Validation

Here we compare observations of CO, OCS, H₂O, SO₂, H₂S, HCl, S₃, SO, to model predictions (Figure S3 and Table S2). As shown in (Greaves *et al.* 2020), all species agree with observations to within an order of magnitude in concentration, within +/- 5 km, with the exception of H₂O and O₂. Photolysis of water is very efficient for our model, and depletion by reaction with SO₃ is significant, so that in our model predicted water vapor drops off rapidly above 70 km, leading to a discrepancy between observed H₂O and model H₂O of several orders of magnitude. This discrepancy is accompanied by higher concentrations of OH and O above 70 km, and so we probably underestimate the lifetime for phosphine above 70 km. However, the lifetime of phosphine at these heights is very short, on the order of days to seconds, for all published models of Venus's middle atmosphere (e.g. by Zhang (Zhang *et al.* 2012) and Bierson & Zhang (Bierson and Zhang 2019)). Our model also predicts too much O₂ in the middle atmosphere of Venus,

within an order of magnitude of the concentrations predicted by Zhang (Zhang *et al.* 2012) and Bierson & Zhang (Bierson and Zhang 2019).

We consider the possibility that our model contains an idiosyncrasy or error that leads to significant underestimates of PH₃ lifetime, and hence overestimates the difficulty of abiotic buildup. To assess this possibility, we repeated our calculations of PH₃ lifetime and required production rates using concentration profiles of H, OH, O, Cl, and SO₂ drawn from (Bierson and Zhang 2019) (aided by C. Bierson, personal communication, 2-Aug-2019). This model excludes PH₃; consequently, it may overestimate lower-atmosphere radical abundances and underestimate PH₃ lifetimes. Use of these radical profiles, instead of the profiles drawn from our model, result in PH₃ lifetimes becoming short ($<10^3$ s) at an altitude of 71 or 80 km instead of 63 km in our model, depending on which of the scenarios from Bierson & Zhang we adopt (their nominal vs. their low $K_{zz}+S_8$ scenarios). However, this change in destruction altitude does not affect the upper limits on lifetime we calculate strongly enough to affect the conclusions of this paper.

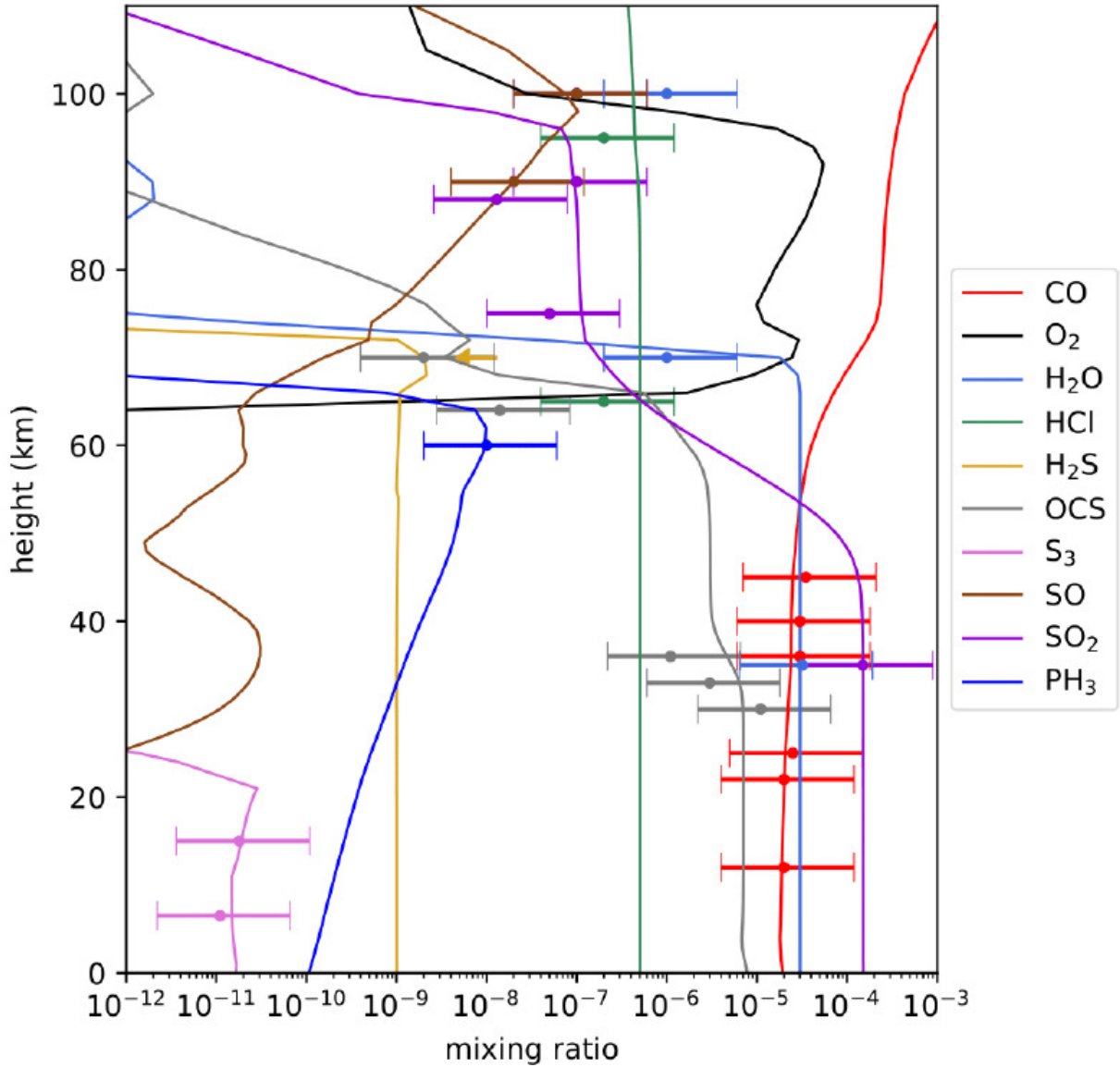


Fig. S3. Comparison of Venus model to observations. Mixing ratios (x axis) of various species versus atmospheric height (km) (y axis). From (Greaves *et al.* 2020), their Fig. S11.

Species	Atmospheric Height	Mixing Ratio	Error	Reference
CO	12 km	2×10^{-5}	$\pm 5 \times 10^{-6}$	(Krasnopolsky 2013)
	22 km	2×10^{-5}	$\pm 5 \times 10^{-6}$	(Krasnopolsky 2013)
	25 km	2.5×10^{-5}	$\pm 5 \times 10^{-6}$	(Krasnopolsky 2013)
	36 km	3×10^{-5}	$(-7, +9) \times 10^{-6}$	(Marcq <i>et al.</i> 2008)
	40 km	3×10^{-5}	$\pm 5 \times 10^{-6}$	(Krasnopolsky 2013)
	45 km	3.5×10^{-5}	$\pm 5 \times 10^{-6}$	(Krasnopolsky 2013)
OCS	30 km	1.1×10^{-5}	$\pm 1 \times 10^{-6}$	(Krasnopolsky 2013)
	33 km	3×10^{-6}	$\pm 2 \times 10^{-6}$	(Marcq <i>et al.</i> 2008)

	36 km	1.1×10^{-6}	$\pm 1 \times 10^{-7}$	(Krasnopolsky 2013)
	64 km	1.4×10^{-8}	$(-1.2,+2.8) \times 10^{-8}$	(Krasnopolsky 2008)
	70 km	2×10^{-9}	$(-1.8,+6) \times 10^{-9}$	(Krasnopolsky 2008)
H ₂ O	35 km	3.2×10^{-5}	$\pm 4 \times 10^{-6}$	(Marcq <i>et al.</i> 2008)
	70 km – 100 km	1×10^{-6}	$(-5,+20) \times 10^{-7}$	(Bertaux <i>et al.</i> 2007), Constant between these heights
SO ₂	35 km	1.5×10^{-4}	$\pm 1.4 \times 10^{-4}$	(Marcq <i>et al.</i> 2008)
	75 km	5×10^{-8}	$(-4,+45) \times 10^{-8}$	(Belyaev <i>et al.</i> 2012), Average from several observations
	90 km	1×10^{-7}	$(-9,+90) \times 10^{-8}$	(Belyaev <i>et al.</i> 2012), Average from several observations
	100 km	1×10^{-7}	$(-9,+90) \times 10^{-8}$	(Belyaev <i>et al.</i> 2012), Average from several observations
H ₂ S	70 km	$< 2.3 \times 10^{-8}$		(Krasnopolsky 2008), Upper Limit
HCl	65 km – 95 km	2×10^{-7}	$\pm 5 \times 10^{-8}$ at 65 km $\pm 2 \times 10^{-7}$ at 95 km	(Bertaux <i>et al.</i> 2007), Constant between these heights
S ₃	6.5 km	1.1×10^{-11}	$\pm 3 \times 10^{-12}$	(Krasnopolsky 2013), Heights are approximate
	15 km	1.8×10^{-11}	$\pm 3 \times 10^{-12}$	(Krasnopolsky 2013), Heights are approximate
SO	90 km	2×10^{-8}	$\pm 1 \times 10^{-8}$	(Belyaev <i>et al.</i> 2012), Average from several observations
	100 km	1×10^{-7}	$(-9,+90) \times 10^{-8}$	(Belyaev <i>et al.</i> 2012), Average from several observations
PH ₃	60 km	1×10^{-8}	$(-0.5,+1) \times 10^{-8}$	This work and (Greaves <i>et al.</i> 2020)

Table S2. Observational constraints on atmospheric concentrations. Adapted from (Greaves *et al.* 2020), their Table S3.

1. 1. 5. Details of Estimation of the Lifetime of PH₃ in the Venusian Atmosphere

The lifetime of phosphine in the Venusian atmosphere is computed in the photochemical code. Here we break down the destruction rate into its components to gain a better understanding of the

chemical sinks of PH₃ as a functional of altitude and to enable comparison with other models of the Venusian atmosphere.

The destruction rate components of phosphine are: reactions with O, H, OH, and Cl radicals, direct photolysis by UV radiation, and thermolytic decay, discussed above, in Supplementary Section 1.1.1. The destruction rates due to each of these radicals are shown in Figure 2, in the main text. We also examine the vertical transport of PH₃ in the atmosphere of Venus (Supplementary Section 1.1.5.1.) and its effects on the on the final lifetime calculations (Supplementary Section 1.1.5.2.). We close this section with the discussion of the limitations of our lifetime calculations (Supplementary Section 1.1.5.3.).

1. 1. 5. 1. Vertical Transport Lifetime of PH₃

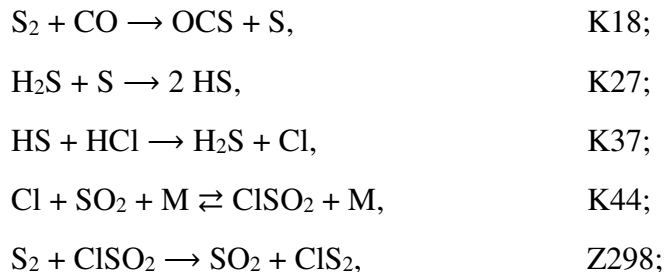
The photochemical lifetime of PH₃ can be long in the deep atmosphere (<50 km), but is always short in the high atmosphere (>60-80 km) where UV-generated radicals efficiently destroy PH₃. In the deep atmosphere, transport to the upper atmosphere limits PH₃ lifetime. To account for the effects of transport on PH₃ lifetime, we calculate the transport timescale for PH₃ at altitude z_1 due to eddy diffusion, via $t_{\text{transport}} = \Delta z^2 / K_{zz}$, where K_{zz} is the eddy diffusion coefficient, and $\Delta z = z_0 - z_1$, where z_0 is the vertical altitude at which PH₃ lifetimes are short due to photochemistry. The pseudo-first order rate constant of PH₃ loss due to eddy diffusion is thus $1 / t_{\text{transport}} = K_{zz} / \Delta z^2$. We conservatively adopt $K_{zz} = K_{zz}(z_1)$; since K_{zz} monotonically nondecreases with z , this underestimates K_{zz} , overestimates $t_{\text{transport}}$, and underestimates the destruction rate.

1. 1. 5. 2. Overall Lifetime Calculation

In each altitude bin, we adopt the minimum of the transport timescale to 63 km (where the photochemical lifetimes are, $\leq 10^4$ s; Figure 2, in the main text) and the photochemical lifetime as our overall lifetime. We invert the lifetime to obtain the pseudo-first-order destruction rate constant. This approach assumes that molecules are lost either to transport or to photochemistry. In reality, both loss mechanisms apply; consequently, this approach underestimates PH₃ destruction rates and overestimates the PH₃ lifetime.

1. 1. 5. 3. Chlorine atom chemistry in the lower and middle atmosphere of Venus

In our model Cl peaks at the surface and at 25-35 km. The surficial peak is due to thermal chemistry common to the models of (Zhang *et al.* 2012) and (Krasnopolsky 2007). The reason for the Cl peak between 25 – 35 km in our model is due to the combination of the networks of K07 (Krasnopolsky 2007) and Z12 (Zhang *et al.* 2012). Within 5 km of the surface of Venus, the temperatures are great enough for the following reactions occur with reasonable efficiency (reaction numbers given from in the form of K# for K07 and Z# for Z12):



The ClS₂ diffuses upward and is photodissociated with increasing efficiency with altitude, since the photodissociation rate depends on a cross-section that is reasonably large and that extends in wavelength to 485 nm (Zhang *et al.* 2012). At heights greater than 30 km, Cl becomes consumed by the products of H₂SO₄ dissociation from the bottom of the clouds. The specifics of where the transitions between

There are differences in lower atmospheric Cl abundances of two or more orders of magnitude between each of the models. In our model, the number density of Cl between 25 and 35 km is between 100 and 702 cm⁻³, which is much greater at that height than the number densities of Bierson (Bierson and Zhang 2019), with a maximum of 128 cm⁻³ at 10 km, or Krasnopolsky (Krasnopolsky 2007), which has a maximum Cl density at the surface of 105 cm⁻³, dropping rapidly to less than 1 cm⁻³ at >27 km. Consequently, between 25 and 35 km, our predicted lifetime for PH₃ is substantially shorter than that inferred from other models, and is shorter even than thermochemical destruction or the diffusion timescale. This explains the peak that is present in our model but not in the models of Krasnopolsky (Krasnopolsky 2007) or Bierson (Bierson and Zhang 2019).

1. 1. 5. 4. *Caveats and Limitations of the Lifetime Calculation*

The main limitations of the calculations presented here is that they likely underestimate the PH₃ destruction rate and overestimate the PH₃ lifetimes in the deep atmosphere. We have already remarked on our use of room-temperature rate constants for Cl attack, our neglect of N attack, and that our calculation methodology may overestimate diffusion timescale and hence underestimate loss due to vertical transport. For transport, we have further assumed that PH₃ must be transported to the high atmosphere to be destroyed, whereas in some cases transport to the bottom of the atmosphere where thermolytic decay is fastest may even more efficiently destroy PH₃. We may have neglected other relevant loss processes, due primarily to incompleteness of knowledge of PH₃ loss. Nearly all modern phosphine degradation kinetics measurements come from the organometallic vapor phase epitaxy (MOVPE/OMVPE) literature, which is concerned with fractional breakdown of organophosphines over semi-conductor surfaces, in which phosphine is sometimes included as a reference compound. Similarly, theoretical work on thermal decomposition of PH₃ is lacking. An early isolated theoretical study that calculates a theoretical rate of thermal decomposition of phosphine gives reaction constant values corresponding to lifetime of 2630 years at 673 K (Buchan and Jasinski 1990), a result that differs significantly from the extrapolated experimental measurements. Only two experimental

studies by (Hinshelwood and Topley 1924; Larsen and Stringfellow 1986) give data, on large enough volumes and without catalytic metals, from which free gas kinetics can be extracted, and suggest a half-life of phosphine to thermal breakdown under Venusian surface conditions is 27.2 hours, or 4.2 days at 670 K, which is consistent with the textbook comment that phosphine breaks down 'slowly' at 400 °C (Prescott 1939). For example, the silica surface-catalyzed thermal decomposition of phosphine is well-known from the semi-conductor industry, where surface-catalyzed rates are several orders of magnitude faster than gas phase rates (Hinshelwood and Topley 1924; Larsen and Stringfellow 1986). If similar surface catalysts exist on the surface of Venus, PH_3 thermolysis rates may be larger than we have modeled here.

1.2. Creation of the Forward Chemical Kinetic Network of Phosphorus Species

Many photochemically generated radicals in the Venusian atmosphere (e.g. H) can in principle, very efficiently react with oxidized phosphorus species in the atmosphere leading to their reduction and hence to the potential formation of phosphine. We explore the potential photochemical phosphine production by modeling the kinetics of the chemical reactions between the photochemically generated radicals and the oxidized phosphorus species. We construct a network of possible reactions, and calculate the maximum possible flux through the forward chemical kinetic network (*neglecting* any back reactions), as a function of altitude.

We consider phosphoric acid (H_3PO_4) as a starting point of the network because the kinetics of other oxidized phosphorus species, that could serve as alternative starting points of the network (e.g. P_4O_6 , P_4O_{10}) are unknown, and because H_3PO_4 is predicted to be the dominant form of phosphorus in the clouds of Venus (See Section 3.2.1.1 of the main paper for the discussion of the dominant phosphorus species in the atmosphere of Venus). We note that choosing H_3PO_4 as a starting point is a conservative approach and the “best case scenario” for the production of phosphine. In contrast to other dominant phosphorus species H_3PO_4 can serve as a source of both P and H needed for the formation of PH_3 in the network. The network contains all reaction rates where their kinetics parameters (which give rate as a function of temperature) are known. Kinetic data for reactions were extracted from the NIST kinetics database (Linstrom and Mallard 2001), supplemented by (Kaye and Strobel 1984) and (Bolshova and Korobeinichev 2006) . The network is shown in Figure S4.

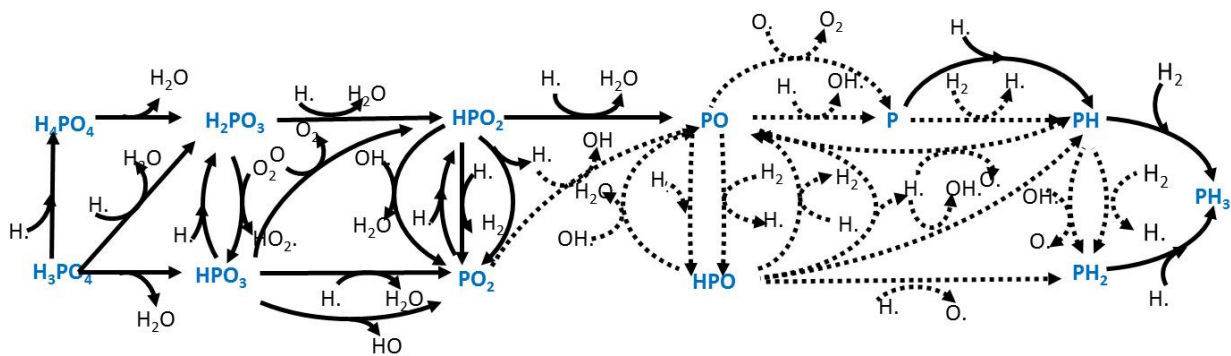


Fig. S4. The forward reaction network of phosphorus species to form phosphine. Solid lines represent reactions of phosphorus species for which kinetic data is available in the NIST reaction kinetics database or in (Kaye and Strobel 1984) or (Bolshova and Korobeinichev 2006) are considered. Dotted lines are reactions where phosphorus species kinetics are not known and the analogous nitrogen species reaction kinetics was used instead (see Supplementary Section 1.2.2.). Figure modified from (Greaves *et al.* 2020).

For each sequence of reactions that lead to PH_3 , there will be one reaction that is slower than the rest. Such reaction is the “rate-limiting step” and the rate of this reaction accurately represents the rate of the entire sequence of reactions. We next consider whether the rate of this reaction is sufficient to explain the observed amounts of phosphine in Venus’ atmosphere. We illustrate the rationale for the approach on a simpler example that considers just six reactions (Figure S5). If *any* of the reactions are too slow to produce the required flux of phosphine, then production of phosphine is not kinetically possible *no matter* how fast the other steps are, or what are the concentration of the other intermediates. For example, if reaction 4 in the simplified network presented on Figure S5 could only proceed at 10^{-4} times the rate needed to compensate for the rate of destruction of phosphine, phosphine would not be produced at the required rate to explain the observed abundance of phosphine. This holds even if all the phosphorus in the atmosphere was present as PO, and regardless of the rates of reactions 1, 2, 3, 5 and 6. In the case where reaction 4 is the slowest, most of the non-phosphine phosphorus in the atmosphere would be present as PO. If one reaction in a network of reactions such as that in Figure S4 is the rate limiting step from start to end product, then most of the phosphorus species will ‘accumulate’ as reactants for that reaction. Therefore, as a limiting case, we calculated the rate of reaction assuming that *all* the phosphorus in the atmosphere was present as the reacting phosphorus species in *each* reaction. We realize that this is not self-consistent. In the simple reaction scheme in Figure S5, all the atmosphere’s phosphorus cannot be present as H_3PO_4 and H_2PO_3 and HPO_2 etc. Such approach will overestimate the rate of reaction through the network and is consistent with our goal of estimating the maximum possible rate at which phosphine could be produced through reaction of oxidized phosphorus species with photochemical intermediates.

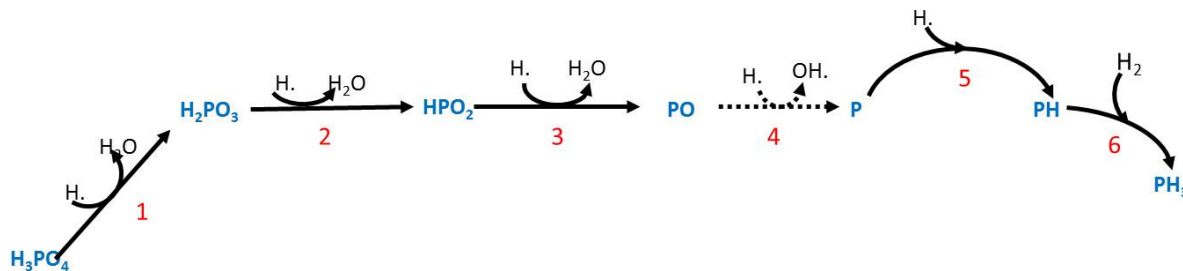


Fig. S5. Illustration of the rationale behind the creation of the network of reactions of phosphorus species with Venusian atmospheric components. We assess which reactions in the network are “rate limiting” and are too slow to produce the required flux of phosphine. In the simplified reaction network shown, the reaction 4 is the “rate limiting” step (dotted line).

The rate of reaction for all of the reactions shown in Figure S4 was calculated for 1 km steps in altitude from 0 to 115 km. Reactions were calculated to 115 km because this is the limit of the estimated number densities for H, OH and O species. Some of the reactions between reactive radicals such as H and PO are expected to happen on timescales relevant to this study (i.e. days or hours) even at ~ 180 K, the temperature of Venus’ atmosphere at 115 km. (this contrasts to the thermodynamic calculations discussed below, where reactions are between stable species and hence will happen at negligible rates below ~ 260 K). The concentration of all species except the phosphorus species was taken from the photochemical model as described above. We emphasize that our network is purely a model of the reductive reactions in the phosphorus species network. It is not an equilibrium model incorporating the back reactions. This therefore represents the maximum possible rate of production of phosphine.

1. 2. 1. Estimation of the Gas Phase Concentration of Phosphorus Species.

The concentration of the dominant phosphorus species in the Venusian atmosphere is uncertain. The only measure of atmospheric phosphorus was provided by the Vega descent probe. With an exception of the detection of the trace ~ 20 ppb of phosphine by (Greaves *et al.* 2020), no subsequent studies comment on the presence of the phosphorus species in Venus’ atmosphere.

The Vega descent probe found fluctuating level of phosphorus in an elemental analysis of materials captured on a filter. In the altitude range of 52 and 47 km the abundance of phosphorus appears to be in the same order as the abundance of sulfur (Andreichikov 1987; Andreichikov 1998b; Surkov *et al.* 1974; Vinogradov *et al.* 1970a), as reviewed in (Titov *et al.* 2018). Above 52 km no phosphorus was detected, and at 47 km the probe appeared to fail. It is therefore plausible that phosphorus is present as a condensed, liquid or solid, phase in the cloud layer. We therefore assume that phosphorus in the gas phase is a saturated vapor over phosphorus in a condensed phase above the base of the clouds. Below the clouds, gaseous phosphorus is assumed to be well-mixed (Figure S6). We estimate the vapor pressure of phosphorus species as follows.

We use the vapor pressure of P_4O_{10} over solid P_4O_{10} as estimate of the vapor pressure over condensed phosphorus species in the clouds, as P_4O_{10} represents the oxidation state of phosphorus expected to be most abundant at the level of the clouds that has a well defined vapour pressure. We note that phosphorus at the altitude of the clouds is expected to be overwhelmingly present as oxidized phosphorus species. H_3PO_4 does not have a well-defined vapor pressure as it decomposes on boiling to mixed anhydrides, of which P_4O_{10} is the end member. We describe the estimation of the vapor pressure over P_4O_{10} below (Supplementary Section 1.3.2.2.).

Our results formally over-estimate the vapor pressure of phosphorus species, as some phosphorus in the clouds will be in the thermodynamically most favored state, H_3PO_4 . The likely over-estimation of the concentration of the phosphorus species in the gas phase is a conservative approach that overall favors the formation of phosphine in the atmosphere of Venus.

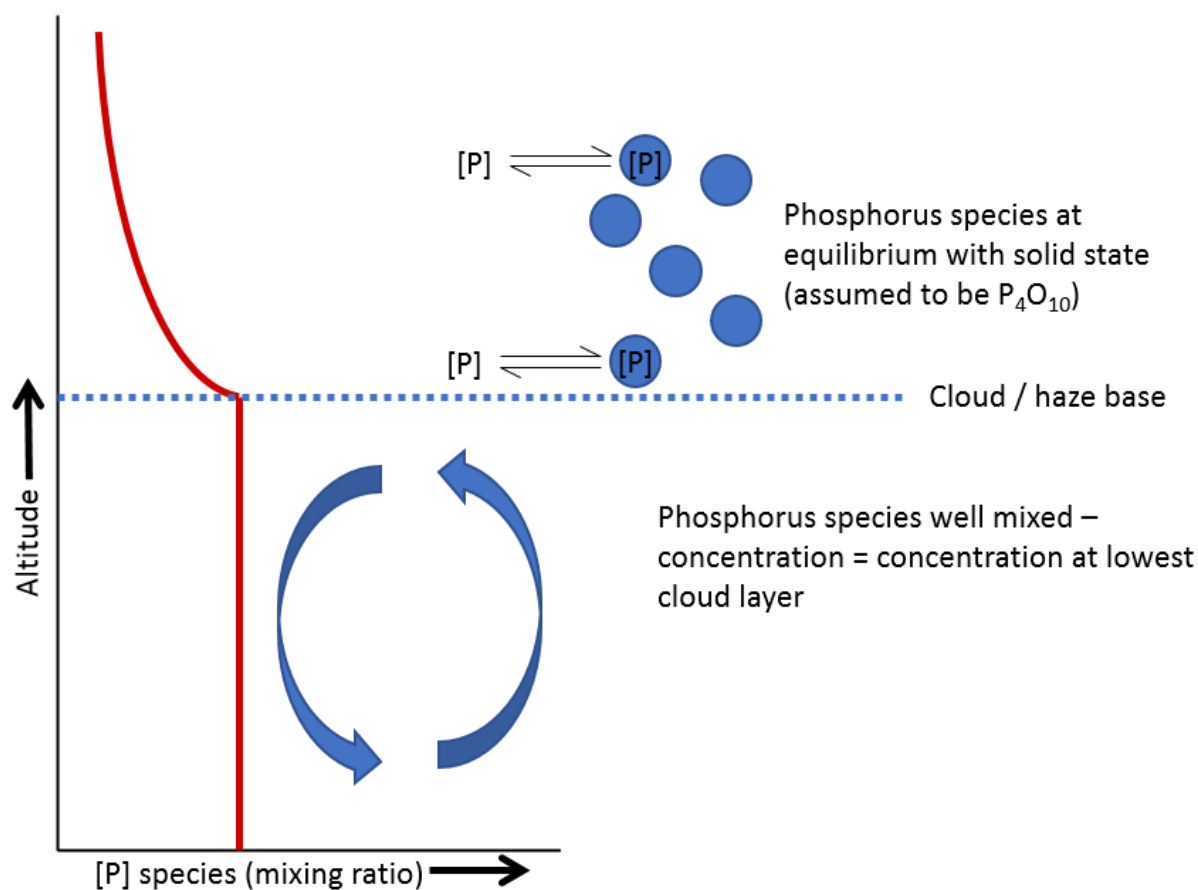


Fig. S6. Model of the concentration of phosphorus species in Venus' atmosphere. x axis: gas phase concentration of the phosphorus species in the atmosphere of Venus. y axis: the altitude in the atmosphere of Venus. Gas phase phosphorus is assumed to be saturated over condensed, liquid or solid phase phosphorus in the clouds. The vapor pressure of the gas phase phosphorus species (i.e. the concentration of the gaseous phosphorus species) falls as the

altitude rises (as the temperature decreases). The concentration of the gaseous phosphorus species below the cloud decks (~48 km) is unknown and is assumed to be well-mixed (see Supplementary Section 1.1.5.1 on vertical mixing below the cloud layer). See Supplementary Section 1.3.2.2. for more details on the estimation of the temperature dependent vapor pressure of the phosphorus species.

1. 2. 2. Kinetic data for Nitrogen Species as a Substitute for Missing Phosphorus Reactions

The crucial kinetic data for some reactions of phosphorus species are missing. For example, the kinetics of reactions in which a P=O bond is reduced to a P-H bond have not been studied in the gas phase.

To fill in missing kinetic data we construct the kinetic network where reactions of nitrogen species are used as a replacement for analogous reactions of phosphorus species. In particular, we are concerned to model the steps from PO and PO₂ to P and PH (by analogy from NO, NO₂, N and NH respectively), which are crucial steps in the formation of phosphine (Figure S4).

The likely reason that the P=O → P-H class of reactions has not been studied is because P=O radical chemistry is investigated exclusively in the context of (terrestrial) combustion (Ballistreri *et al.* 1983; Haraguchi and Fuwa 1976), and especially in relation to phosphorus compounds as flame retardants. In these circumstances, P=O is the most abundant phosphorus-containing species present in the flame (Peters 1979), but in the presence of oxygen gas and its excited states P and PH species are not expected to exist. HP=O and P=O are not as stable as their nitrogen analogues HN=O and N=O, and cannot be isolated as pure gases at STP (Dittrich and Townshend 1986). PO²⁻ is the phosphorus analogue of nitrite (NO²⁻), and is also known. P=O double bonds are very common in phosphorus chemistry, being formed in H₃PO₄, H₃PO₃, and P₄O₁₀. Hypophosphite (H₂PO₂⁻) forms a P=O double bond in preference to a structure with two single P-O bonds (although hypophosphite is only stable in aqueous solution).

The chemistry of phosphorus and nitrogen species is similar in some respects and such analogies between N and P elements are widely validated, e.g. in the theoretical spectroscopy literature (e.g. (Sousa-Silva *et al.* 2014; Sousa-Silva *et al.* 2016)).

We further justify the analogy between N and P in detail below and on Figure S7.

The bond energies of P=O (~588 kJ/mol) (Rao *et al.* 1981; Toy 2016) and N=O (~639 kJ/mol) (Mayer 1969) are similar (Figure S7(a)). The energy of forming the transition state in cleavage of H-N=O and H-P=O is also similar (Figure S7(b)). Similarly, the reaction chemistry of N=O and P=O forming metal complexes is similar across a wide range of metals (Corrigan *et al.* 1994; Herrmann 1991; Johnson *et al.* 1997; Scherer *et al.* 1991). We note that this is consistent with our informal observation of the close similarity in shape and orientation of HOMO and LUMO

orbitals in P=O and N=O. Such P=O and N=O metal complexes are relatively stable at STP (Bércecs *et al.* 2000; Scoles *et al.* 2001; Yamamoto *et al.* 1998).

Reactions of N=O- and P=O-containing species with H and OH radicals in which the P=O and N=O bonds are broken have similar kinetics overall (data from NIST (Linstrom and Mallard 2001)) (Figure S7(c), (d)). In the four cases where equivalent reactions have kinetic data available for N and P species, presented on (Figure S7(c), (d)), reactions of phosphorus are slower than reactions of nitrogen, so assuming that N reactions are representative of P reactions, the modelling a phosphorus reaction with a nitrogen reaction analogue will slightly over-estimate the rate of that reaction.

By contrast, reactions where the P-H bond is broken are very substantially faster than reactions where the N-H bond is broken, as would be expected from the much lower energy of the P-H bond compared to the N-H bond (as noted above in the discussion of the thermolytic decay of phosphine), therefore further formally overestimating the possibility of the formation of phosphine (Figure S7(e)).

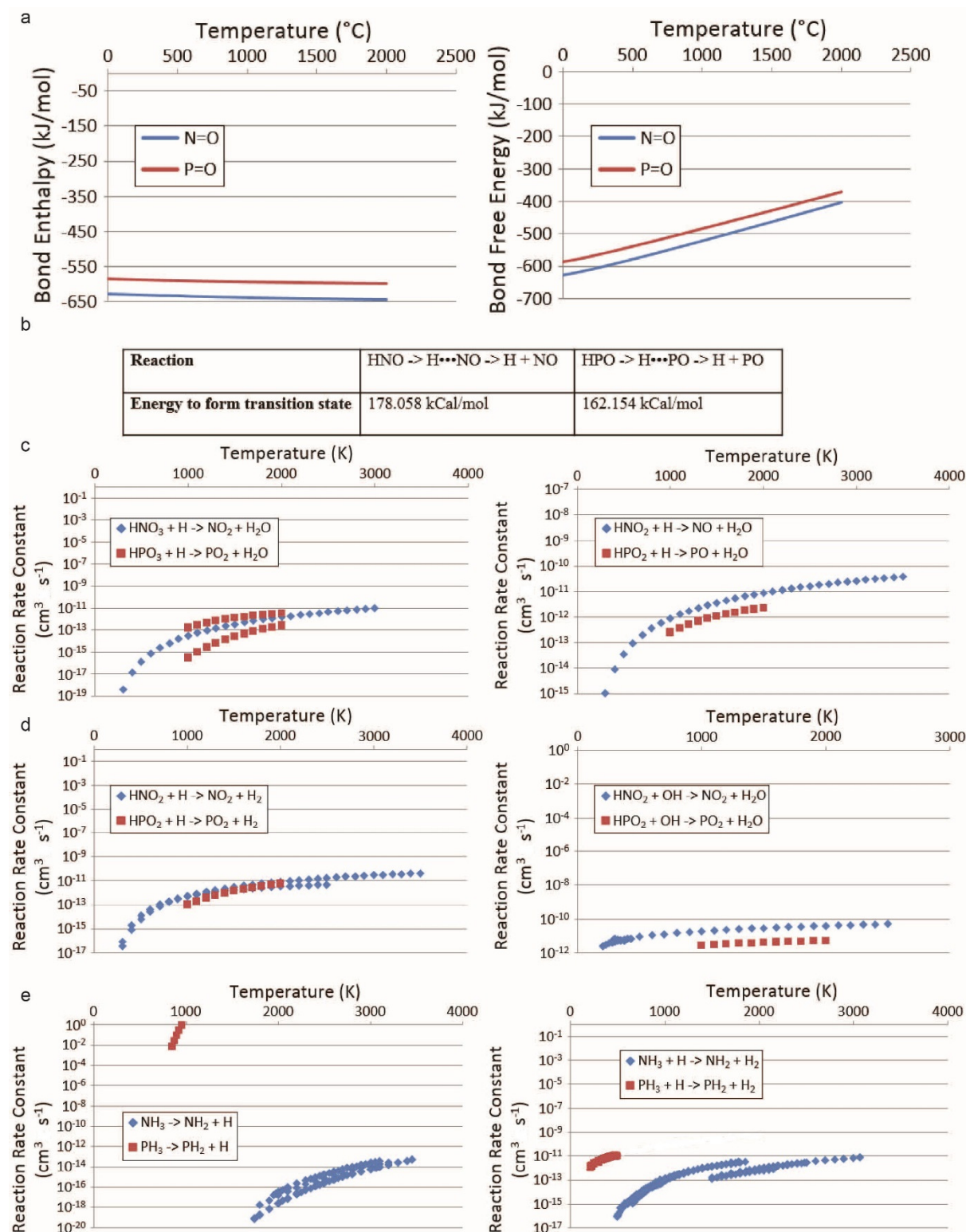


Fig. S7. The analogy between N and P chemistry. (a) Bond enthalpy (*left panel*) energy and Gibbs free energy of formation (*right panel*) for N=O and P=O are similar. x axis: Temperature ($^{\circ}\text{C}$), y axis: Bond Enthalpy (kJ/mol) and Bond Energy (kJ/mol). The bond enthalpy and bond energy values are calculated from JANAF tables of free energy and entropy for reactions $\text{N} + \text{O} \rightarrow \text{NO}$ and $\text{P} + \text{O} \rightarrow \text{PO}$ (Chase 1998). (b) The energy of forming the transition state in cleavage of H-N=O and H-P=O is similar. The energy values are calculated using *Ab initio* methods using

B3LYP approximation to 6-311G level of theory, using GAMESS (Schmidt *et al.* 1993). (c-e) For reactions where temperature-dependent rate information is available and is consistent between experiments, reactions of N=O and P=O-containing species with H and OH radicals have similar kinetics (data from NIST (Linstrom and Mallard 2001)). x axis: Temperature (K), y axis: Reaction Rate Constant (cm^3s^{-1}). (c) *Left panel*: $\text{HNO}_3 + \text{H} \rightarrow \text{NO}_2 + \text{H}_2\text{O}$ vs $\text{HPO}_3 + \text{H} \rightarrow \text{PO}_2 + \text{H}_2\text{O}$. Note that two sources gave significantly different rates for the phosphorus reaction, which bracket the nitrogen value *Right panel*: $\text{HNO}_2 + \text{H} \rightarrow \text{NO} + \text{H}_2\text{O}$ vs $\text{HPO}_2 + \text{H} \rightarrow \text{PO} + \text{H}_2\text{O}$. N species react ~3-fold faster than P species. (d) *Left panel*: $\text{HNO}_2 + \text{H} \rightarrow \text{NO}_2 + \text{H}_2$ vs $\text{HPO}_2 + \text{H} \rightarrow \text{PO}_2 + \text{H}_2$. The phosphorus reaction has only been measured at high temperatures, where it has a rate very similar to the nitrogen reaction. *Right panel*: $\text{HNO}_2 + \text{OH} \rightarrow \text{NO}_2 + \text{H}_2\text{O}$ vs $\text{HPO}_2 + \text{OH} \rightarrow \text{PO}_2 + \text{H}_2\text{O}$. Reaction rate constants differ by a factor of ~5 over the range where both are measured. (e) *Left panel*: $\text{NH}_3 \rightarrow \text{NH}_2 + \text{H}$ vs $\text{PH}_3 \rightarrow \text{PH}_2 + \text{H}$. Note that the reactions have not been measured at the same temperature range, but it is clear that the two sets of points belong to substantially different curves. *Right panel*: $\text{NH}_3 + \text{H} \rightarrow \text{NH}_2 + \text{H}_2$ vs $\text{PH}_3 + \text{H} \rightarrow \text{PH}_2 + \text{H}_2$. Note that the phosphorus species data is only for low temperatures. In both reactions (left and right panels) the P-H bond is broken much faster than the N-H bond. PH_3 is expected to be much more efficiently destroyed than its nitrogen counterpart, NH_3 , which leads to the formal overestimation of the formation of phosphine.

1. 3. Methods Used in the Thermodynamic Analysis of Potential Phosphine-Producing Reactions

1. 3. 1. Overview of Method for Calculating the Gibbs Free Energy of the Reaction (ΔG)

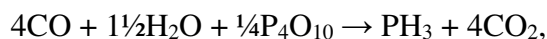
We calculate the Gibbs Free Energy on the basis of established textbook knowledge (Greiner *et al.* 2012; Perrot 1998) and previously published work (Bains *et al.* 2019). In brief, the free energy of a reaction occurring in non-standard conditions is given by

$$\Delta G = \Delta G^0 + R.T.\ln(Q). \quad (24)$$

Here ΔG is the free energy of reaction, ΔG^0 is the standard free energy (i.e. the energy where all the reagents are in their standard state), R is the gas constant, T is the absolute temperature and Q is the reaction quotient. The standard free energy of a reaction is the sum of the standard free energy of the products minus the standard free energy of the reactants. The reaction quotient Q is given by

$$Q = \frac{\prod_1^n ap_i^{s_i}}{\prod_1^m ar_i^{s_i}} \quad (25)$$

Where ap_i is the activity of product number i , and s_i is the number of moles of product i in the reaction, and ar_i is the activity of the reactant i , and again s_i is the number of moles of that reactant in the reaction. Thus, for the reaction



$$Q = \frac{\{\text{PH}_3\}\{\text{CO}_2\}^4}{\{\text{CO}\}^4\{\text{H}_2\text{O}\}^{1.5}\{\text{P}_4\text{O}_{10}\}^{0.25}} \quad (26)$$

where {species} is the activity of that species.

Thus, to calculate the free energy of a reaction, and hence estimate whether it will proceed spontaneously, we need to know the standard free energy of the reactants and products and the activities of the reactants and products.

The standard free energy of reaction is itself a function of temperature. The values for the standard free energy (ΔG^0) as a function of temperature between 250 K and 1000 K (where relevant – e.g. there is no free energy of liquid water at temperatures over 673 K because liquid water does not exist above this temperature) were obtained from the sources listed in Table S3.

Species and phase	Source
P ₄ O _{10(g)} , P ₄ O _{10(s)} , H ₃ PO _{4(s/l)} , H ₂ SO _{4(g)} , PH _{3(g)} , H ₂ O _(l) , H ₂ O _(g) , SO _{2(g)} , CO _(g) , CO _{2(g)} , H ₂ S _(g) , S _(g) , OCS _(g)	(Chase 1998)
H ₃ PO _{3(aq)} , H ₃ PO _{4(aq)}	(Barner and Scheurman 1978)
H ₃ PO _{3(cr/l)}	Calculated from (Barner and Scheurman 1978; Guthrie 1979)
PH _{3(aq)}	Calculated from (Chase 1998; Fu <i>et al.</i> 2013)
SO _{2(aq)} , CO _{2(aq)} , CO _(aq) , H ₂ S _(aq)	(Amend and Shock 2001)
CaO _(s) , Al ₂ O _{2(s)} , MgO _(s) , CaF _{2(s)} , AlPO _{4(s)} , Ca ₃ (PO ₄) _{2(s)} , Ca ₅ (PO ₄) ₃ F _(s) , Mg ₃ (PO ₄) _{2(s)} , CaSO _{4(s)} , MgSO _{4(s)} , FeO _(s) , FeS _{2(s)} , Fe ₂ O _{3(s)} , Fe ₃ O _{4(s)}	(Robie and Hemingway 1995)
NAD _(aq) , FAD _(aq) , Coenzyme-Q _(aq)	(Lehninger 2004; Pratt and Cornley 2014)
Ferredoxins _(aq)	(Smith and Feinberg 1990)

Table S3. Sources for the values for the standard free energy (ΔG^0) as a function of temperature between 250 K and 1000 K for chemical species used in this study.

At high pressures gas activities differ significantly from their partial pressures. Gas activity was corrected for pressure and temperature according to Berthelot's equation (Rock 1969):

$$a = P \cdot \exp \left[\frac{9T_c}{128P_c T} \cdot \left(1 - \frac{6T_c^2}{T^2} \right) \cdot P \right], \quad (27)$$

where a is the activity of the species, P is the pressure, T is the absolute temperature, T_c is the species' critical temperature and P_c is the species critical pressure. Critical pressures and temperatures were obtained from the sources listed in Table S4.

Species	T _c , P _c source
CO ₂ , H ₂ S, H ₂ O, N ₂	(Ballesteros <i>et al.</i> 2019)
SO ₂	(Médard 2019)
OCS	(Robinson and Senturk 1979)
CO	(ToolBox 2003)
H ₂	(Hoge and Lassiter 1951)

Table S4. Sources for critical pressure (P_c) and critical temperature (T_c) values of gaseous chemical species used to calculate their gas activities in this study.

The critical temperature of H₃PO₄, P₄O₁₀ and P₄O₆ were assumed to be sufficiently high that these species behaved like a near perfect gas at Venus temperatures.

The activity of solids was assumed to be 1. The standard state of a *pure* solid reagent is 1; mixtures may have different activities, but as the nature of the mixtures are not known all solids were assumed to be single chemical species. At Venus surface pressures, pressure corrections will not introduce material activity changes in solids. Changes in free energy with temperature are included in the sources given above in Table S3.

1. 3. 2. Modelling of the Thermodynamics of the Atmospheric and Surface Reactions

Next, we discuss our reasoning behind the choice of chemical reactants (Section 1.3.2.1) and their input concentrations (Section 1.3.2.2). We also present the relevant chemical reactions that could in principle lead to the phosphine formation in the Venusian environment (Section 1.3.2.3).

1. 3. 2. 1. Choice of Reactants

Choice of dominant atmospheric phosphorus species. Phosphorus-containing species have not been modeled for Venus' atmosphere before and our work represents the first attempt to model the dominant phosphorus species in Venusian atmosphere.

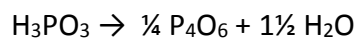
We analyzed what phosphorus-containing chemicals are likely to be present in Venus' atmosphere by calculating which species would be most thermodynamically stable under Venusian atmospheric conditions (e.g., concentrations of water and reducing gases).

The equilibrium between the four phosphorus species was calculated as follows by calculating the $\ln(Q)$ values for each of the following reactions which would result in a $\Delta G=0$. In all cases, the activities of the other components were calculated as described in the main text, and therefore the calculated concentration of phosphorus species cover a range of values.

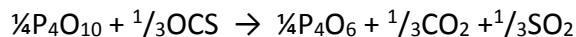
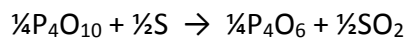
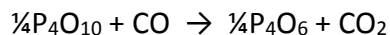
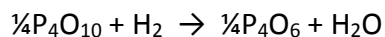
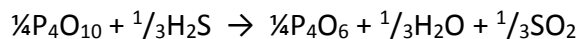
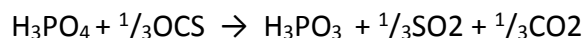
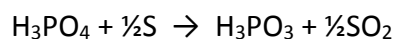
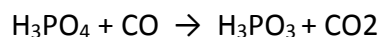
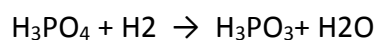
There are two classes of reactions involved; dehydration reactions and reduction reactions. For dehydration reactions only one reaction is possible. For reduction reactions five reactions are

considered, corresponding to the five reducing gases likely to be present in trace amounts in Venus' atmosphere, and the average free energy of the reactions was used. (Note that if the atmosphere were at equilibrium then each of the reactions would give that same result; however, the atmosphere is not at equilibrium.)

Dehydration reactions



Reduction reactions



Choice of reducing agents. The conversion of the oxidized variant of phosphorus in the P(+3) or P(+5) oxidation state to phosphine requires a reducing agent and a source of hydrogen atoms.

Two reducing agents – H₂S and H₂ – are themselves sources of hydrogen atoms, a further three reducing gases – CO, OCS and elemental sulfur – contain no hydrogen atoms, and hence require a reaction involving water to provide hydrogen. Gas phase elemental sulfur is taken as the most stable species (S₂ or S₈) at each temperature. In principle, N₂ (which can be oxidized to HNO₃) or HCl (which can be oxidized to perchlorate) could also act as reducing agents. Preliminary calculations suggested that the energy requirements to use the oxidation of N₂ or HCl as a source of electrons to reduce phosphates to phosphine were very high, and so these reactions were not considered further.

The reducing agents on the surface of Venus are unknown, but solid mineral reducing agents are likely to be salts of redox active metals. Iron(II) compounds are potential reductants for phosphorus species (Herschy et al. 2018), and the presence of H₂S and HCl in the Venusian atmosphere suggest that FeS₂ and FeCl₂ should be considered as potential reductants. In the presence of excess liquid water Fe(II) oxidation (serpentinization reactions) have been shown to be capable to reducing phosphate to phosphite at 25°C (Pasek *et al.* 2020), although of course

this chemistry could not happen on Venus' surface as there is negligible water there, and water is present in gas phase only. In addition, FeS_2 is unstable under Venus surface conditions (Fegley 1997) and FeCl_2 may be unstable below the cloud deck level on Venus (Figure S8), both spontaneously forming Fe(III) species. We therefore ignored calculations involving FeCl_2 at altitudes below which FeO is thermodynamically favored over FeCl_2 .

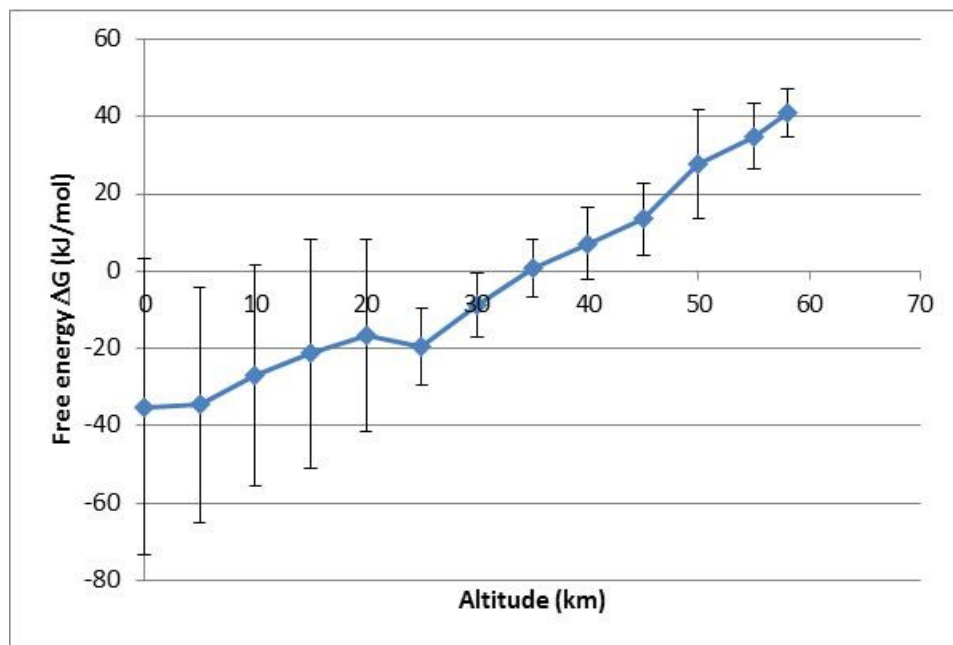


Figure S8. FeCl_2 may be unstable below the cloud deck level on Venus. x axis: altitude. y axis: free energy of reaction of hydrolysis of FeCl_2 by atmospheric water under Venus conditions. Bars show range of ΔG values resulting from different partial pressures of HCl and H_2O . The free energy of the reaction $\text{FeCl}_2 + \text{H}_2\text{O} \rightarrow \text{FeO} + 2\text{HCl}$ was calculated as explained in the main text. We ignored calculations involving FeCl_2 at altitudes below that at which the free energy of the reaction forming FeCl_2 from FeO and HCl was negative (i.e. at altitudes below which FeO is thermodynamically favored over FeCl_2).

Choice of the surface minerals. The chemical composition of the surface minerals of Venus is poorly known. The only data on the crustal composition of Venus comes from the X-ray fluorescence measurements of the bulk composition of the crust by Vega (Surkov *et al.* 1986) and Venera (Surkov *et al.* 1984) landers. The measurements suggest that the Venus' crustal composition is extremely similar to terrestrial tholeiitic basalts. Terrestrial basalts contain very low amounts of phosphorus (0.08% - 0.45%). If phosphorus is present on the surface of Venus, it is likely to be in the form of phosphate salts. We have considered phosphate salts of Mg, Ca, Al and K, with fluorapatite included as well as HF is probably present in the atmosphere. Phosphate minerals were assumed to be present as differentiated minerals, i.e. as pure solids whose activity is 1. The presence of pure solids is geologically unlikely, but (as with many other assumptions in this paper) presents a 'best case scenario' for making phosphine chemically. Reduction of these minerals by all the reducing atmospheric gases mentioned above was also modeled.

The selection of relevant reactants that build subsurface rocks and minerals of Venus is discussed in Section 1.3.3.

1.3.2.2. Choice of Vertical Concentration Profiles

For each of the trace gases in Venus' atmosphere, we use two different vertical concentration profiles, representing a maximum and minimum concentration as reported in the literature (Table S5). Some sources are either directly measured but most gas species are theoretically estimated (Table S5). Gas concentrations were only explored up to 60 km altitude, above which the temperature is below 260 K and reactions would be so slow that thermodynamics would not effectively predict what species would be present. Note that 60 km is a lower height limit than was applied for the kinetics modeling above in Section 1.2. This is because in this section we are concerned with the reactions of stable chemical species with each other. These have extremely slow reaction kinetics below the freezing point of water, and so we can neglect any reaction by these species above 60 km, where the temperature <260 K. By contrast, the reaction network shown in Section 1.2. involved reactive radicals, which have very fast reaction kinetics at temperatures above 150 K. The difference is illustrated from everyday experience on Earth. Chemicals such as isoprene are stable for decades even in the presence of oxygen in the absence of light, because the kinetics of direct reaction of oxygen with isoprene are immeasurably slow. However, the reaction destroys isoprene in the range of hours or minutes under sunlight because photolysis generates reactive radicals which then initiate reaction (Zhan *et al.* 2020).

Temperature (K)	Pressure (bars)	Altitude (km)	Lowest partial pressure	T (theoretical) vs M (measured)	Reference	Highest partial pressure	T (theoretical) vs M (measured)	Reference
SO ₂								
735	92.1	0	1.7E-06	T	A	2.3E-04	T	A
697	66.5	5	1.8E-06	M	F	2.3E-04	T	A
658	47.4	10	4.5E-06	M	F	5.0E-04	M	B
621	33.0	15	2.2E-05	T	G	1.9E-04	M	B
579	22.5	20	2.3E-05	T	G	1.9E-04	T	A
537	14.9	25	2.4E-05	T	A	1.9E-04	T	A
495	9.85	30	2.5E-05	M	F	1.9E-04	T	G
453	5.92	35	2.5E-05	M	F	2.0E-04	T	A
416	3.50	40	2.6E-05	T	G	2.0E-04	T	A
383	1.98	45	3.0E-05	T	G	2.0E-04	T	A
348	1.07	50	3.3E-05	M	F	2.0E-04	T	A
300	0.53	55	3.7E-05	T	G	2.1E-04	T	A
263	0.24	60	4.3E-05	M	F	2.2E-04	T	A
H ₂ S								
735	92.1	0	5.0E-09	T	B	2.2E-06	T	A
697	66.5	5	1.4E-08	T	B	2.2E-06	T	A
658	47.4	10	3.7E-08	T	B	2.2E-06	T	A
621	33.0	15	7.7E-08	T	C	2.2E-06	T	A
579	22.5	20	7.8E-08	T	B	2.3E-06	T	A
537	14.9	25	9.0E-08	T	B	2.3E-06	T	B

495	9.85	30	1.0E-07	T	C	9.1E-07	T	A
453	5.92	35	1.2E-07	T	C	2.1E-06	T	A
416	3.50	40	1.2E-07	T	B	2.1E-06	T	A
383	1.98	45	1.4E-07	T	C	2.2E-06	T	A
348	1.07	50	1.6E-07	T	C	2.2E-06	T	A
300	0.53	55	1.7E-07	T	C	2.2E-06	T	A
263	0.24	60	1.7E-07	T	C	2.2E-06	T	A
S								
735	92.1	0	8.8E-10	T	B	3.4E-06	T	C
697	66.5	5	8.8E-10	T	B	5.7E-06	T	C
658	47.4	10	8.8E-10	T	B	9.3E-06	T	C
621	33.0	15	8.8E-10	T	B	1.4E-05	T	C
579	22.5	20	8.8E-10	T	B	2.2E-05	T	C
537	14.9	25	8.8E-10	T	B	3.0E-05	T	C
495	9.85	30	1.1E-09	T	B	3.2E-05	T	C
453	5.92	35	3.7E-09	T	B	3.4E-05	T	C
416	3.50	40	1.0E-08	T	B	2.1E-07	T	B
383	1.98	45	1.3E-08	T	B	4.0E-07	T	B
348	1.07	50	1.5E-08	M	E	4.0E-07	T	B
300	0.53	55	1.5E-08	M	E	5.9E-07	T	B
263	0.24	60	2.0E-08	M	E	1.5E-06	T	C
OCS								
735	92.1	0	7.0E-12	T	B	2.6E-05	T	C
697	66.5	5	4.6E-10	T	B	2.7E-05	T	C
658	47.4	10	6.5E-10	T	B	5.6E-05	T	A
621	33.0	15	6.0E-09	T	B	5.9E-05	T	A
579	22.5	20	1.0E-08	M	E	6.0E-05	T	A
537	14.9	25	1.2E-08	T	B	6.0E-05	T	A
495	9.85	30	1.6E-08	T	A	6.1E-05	T	A
453	5.92	35	2.1E-08	T	A	6.2E-05	T	A
416	3.50	40	2.6E-08	T	A	1.3E-05	T	A
383	1.98	45	4.2E-08	T	A	1.5E-05	M	E
348	1.07	50	1.1E-07	T	B	1.6E-05	T	C
300	0.53	55	1.3E-07	T	B	2.0E-05	T	C
263	0.24	60	2.8E-07	T	A	2.3E-05	T	C
H ₂ O								
735	92.1	0	5.7E-06	T	A	1.4E-03	T	B
697	66.5	5	1.1E-05	T	A	1.4E-03	T	B
658	47.4	10	1.9E-05	T	A	2.2E-03	M	B
621	33.0	15	2.3E-05	T	C	5.2E-03	M	B
579	22.5	20	2.4E-05	T	G	8.0E-03	M	I
537	14.9	25	2.4E-05	T	G	1.4E-03	T	B
495	9.85	30	2.5E-05	M	E	1.4E-03	T	B
453	5.92	35	2.5E-05	M	E	1.4E-03	T	B
416	3.50	40	2.5E-05	M	E	1.4E-03	T	B
383	1.98	45	2.5E-05	M	E	1.4E-03	T	B
348	1.07	50	2.6E-05	M	E	1.4E-03	T	B
300	0.53	55	2.6E-05	M	E	1.4E-03	T	B
263	0.24	60	2.6E-05	M	E	1.4E-03	T	B
CO								
735	92.1	0	1.6E-12	T	B	3.4E-05	T	A
697	66.5	5	1.8E-12	T	B	3.7E-05	T	C
658	47.4	10	3.3E-11	T	B	3.8E-05	T	C
621	33.0	15	3.7E-11	T	B	4.2E-05	T	A
579	22.5	20	4.9E-10	T	B	4.2E-05	T	A

537	14.9	25	5.4E-10	T	B	4.5E-05	T	A
495	9.85	30	5.3E-09	T	B	4.6E-05	T	A
453	5.92	35	5.7E-09	T	B	2.3E-05	T	C
416	3.50	40	4.1E-08	T	B	2.4E-05	T	A
383	1.98	45	4.4E-08	T	B	2.9E-05	T	C
348	1.07	50	2.2E-07	T	B	3.0E-05	M	E
300	0.53	55	2.4E-07	T	B	3.0E-05	M	B
263	0.24	60	8.8E-07	T	B	3.2E-05	M	B
H ₂								
735	92.1	0	3.0E-13	T	B	5.8E-08	T	B
697	66.5	5	2.1E-12	T	B	8.2E-08	T	B
658	47.4	10	1.1E-11	T	B	8.8E-08	T	B
621	33.0	15	3.4E-11	T	B	1.1E-07	T	B
579	22.5	20	4.9E-11	T	B	1.3E-07	T	B
537	14.9	25	1.7E-10	T	B	1.4E-07	T	B
495	9.85	30	4.7E-10	T	B	4.5E-09	T	D
453	5.92	35	7.8E-10	T	B	4.5E-09	T	D
416	3.50	40	1.1E-09	T	B	4.6E-09	T	D
383	1.98	45	1.9E-09	T	B	4.7E-09	T	D
348	1.07	50	2.6E-09	T	B	4.9E-09	T	D
300	0.53	55	3.0E-09	T	B	7.5E-09	T	B
263	0.24	60	3.0E-09	T	D	3.5E-08	T	B
HCl								
735	92.1	0	2.0E-07	T	D	5.4E-07	T	A
697	66.5	5	2.0E-07	T	D	5.5E-07	T	A
658	47.4	10	2.0E-07	T	D	5.5E-07	T	A
621	33.0	15	4.2E-07	M	E	5.6E-07	T	A
579	22.5	20	4.2E-07	M	E	3.1E-06	T	H
537	14.9	25	4.2E-07	M	E	8.6E-06	T	H
495	9.85	30	5.0E-07	T	A	1.3E-05	T	H
453	5.92	35	5.0E-07	T	A	1.3E-05	T	H
416	3.50	40	5.2E-07	T	A	1.7E-05	T	H
383	1.98	45	5.3E-07	T	A	3.6E-05	T	H
348	1.07	50	5.3E-07	T	A	5.3E-07	T	A
300	0.53	55	5.3E-07	T	A	5.3E-07	T	A
263	0.24	60	5.4E-07	T	A	5.4E-07	T	A

Table S5. List of sources for gas concentrations were collected from the available literature and are either directly measured or theoretically estimated. References used: A: (Taylor and Hunten 2014), B: (Oyama *et al.* 1980), C: (Krasnopolsky 2007), D: (Krasnopolsky 2012), E: (Marcq *et al.* 2018), F: (Vandaele *et al.* 2017), G: (Andreichikov 1998a), H: (Hoffman *et al.* 1979), I: (Vinogradov *et al.* 1970b).

We estimated the total concentration of phosphorus species in the gas phase as a saturated vapor over phosphorus species in a condensed phase above the base of the clouds.

The vapor pressure of P₄O₁₀ over solid P₄O₁₀ as a function of temperature is predicted from equations that were developed to empirically predict that vapor pressure. Three such equations are available; the geometric mean was taken as the value for this work.

$$P_v = \sqrt[3]{\alpha \cdot \beta \cdot \gamma}, \quad (28)$$

where P_v =vapor pressure and α , β , γ are the results of the predictive equations from:

α from (DIPPR (<https://dippr.aiche.org/>))

$$LN(V_p) = 79.33 - \frac{12766}{K} - 7.3289 \cdot LN(K) + 1.1 \cdot 10^{-18} \cdot K^6 \text{ (over solid, in pascals)} \quad (29)$$

β from (DIPPR (<https://dippr.aiche.org/>))

$$LN(V_p) = -10.768 - \frac{9004.2}{K} - 5.8118 \cdot LN(K) - 2.5 \cdot 10^{-6} \cdot K^2 \text{ (over liquid, in pascals)} \quad (30)$$

γ from ((Yaws and Knovel 1999))

$$LOG_{10}(P_v) = -55.9316 - \frac{2852.9}{K} + 27.0 \cdot LOG_{10}(K) - 0.029138 \cdot K + 9.47 \cdot 10^{-6} \cdot K^2 \text{ (over solid, in mm Hg)} \quad (31)$$

Some reactions only occur in the clouds, and so the cloud top altitude also affects our calculations. For completeness, we varied cloud bases from 35 km to 60 km, and cloud tops from 40 km to 60 km, with the caveat that a 5 km thick cloud layer was always assumed. In the droplet phase in the clouds, phosphorus species concentration is assumed to be 1 molal. This is an arbitrary amount, chosen purely for convenience, as the concentration of phosphorus species in the cloud droplet phase is unknown. We note that this is likely an overestimation of the concentration of phosphorus, and a conservative approach aimed to make phosphine production more favorable. If phosphorus species are less abundant then the formation of phosphine is much less likely.

Concentration of sulfuric acid. It is widely assumed that cloud droplets are composed primarily of sulfuric acid. (Titov *et al.* 2018). Given the water vapor profile presented in the Table S5, the concentration of sulfuric acid can be calculated from the relationship between the vapor pressure of water over sulfuric acid with temperature and concentration of the acid (Greenewalt 1925). Notably, at lower cloud levels this calculation gives concentrations of slightly over 100%, which is consistent with the suggestion that there is SO_3 in the lower atmosphere of Venus, likely dissolved in the sulfuric acid droplets (Craig *et al.* 1983) to give ‘oleum’ (Greenwood and Earnshaw 2012). Given the vapor pressure of gaseous sulfuric acid over liquid sulfuric acid from (Ayers *et al.* 1980), the partial pressure of gaseous sulfuric acid at the base of the clouds can be calculated, and this is assumed to be well mixed throughout the atmosphere below the clouds. This means that the partial pressure of sulfuric acid is dependent on the altitude of the base of the clouds.

Concentration of gases dissolved in cloud droplets. For completeness, we assume that all species present in the gas phase are also present in droplets. The solubility of atmospheric gases in cloud and haze droplets is unknown. Of the components of the Venusian atmosphere, only the

solubility of carbon dioxide and sulfur dioxide in concentrated sulfuric acid have been studied (Hayduk *et al.* 1988; Markham and Kobe 1941; Zhang *et al.* 1998). However, assuming that the gaseous species are chemically stable in cloud droplets, then their solubility is not important for calculating the thermodynamics of the reaction with species originally in the gas phase. If trace gases in the atmosphere are at equilibrium with solvated species in droplets then, by definition, any energy released by their solution must be compensated by their greater concentration in the liquid phase, so the net free energy of reaction is not affected.

1. 3. 2. 3. *Choice of Reactions*

To probe the source of phosphine in Venusian atmosphere we have assembled a representative list of all possible chemical reactions involving the species (summarized in Table S5) that could theoretically lead to the reduction of oxidized phosphorus species in Venusian atmosphere, surface, and subsurface and the formation of phosphine.

We identified 75 potential reactions that could involve various oxidized phosphorus species and reducing agents present in the Venusian environment (see Table S6 for the list of all chemical reactions considered). We calculated the Gibbs Free Energy for each reaction, for a total of 256 partial pressure and 15 cloud altitude combinations. A total of 3840 conditions were tested for each of the 75 reactions. Below we describe particulars of both the choice of phosphorus species and their reactions with reductants.

Because phosphorus could be present in gas phase as P_4O_6 , P_4O_{10} and H_3PO_4 (albeit at very different partial pressures), the reactions of all three species were modelled (see Supplementary Section 1.3.2.1 and Section 3.2.1.1 in the main text for details on the dominant phosphorus species on Venus).

Some reactions can only take place in liquid or solid phases. The examples of such reactions include reduction of phosphorus species to phosphite (H_3PO_3), reduction by solid phase sulfur in hazes or reduction of solid phosphate minerals.

Reduction of phosphite to phosphine can only occur in liquid phase as phosphites disproportionate before they evaporate. Phosphite could be made in cloud or haze droplets at high altitude, therefore the reactions of reduction of H_3PO_3 to phosphine by atmospheric gases or by minerals transported to the atmosphere as dust are only considered in the clouds.

Reduction by solid phase sulfur in hazes in the atmosphere of Venus is considered to take place only in solid (or liquid/melt) phase, i.e. where the activity of sulfur ~ 1 .

Solid mineral phosphates could be reduced by atmospheric gases to phosphine. Such reactions are most likely to occur on the surface. In principle, surface dust could be carried into the atmosphere either by air movement, or volcanic eruptions. While there is no evidence for either

process transporting significant mineral mass into Venus' atmosphere, we have considered the reactions of reduction of minerals at all altitudes for completeness.

Gas and cloud phase reactions
<i>Reduction of H₃PO₄ to PH₃</i>
1) H ₂ S + H ₃ PO ₄ → PH ₃ + H ₂ SO ₄
2) $\frac{4}{3}$ H ₂ S + H ₃ PO ₄ → PH ₃ + $\frac{4}{3}$ SO ₂ + $\frac{4}{3}$ H ₂ O
3) 4H ₂ + H ₃ PO ₄ → PH ₃ + 4H ₂ O
4) 4CO + H ₃ PO ₄ → PH ₃ + 4CO ₂
5) 2S + H ₃ PO ₄ → PH ₃ + 2SO ₂
6) $\frac{4}{3}$ OCS + H ₃ PO ₄ → PH ₃ + $\frac{4}{3}$ SO ₂ + $\frac{4}{3}$ CO ₂
7) $\frac{4}{5}$ FeS ₂ + H ₃ PO ₄ → PH ₃ + $\frac{4}{5}$ FeO + $\frac{8}{5}$ SO ₂
8) $\frac{8}{11}$ FeS ₂ + H ₃ PO ₄ → PH ₃ + $\frac{4}{11}$ Fe ₂ O ₃ + $\frac{16}{11}$ SO ₂
9) 8FeO + H ₃ PO ₄ → PH ₃ + 4Fe ₂ O ₃
10) 8FeCl ₂ + 8H ₂ O + H ₃ PO ₄ → PH ₃ + 4Fe ₂ O ₃ + 16HCl
<i>Reduction of P₄O₁₀ to PH₃</i>
11) H ₂ S + 1½H ₂ O + ¼P ₄ O ₁₀ → PH ₃ + H ₂ SO ₄
12) $\frac{4}{3}$ H ₂ S + ¼P ₄ O ₁₀ + $\frac{1}{6}$ H ₂ O → PH ₃ + $\frac{4}{3}$ SO ₂
13) 4H ₂ + ¼P ₄ O ₁₀ → PH ₃ + 2½H ₂ O
14) 4CO + 1½H ₂ O + ¼P ₄ O ₁₀ → PH ₃ + 4CO ₂
15) 2S + 1½H ₂ O + ¼P ₄ O ₁₀ → PH ₃ + 2SO ₂
16) $\frac{4}{3}$ OCS + 1½H ₂ O + ¼P ₄ O ₁₀ → PH ₃ + $\frac{4}{3}$ SO ₂ + $\frac{4}{3}$ CO ₂
17) $\frac{4}{5}$ FeS ₂ + 1½H ₂ O + ¼P ₄ O ₁₀ → PH ₃ + $\frac{4}{5}$ FeO + $\frac{8}{5}$ SO ₂
18) $\frac{8}{11}$ FeS ₂ + 1½H ₂ O + ¼P ₄ O ₁₀ → PH ₃ + $\frac{4}{11}$ Fe ₂ O ₃ + $\frac{16}{11}$ SO ₂
19) 8FeO + 1½H ₂ O + ¼P ₄ O ₁₀ → PH ₃ + 4Fe ₂ O ₃
20) 8FeCl ₂ + 9½H ₂ O + ¼P ₄ O ₁₀ → PH ₃ + 4Fe ₃ O ₄ + 16HCl
<i>Reduction of P₄O₆ to PH₃</i>
21) $\frac{3}{4}$ H ₂ S + 1½H ₂ O + ¼P ₄ O ₆ → PH ₃ + $\frac{3}{4}$ H ₂ SO ₄
22) H ₂ S + ¼P ₄ O ₆ + ½H ₂ O → PH ₃ + SO ₂
23) 3H ₂ + ¼P ₄ O ₆ → PH ₃ + 1½H ₂ O
24) 3CO + 1½H ₂ O + ¼P ₄ O ₆ → PH ₃ + 3CO ₂
25) 1½S + 1½H ₂ O + ¼P ₄ O ₆ → PH ₃ + 1½SO ₂
26) OCS + 1½H ₂ O + ¼P ₄ O ₆ → PH ₃ + SO ₂ + CO ₂
27) $\frac{3}{5}$ FeS ₂ + 1½H ₂ O + ¼P ₄ O ₆ → PH ₃ + $\frac{3}{5}$ FeO + $\frac{6}{5}$ SO ₂
28) $\frac{6}{11}$ FeS ₂ + 1½H ₂ O + ¼P ₄ O ₆ → PH ₃ + $\frac{3}{11}$ Fe ₂ O ₃ + $\frac{12}{11}$ SO ₂
29) 6FeO + 1½H ₂ O + ¼P ₄ O ₆ → PH ₃ + 3Fe ₂ O ₃
30) 6FeCl ₂ + 7½H ₂ O + ¼P ₄ O ₆ → PH ₃ + 3Fe ₂ O ₃ + 12HCl
<i>Disproportionation of H₃PO₃ (in droplets) and P₄O₆ (in gas phase)</i>
31) P ₄ O ₆ + 1½H ₂ O → PH ₃ + $\frac{3}{4}$ P ₄ O ₁₀
32) 4H ₃ PO ₃ → PH ₃ + 3H ₃ PO ₄

<i>Reduction of H₃PO₃ (in droplets) to PH₃</i>
33) $\frac{3}{4}\text{H}_2\text{S} + \text{H}_3\text{PO}_3 \rightarrow \text{PH}_3 + \frac{3}{4}\text{H}_2\text{SO}_4$
34) $\text{H}_2\text{S} + \text{H}_3\text{PO}_3 \rightarrow \text{PH}_3 + \text{SO}_2 + \text{H}_2\text{O}$
35) $3\text{H}_2 + \text{H}_3\text{PO}_3 \rightarrow \text{PH}_3 + 3\text{H}_2\text{O}$
36) $3\text{CO} + \text{H}_3\text{PO}_3 \rightarrow \text{PH}_3 + 3\text{CO}_2$
37) $1\frac{1}{2}\text{S} + \text{H}_3\text{PO}_3 \rightarrow \text{PH}_3 + 1\frac{1}{2}\text{SO}_2$
38) $\text{OCS} + \text{H}_3\text{PO}_3 \rightarrow \text{PH}_3 + \text{SO}_2 + \text{CO}_2$
39) $\frac{3}{5}\text{FeS}_2 + \text{H}_3\text{PO}_3 \rightarrow \text{PH}_3 + \frac{3}{5}\text{FeO} + \frac{6}{5}\text{SO}_2$
40) $\frac{8}{11}\text{FeS}_2 + \text{H}_3\text{PO}_4 \rightarrow \text{PH}_3 + \frac{4}{11}\text{Fe}_2\text{O}_3 + \frac{16}{11}\text{SO}_2$
41) $6\text{FeO} + \text{H}_3\text{PO}_3 \rightarrow \text{PH}_3 + 3\text{Fe}_2\text{O}_3$
42) $6\text{FeCl}_2 + 6\text{H}_2\text{O} + \text{H}_3\text{PO}_3 \rightarrow \text{PH}_3 + 3\text{Fe}_2\text{O}_3 + 12\text{HCl}$
Reactions with sulphur haze
<i>Reduction by sulphur haze</i>
43) $2\text{S}_{(s)} + \frac{1}{4}\text{P}_4\text{O}_{10} + 1\frac{1}{2}\text{H}_2\text{O} \rightarrow \text{PH}_3 + 2\text{SO}_2$ [solid sulphur in haze particles]
Reduction of phosphate minerals at the surface of the planet or as dust in atmosphere
<i>Whitlockite (Ca₃(PO₄)₂)</i>
44) $1\frac{1}{2}\text{H}_2\text{S} + \frac{1}{2}\text{Ca}_3(\text{PO}_4)_2 \rightarrow \text{PH}_3 + \frac{1}{2}\text{CaSO}_4 + \text{CaO} + \frac{1}{2}\text{S} + \frac{1}{2}\text{SO}_2$
45) $4\text{H}_2\text{S} + \frac{1}{2}\text{Ca}_3(\text{PO}_4)_2 \rightarrow \text{PH}_3 + \frac{3}{2}\text{CaO} + 2\frac{1}{2}\text{H}_2\text{O} + 4\text{S}$
46) $4\text{H}_2 + \frac{1}{2}\text{Ca}_3(\text{PO}_4)_2 \rightarrow \text{PH}_3 + \frac{3}{2}\text{CaO} + 2\frac{1}{2}\text{H}_2\text{O}$
47) $4\text{CO} + \frac{1}{2}\text{Ca}_3(\text{PO}_4)_2 + 1\frac{1}{2}\text{H}_2\text{O} \rightarrow \text{PH}_3 + 1\frac{1}{2}\text{CaO} + 4\text{CO}_2$
48) $1\frac{1}{2}\text{S} + \frac{1}{2}\text{Ca}_3(\text{PO}_4)_2 + 1\frac{1}{2}\text{H}_2\text{O} \rightarrow \text{PH}_3 + \text{CaSO}_4 + \frac{1}{2}\text{CaO} + \frac{1}{2}\text{SO}_2$
49) $\text{OCS} + \frac{1}{2}\text{Ca}_3(\text{PO}_4)_2 + 1\frac{1}{2}\text{H}_2\text{O} \rightarrow \text{PH}_3 + \text{CaSO}_4 + \text{CO}_2 + \frac{1}{2}\text{CaO}$
<i>Fluorapatite (Ca₅(PO₄)₃F)</i>
50) $1\frac{1}{2}\text{H}_2\text{S} + \frac{1}{3}\text{Ca}_5(\text{PO}_4)_3\text{F} \rightarrow \text{PH}_3 + \frac{1}{6}\text{CaF}_2 + \frac{1}{3}\text{CaSO}_4 + \frac{1}{6}\text{CaO} + \frac{3}{4}\text{SO}_2 + \frac{5}{12}\text{S}$
51) $4\text{H}_2 + \frac{1}{3}\text{Ca}_5(\text{PO}_4)_3\text{F} \rightarrow \text{PH}_3 + \frac{1}{6}\text{CaF}_2 + 1\frac{1}{2}\text{CaO} + 2\frac{1}{2}\text{H}_2\text{O}$
52) $4\text{CO} + 1\frac{1}{2}\text{H}_2\text{O} + \frac{1}{3}\text{Ca}_5(\text{PO}_4)_3\text{F} \rightarrow \text{PH}_3 + \frac{1}{6}\text{CaF}_2 + 1\frac{1}{2}\text{CaO} + 4\text{CO}_2$
53) $2\text{S} + 1\frac{1}{2}\text{H}_2\text{O} + \frac{1}{3}\text{Ca}_5(\text{PO}_4)_3\text{F} \rightarrow \text{PH}_3 + \frac{1}{6}\text{CaF}_2 + 1\frac{1}{2}\text{CaO} + 2\text{SO}_2$
54) $1\frac{1}{3}\text{OCS} + 1\frac{1}{2}\text{H}_2\text{O} + \frac{1}{3}\text{Ca}_5(\text{PO}_4)_3\text{F} \rightarrow \text{PH}_3 + \frac{1}{6}\text{CaF}_2 + 1\frac{1}{2}\text{CaO} + 1\frac{1}{3}\text{CO}_2 + 1\frac{1}{3}\text{SO}_2$
<i>Magnesium phosphate (Mg₃(PO₄)₂)</i>
55) $1\frac{1}{2}\text{H}_2\text{S} + \frac{1}{2}\text{Mg}_3(\text{PO}_4)_2 \rightarrow \text{PH}_3 + \frac{1}{2}\text{MgSO}_4 + \text{MgO} + \frac{1}{2}\text{S} + \frac{1}{2}\text{SO}_2$
56) $4\text{H}_2\text{S} + \frac{1}{2}\text{Mg}_3(\text{PO}_4)_2 \rightarrow \text{PH}_3 + \frac{3}{2}\text{MgO} + 2\frac{1}{2}\text{H}_2\text{O} + 4\text{S}$
57) $4\text{H}_2 + \frac{1}{2}\text{Mg}_3(\text{PO}_4)_2 \rightarrow \text{PH}_3 + \frac{3}{2}\text{MgO} + 2\frac{1}{2}\text{H}_2\text{O}$
58) $4\text{CO} + \frac{1}{2}\text{Mg}_3(\text{PO}_4)_2 + 1\frac{1}{2}\text{H}_2\text{O} \rightarrow \text{PH}_3 + 1\frac{1}{2}\text{MgO} + 4\text{CO}_2$
59) $1\frac{1}{2}\text{S} + \frac{1}{2}\text{Mg}_3(\text{PO}_4)_2 + 1\frac{1}{2}\text{H}_2\text{O} \rightarrow \text{PH}_3 + \text{MgSO}_4 + \frac{1}{2}\text{MgO} + \frac{1}{2}\text{SO}_2$
60) $\text{OCS} + \frac{1}{2}\text{Mg}_3(\text{PO}_4)_2 + 1\frac{1}{2}\text{H}_2\text{O} \rightarrow \text{PH}_3 + \text{MgSO}_4 + \text{CO}_2 + \frac{1}{2}\text{MgO}$
<i>Berlinite (AlPO₄)*</i>
61) $2\text{H}_2\text{S} + \text{AlPO}_4 \rightarrow \text{PH}_3 + \frac{1}{2}\text{Al}_2\text{O}_3 + \frac{1}{2}\text{H}_2\text{O} + \text{SO}_2 + \text{S}$

62) $4\text{H}_2\text{S} + \text{AlPO}_4 \rightarrow \text{PH}_3 + \frac{1}{2} \text{Al}_2\text{O}_3 + 2 \frac{1}{2} \text{H}_2\text{O} + 4\text{S}$
63) $4\text{H}_2 + \text{AlPO}_4 \rightarrow \text{PH}_3 + \frac{1}{2} \text{Al}_2\text{O}_3 + 2 \frac{1}{2} \text{H}_2\text{O}$
64) $4\text{CO} + 1\frac{1}{2}\text{H}_2\text{O} + \text{AlPO}_4 \rightarrow \text{PH}_3 + \frac{1}{2}\text{Al}_2\text{O}_3 + 4\text{CO}_2$
65) $2\text{S} + 1\frac{1}{2}\text{H}_2\text{O} + \text{AlPO}_4 \rightarrow \text{PH}_3 + \frac{1}{2} \text{Al}_2\text{O}_3 + 2\text{SO}_2$
66) $1\frac{1}{3}\text{OCS} + 1\frac{1}{2}\text{H}_2\text{O} + \text{AlPO}_4 \rightarrow \text{PH}_3 + \frac{1}{2} \text{Al}_2\text{O}_3 + 1\frac{1}{3}\text{CO}_2 + 1\frac{1}{3}\text{SO}_2$
<i>Potassium phosphate (K₃PO₄)*</i>
67) $\text{K}_3\text{PO}_4 + 4\text{H}_2\text{S} \rightarrow \text{PH}_3 + 1\frac{1}{2}\text{K}_2\text{O} + 2\frac{1}{2}\text{H}_2\text{O} + 4\text{S}$
68) $\text{K}_3\text{PO}_4 + 2\text{H}_2\text{S} \rightarrow \text{PH}_3 + 1\frac{1}{2}\text{K}_2\text{O} + \frac{1}{2}\text{H}_2\text{O} + \text{S} + \text{SO}_2$
69) $\text{K}_3\text{PO}_4 + 4\text{H}_2 \rightarrow \text{PH}_3 + 1\frac{1}{2}\text{K}_2\text{O} + 2\frac{1}{2}\text{H}_2\text{O}$
70) $\text{K}_3\text{PO}_4 + 4\text{CO} + 1\frac{1}{2}\text{H}_2\text{O} \rightarrow \text{PH}_3 + 1\frac{1}{2}\text{K}_2\text{O} + 4\text{CO}_2$
71) $\text{K}_3\text{PO}_4 + 2\text{S} + 1\frac{1}{2}\text{H}_2\text{O} \rightarrow \text{PH}_3 + 1\frac{1}{2}\text{K}_2\text{O} + 2\text{SO}_2$
72) $\text{K}_3\text{PO}_4 + \frac{4}{3}\text{OCS} + 1\frac{1}{2}\text{H}_2\text{O} \rightarrow \text{PH}_3 + 1\frac{1}{2}\text{K}_2\text{O} + \frac{4}{3}\text{SO}_2 + \frac{4}{3}\text{CO}_2$
Excluded reactions
73) $\frac{4}{5}\text{N}_2 + \frac{23}{10}\text{H}_2\text{O} + \frac{1}{4}\text{P}_4\text{O}_{10} \rightarrow \text{PH}_3 + \frac{8}{5}\text{HNO}_3$
74) $\text{HCl} + \frac{1}{4}\text{P}_4\text{O}_{10} + 1\frac{1}{2}\text{H}_2\text{O} \rightarrow \text{PH}_3 + \text{HClO}_4$

Table S6. A complete list of reactions considered in this paper, for all potential PH₃ production pathways. *Aluminum sulfate decomposes at Venus surface temperatures (Truex *et al.* 1977) and so was not considered as a product.

1. 3. 3. Calculation of Subsurface Thermodynamics of Phosphine Production

Oxygen fugacity is a geochemically relevant, quantitative method to calculate the redox state of a mineral, and hence whether that mineral could drive a redox reaction such as the reduction of phosphate to phosphine (Frost 1991). Fugacities are often referred to by reference to standard ‘buffers’. Like the more familiar pH buffer, which provides a stable reference for the concentration of hydrogen ions in solution, an fO₂ buffer provides a stable reference for the chemical activity of molecular oxygen in a rock system, and hence how reduced or oxidized that system is.

For example, the Quartz-Iron-Fayalite (QIF) buffer is based on a mixture of iron, silicon dioxide and iron(II) silicate. The buffer uses the following reaction to buffer O₂:



QIF buffer’s maximum buffering capacity is when:

$$\frac{\{Fe\}^2 \cdot \{SiO_2\}}{\{Fe_2SiO_4\}} = 1 \quad (32)$$

At equilibrium, at this maximum buffering point, the log of oxygen fugacity is directly related to the Gibbs free energy for the reaction described above, as shown by the following formula:

$$\Delta G = 0 = \Delta G^0 + R \cdot T \cdot \ln \left[\frac{\{Fe\}^2 \cdot \{SiO_2\} \cdot \{O_2\}}{\{Fe_2SiO_4\}} \right] \Rightarrow \Delta G^0 = -R \cdot T \cdot \ln[\{O_2\}] \quad (33)$$

Where ΔG is the free energy of reaction and is by definition 0 when the reaction is at equilibrium, and other symbols have meanings given previously. Oxygen fugacity is usually expressed on a log scale, and the more negative it is, the more reducing the rock is. See (Frost 1991) for more detail on the measurement, calculation and application of mineral oxygen fugacity buffers.

A number of standard fO_2 buffers are used in geology as references for the redox states of rock. As iron is the major redox-active metal in the crust by mass, most use the redox states of iron. The four standard fO_2 buffers used as exemplars in this study are shown in Table S7.

Abbreviation	Name	Reaction	Buffered species
QIF	Quartz-Iron-Fayalite	$FeSiO_4 \leftrightarrow Fe + SiO_2 + O_2$	Fe(0) / Fe(+2)
IW	Iron-Wustite	$2Fe_3O \leftrightarrow xFe + O_2$	Fe(0) / Fe(+1 – +1.9)
FMQ	Fayalite-magnetite-quartz	$2 Fe_3O_4 + 3 SiO_2 \leftrightarrow 3Fe_2SiO_4 + O_2$	Fe(+2) / Fe(+2 ^{1/3})
MH	Magnetite-hematite	$6Fe_2O_3 \leftrightarrow 4 Fe_3O_4 + O_2$	Fe(+2 ^{1/3}) / Fe(+3)

Table S7. Four standard fO_2 buffers used in geology as references for the redox states of rock.

We can compare these standard fO_2 buffers with the redox state under which phosphorus present in crustal rocks could be reduced to elemental phosphorus (discussed in Supplementary Section 2.3.2.3.) or to phosphine. Two reactions were modelled to plot the reduction of phosphorus on an oxygen fugacity scale as shown in Table S8, together with three to model the balance between H_2S and SO_2 in the rocks.

Process	Reaction
Reduction of P(+5) to phosphine	$Mg_3(PO_4)_2 + 1\frac{1}{2}SiO_2 + 3H_2O \rightarrow 1\frac{1}{2}Mg_2SiO_4 + 2PH_3 + 4O_2$
Production of elemental phosphorus	$Mg_3(PO_4)_2 + 1\frac{1}{2}SiO_2 \rightarrow 1\frac{1}{2}Mg_2SiO_4 + \frac{1}{2}P_4 + 2\frac{1}{2}O_2$
Production of H_2S from sulphate	$3MgSO_4 + 1\frac{1}{2}SiO_2 + 3H_2O \rightarrow 1\frac{1}{2}Mg_2SiO_4 + 3H_2S + 6O_2$
Production of SO_2 from sulphate	$3MgSO_4 + 1\frac{1}{2}SiO_2 \rightarrow 1\frac{1}{2}Mg_2SiO_4 + 3SO_2 + 1\frac{1}{2}O_2$
Production of H_2S from SO_2	$SO_2 + H_2O \rightarrow H_2S + \frac{1}{2}O_2$

Table S8. Reactions modelled to plot the reduction of phosphorus in the oxygen fugacity scale. Sulphur is assumed to be present in rocks as magnesium sulphate. The ratio of $H_2S:SO_2$ is calculated from the ratio of the energy of production of H_2S from magnesium sulphate rock compared to the energy of production of SO_2 from the same rock.

Following from the equation above (eq. (33)), the oxygen fugacity needed to allow 50% of the phosphorus in a rock to be present as phosphine is given by

$$\Delta G = 0 = \Delta G^0 + RT \ln(Q) \quad (34)$$

and therefore, for production of PH_3 , for example (following the reaction shown in Table S8),

$$\Delta G^0 + R \cdot T \cdot \ln \left(\frac{\{Mg_2SiO_4\}^{1.5} \cdot \{PH_3\}^2 \cdot \{O_2\}^4}{\{Mg_3(PO_4)_2\} \cdot \{SiO_2\}^{1.5} \cdot \{H_2O\}^3} \right) = 0 \quad (35)$$

If we assume $\{\text{SiO}_2\}$ is $\sim \{\text{Mg}_2\text{SiO}_4\}$ (i.e. to within a factor of two or three, the amount of magnesium and the amount of silicon in the rocks is the same), and as we have defined this to be at the reaction half-point, so that by definition $\{\text{PH}_3\}^2 = \{\text{Mg}_3(\text{PO}_4)_2\}$, then

$$\Delta G^0 = -R \cdot T \cdot 2.5 \cdot [\ln(\{O_2\})] \quad (36)$$

and hence

$$\log(\{O_2\}) = \frac{\frac{\Delta G^0}{R \cdot T}}{2.5} \cdot 0.4343 \quad (37)$$

for the reaction shown in Table S8. Because f_{O_2} values typically span tens of orders of magnitudes, they are usually plotted on a \log_{10} scale, hence multiplying the natural log value by 0.4343. f_{O_2} is sensitive to temperature, but relatively insensitive to pressure.

We have also included the $\text{SO}_2/\text{H}_2\text{S}$ couple in our fugacity calculations to validate that the calculation method gave results consistent with real geochemistry that was identified on Earth.

2. Supplementary Results

Below we show the individual curves of free energy of reaction as a function of altitude for the reactions listed in Table S6. For each reaction a maximum and minimum free energy is calculated for each altitude (different free energies result from different assumptions about the gas concentrations in the atmosphere, as discussed above); the overall maximum and minimum values for each set of reactions is show by the two dashed lines on each graph (Figure S9 and Figure S10).

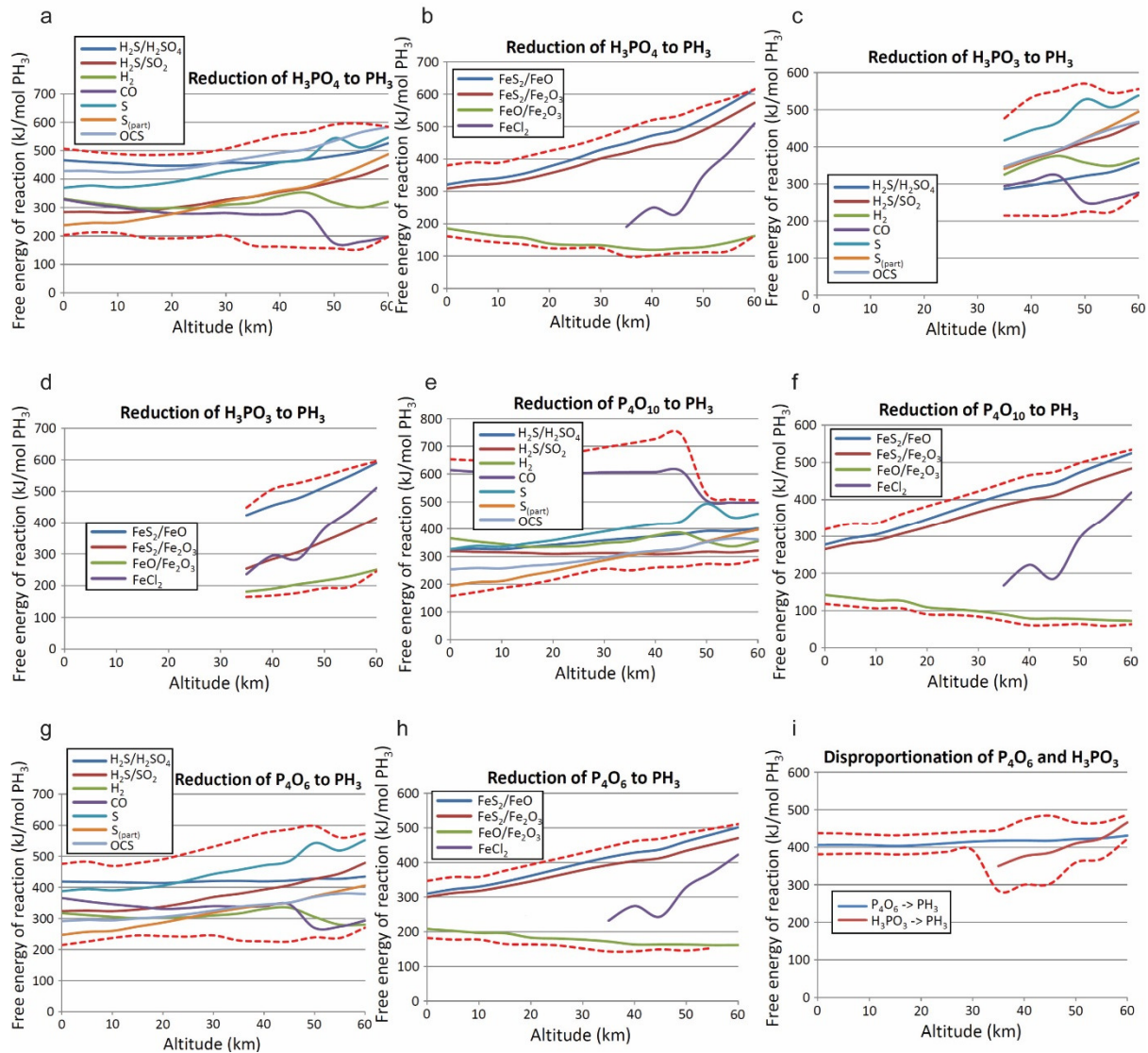


Fig. S9. Thermodynamics of phosphine production in the Venusian atmosphere-surface environment. x axis: altitude (km), y axis: Gibbs free energy of reaction (ΔG) (kJ/mol). Dashed lines show the limits of the free energy found for any combination of gas partial pressures, for any altitude, for any reaction in a set of reactions. Each solid line represents a different reductant, and in the case of H_2S as a reductant, a different oxidized product. ‘S’ is elemental sulfur in gas phase, ‘S_(part.)’ is elemental sulfur in solid (particle) phase. (a) Free energy of reduction of orthophosphoric acid by gaseous reductants under Venus atmosphere conditions. (b) Free energy of reduction of orthophosphoric acid by mineral reductants under Venus atmosphere conditions. Note that the line for FeCl_2 only covers altitudes from 35 km upwards. Below 35 km FeCl_2 is unstable to hydrolysis to HCl and FeO under Venus atmosphere conditions in nearly all scenarios (Figure S8). Calculations are done for altitudes up to 60 km because, in principle, minerals could be carried to the cloud tops as dust. (c) Reduction of H_3PO_3 to phosphine by atmospheric reductants. Note that H_3PO_3 is not stable outside a liquid droplet under Venus temperatures, and so these calculations are only performed for altitudes at which cloud droplets could exist. (d) Reduction of H_3PO_3 to PH_3 by mineral reductants. (e) Reduction of P_4O_{10} to PH_3 by atmospheric components. (f) Reduction of P_4O_{10} to PH_3 by mineral / dust. (g) Reduction of P_4O_6 by atmospheric components. (h) Reduction of P_4O_6 by mineral / dust. (i) Disproportionation of P_4O_6 and H_3PO_3 species to PH_3 . In conclusion (a-i), the formation of phosphine in the Venusian atmosphere-surface environment cannot proceed spontaneously (i.e. none of the conditions considered result in a negative free energy).

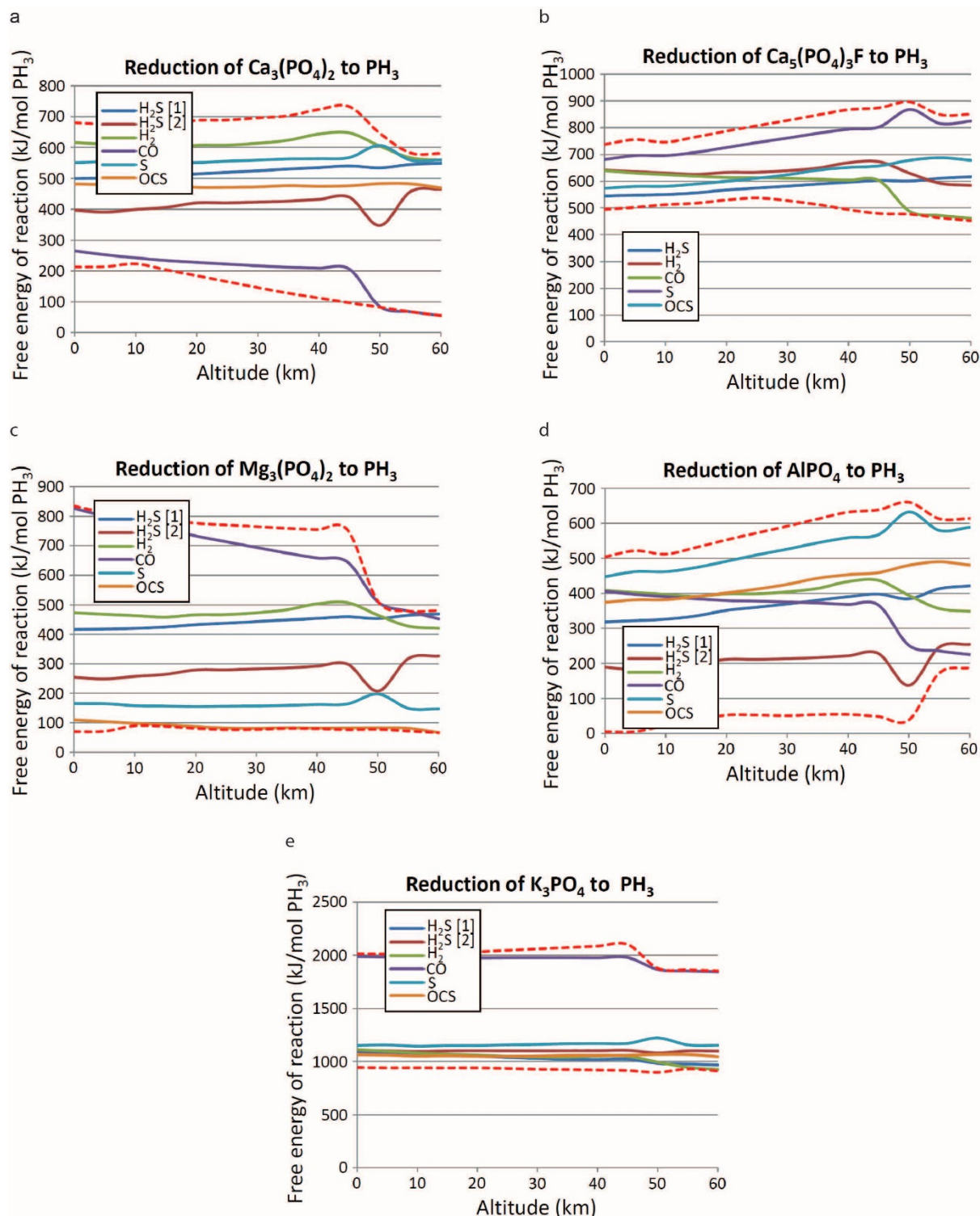


Fig. S10. Thermodynamics of the reduction of mineral phosphates by atmospheric gases. x axis: altitude (km), y axis: Gibbs free energy of reaction (ΔG) (kJ/mol). Dashed lines show the limits of the free energy found for any combination of gas partial pressures, for any altitude, for any reaction in a set of reactions. Each solid line represents a different reductant. (a) Reduction of calcium phosphate (whitlockite) by Venusian trace atmospheric gases. Reactions are calculated to 60km altitude to cover the possibility that dust could be carried into the cloud layer. H_2S [1]: reaction $\frac{1}{2}\text{H}_2\text{S} + \frac{1}{2}\text{Ca}_3(\text{PO}_4)_2 \rightarrow \text{PH}_3 + \frac{1}{2}\text{CaSO}_4 + \text{CaO} + \frac{1}{2}\text{S} + \frac{1}{2}\text{SO}_2$; H_2S [2]: reaction $4\text{H}_2\text{S} + \frac{1}{2}\text{Ca}_3(\text{PO}_4)_2$

-> $\text{PH}_3 + \frac{3}{2}\text{CaO} + 2\frac{1}{2}\text{H}_2\text{O} + 4\text{S}$ (b) Reduction of calcium fluorophosphate (fluorapatite) to PH_3 by atmospheric gases. (c) Reduction of magnesium phosphate ($\text{Mg}_3(\text{PO}_4)_2$) to phosphine by atmospheric gases. (d) Reduction of aluminium phosphate (berlinite) (AlPO_4) to phosphine by atmospheric gases. We note that some combinations of extreme values of the partial pressure of both H_2S and elemental sulfur (S_2) come close to predicting a negative ΔG value for phosphine production at the surface. ΔG values are affected by the substantial uncertainty in the partial pressures of H_2S , H_2O and gas phase elemental sulfur. Constraining the partial pressures of those gases is important to validate whether the reduction of aluminium phosphate could be a source of phosphine. (e) Reduction of potassium phosphate ($\text{K}_3(\text{PO}_4)$) to phosphine by atmospheric gases. In conclusion (a-e), formation of phosphine by reduction of surface mineral phosphates in the Venusian atmosphere-surface environment cannot proceed spontaneously (i.e. none of the conditions considered result in a negative free energy).

2. 1. Sensitivity Analysis to Variations of Venus Atmospheric Gas Concentrations

To test the sensitivity of our results to the assumptions about gas concentrations, we asked how much each gas concentration listed in Table S5 would have to be changed for *any* of the reactions listed in Table S6 to be exergonic for phosphine production at *any* altitude. The results are shown in Figure S11.

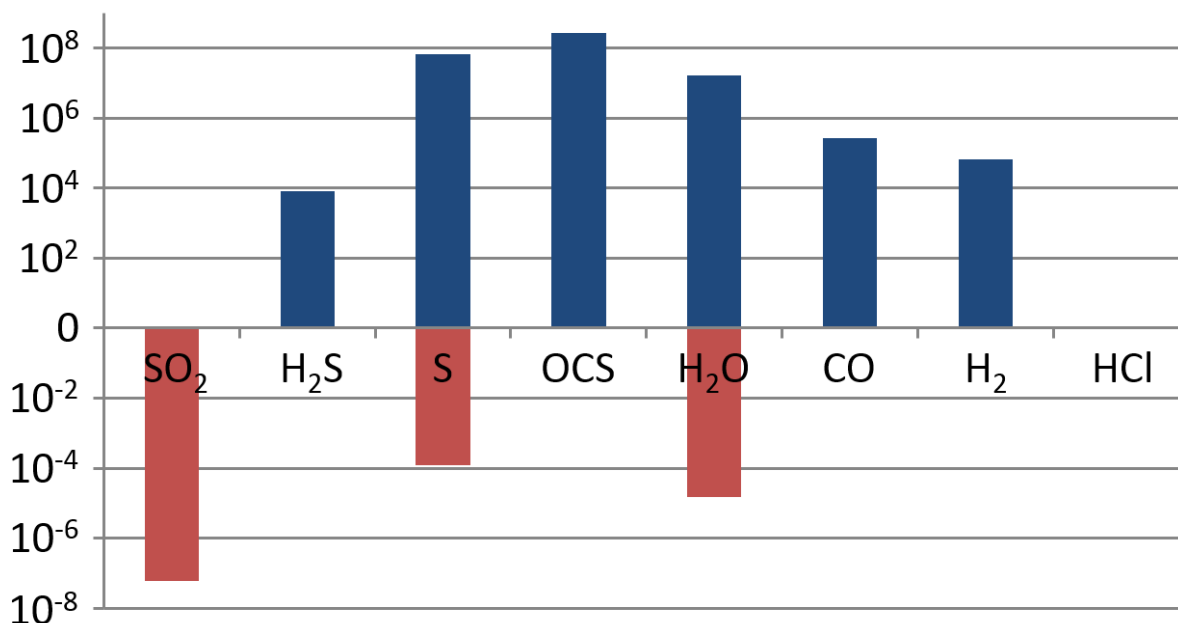


Fig. S11. Fractional change in partial pressure of trace gases needed to produce a negative ΔG value for phosphine production through any chemistry at any altitude. x axis: gaseous reductant. y axis: fold increase ($y > 1$) or decrease ($y < 1$) in partial pressure needed for thermodynamically favorable conditions for phosphine production. Gases were set to the geometric mean of the maximum and minimum values in Table S5, and then each gas was increased in steps to a maximum of 10^9 of its mean value, or decreased to a minimum of 10^{-9} of its mean value. Bars represent the smallest change that would give a negative ΔG for phosphine production at *any* altitude using *any* reaction: bars above $y=1$ imply an increase in partial pressure is favorable, bars below $y=1$ imply a decrease in partial pressure is favorable. If there is no bar above the axis, then no increase in gas concentration can drive phosphine production. Similarly, no bar below the axis implies that no reduction in gas can drive phosphine production. CO_2 was not varied, as its partial pressure is well known to within a few percent. In summary, the estimations of gas

concentrations would have to be incorrect by more than four orders of magnitude for our conclusions to change, i.e. for the formation of phosphine to be exergonic and likely to occur spontaneously.

For example, no tested change in HCl partial pressure resulted in phosphine production. Only H₂S and CO have values which suggest that very substantial systematic errors in measurements or modelling could account for the production of phosphine. If the maximum concentration of H₂S was $\sim 10^4$ -fold higher than the highest level reported in the literature, or that of CO was 3.10^5 -fold higher, then under some conditions they could drive phosphine production. Such an unlikely scenario would be equivalent to 0.1% H₂S or 1% CO in Venus' atmosphere. All other gases would require physically unrealistic changes in their partial pressures to drive phosphine production. For example, a reduction of SO₂ by a factor of 5.8×10^{-8} , necessary to allow phosphine production, implies a partial pressure of 10^{-13} , which is at least 4 orders of magnitude below the detection limits of the instruments that have detected SO₂ on Venus.

2. 2. Validation of the Fugacity Calculations

2. 2. 1. H₂S/SO₂ as a Qualitative Validation of the Fugacity Calculations

As a qualitative validation of the fugacity calculation we calculate the fugacity of the terrestrial H₂S/SO₂ equilibrium (Figure S12 - blue line). For example, at 1000 K (the temperature of the vertical black line, on Figure S12), in a rock with the oxygen fugacity of QIF, at low temperatures, sulfur will predominantly be reduced (yellow QIF line is *below* blue H₂S/SO₂ line), whereas at high temperatures sulfur will predominantly be oxidized (yellow QIF line is *above* blue H₂S/SO₂ line).

The results from the SO₂/H₂S line are qualitatively consistent with field observations on Earth and modelling on Mars. Specifically, Terrestrial and Martian mantle rocks typically have fO₂ values between FMQ-4 and FMQ+3 (Ballhaus *et al.* 1990), a region shaded in grey on the graphs on Figure S12 and Figure S13. The SO₂/H₂S fO₂ curve falls largely within this zone, and indeed terrestrial volcanoes can emit SO₂, H₂S or a mixture from primary degassing. Consistent with this observation, gases evolved from rocks at higher temperature, or rocks containing less water or with higher oxygen fugacity (smaller negative log number) have a lower H₂S/SO₂ ratio (Gerlach 1982; Hoshyaripour *et al.* 2012; Whitney 1984) on Earth and on Mars (Gaillard and Scaillet 2009).

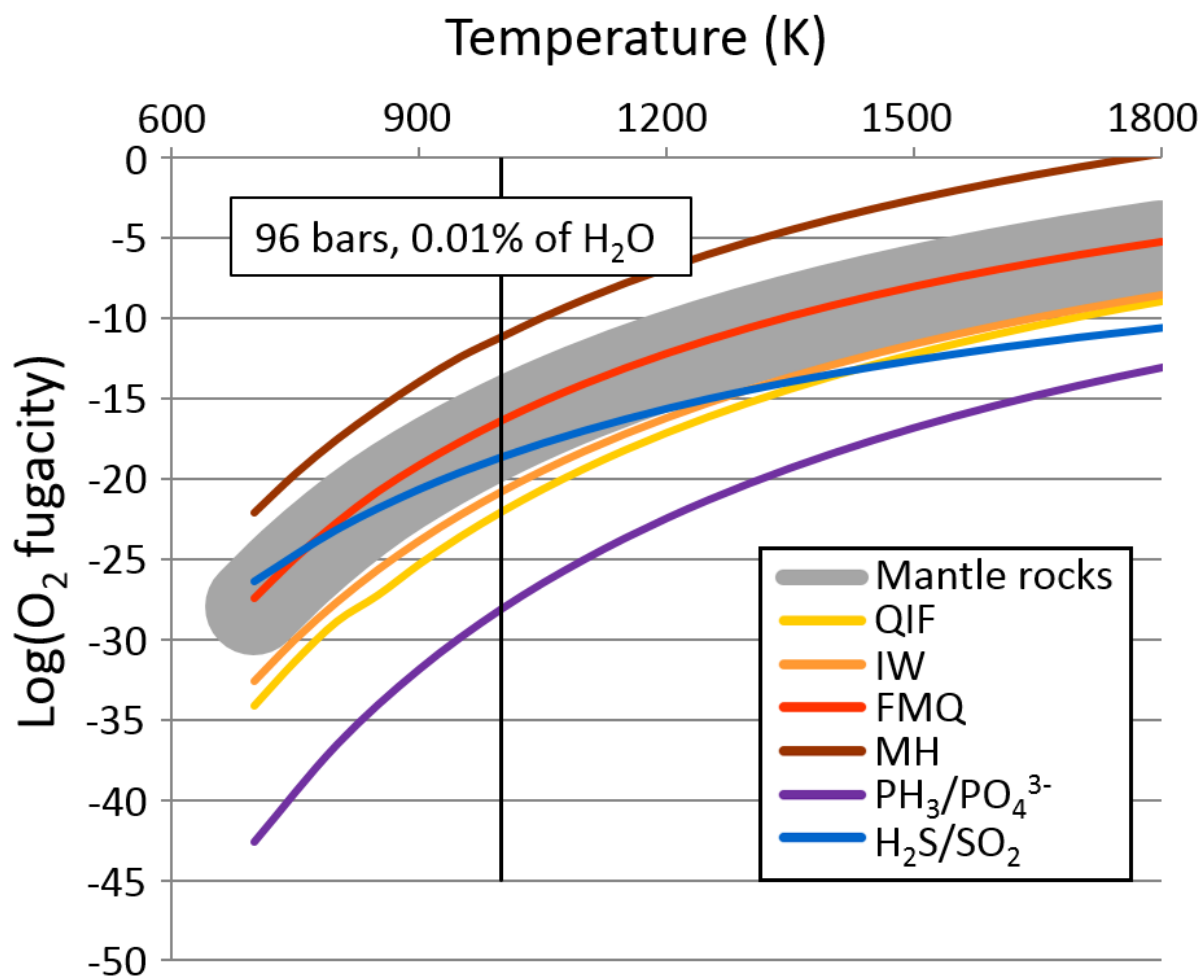


Fig. S12. Comparison of the fugacity of the phosphate/phosphine equilibrium to the fugacity of the standard mineral buffers of terrestrial rocks and the fugacity of the terrestrial H₂S/SO₂ equilibrium (blue line). x axis: log O₂ fugacity, y axis: Temperature (K). Fugacity of the production of phosphine from phosphate minerals is calculated for 96 bars and 0.01% water in the rocks. The fugacity of the phosphate/phosphine equilibrium is shown as a purple line. The other curves are O₂ fugacities of standard rock buffers. The phosphate/phosphine fO₂ curve lies below the QIF buffer line (the most reduced rock of the buffers shown) which falls below the typical fO₂ of terrestrial mantle or crustal rocks (grey band region). Therefore, typical terrestrial rocks are too oxidized to produce PH₃ from phosphates and the formation of phosphine is highly unlikely under Venusian subsurface conditions.

2. 2. 2. Sensitivity Analysis on Subsurface Fugacity Calculations.

We modelled combinations of f(O₂) of the phosphate/phosphine equilibrium in the plausible Venusian pressure range, and for water content of the rocks of 0,01-5% (unrealistically high for modern Venus, but found in some recently subducted rocks on Earth). We note that the mineral redox buffers are also pressure sensitive (Frost 1991), but this effect is trivial at crustal pressures. Phosphine production is not favored under any plausible crustal conditions (Figure S13).

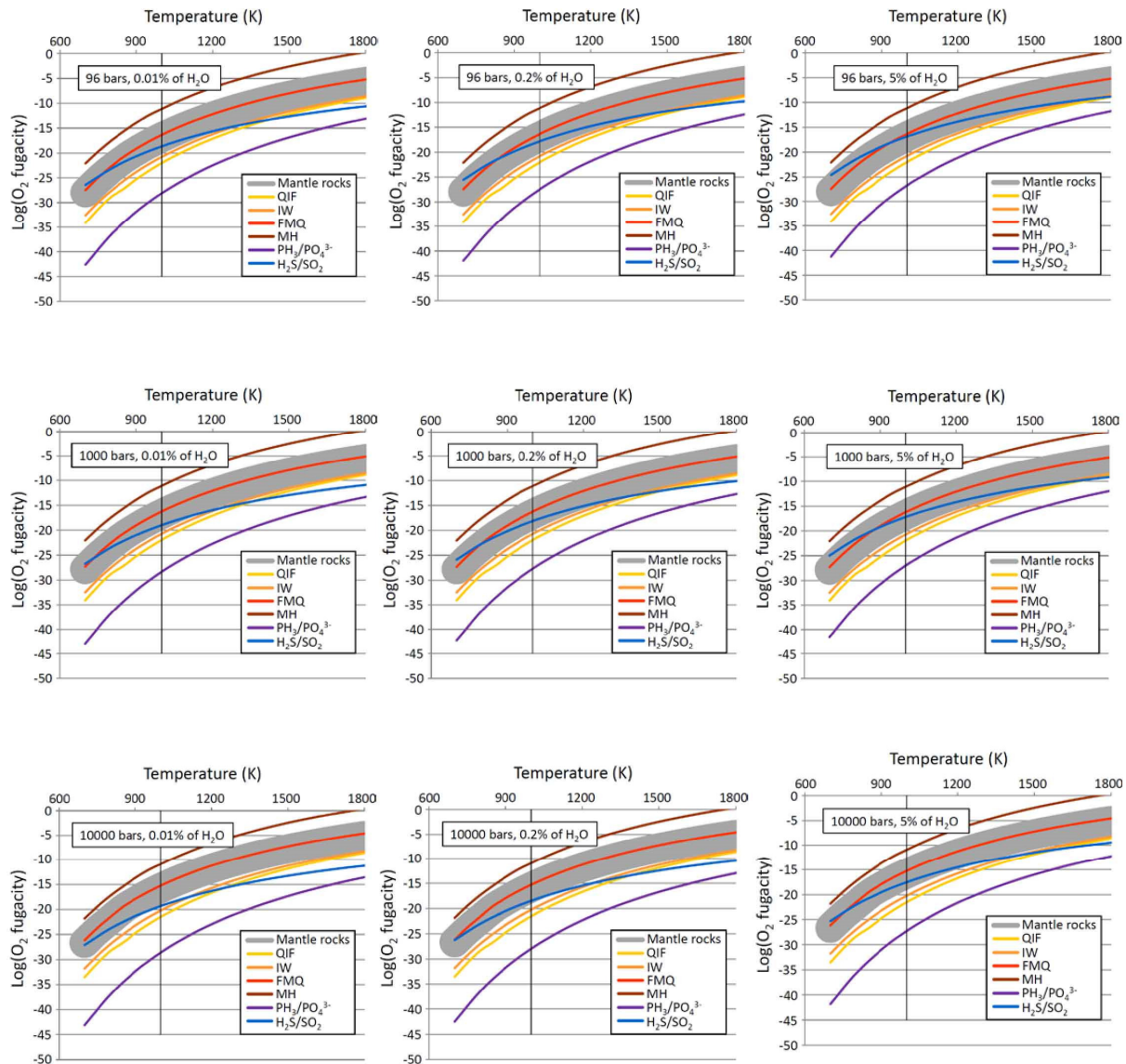


Fig. S13. Oxygen fugacity of the phosphate/phosphine equilibrium under variable pressures and water content values. x axis: logO₂ fugacity, y axis: Temperature (K). Fugacity of the production of phosphine from phosphate minerals is calculated for range of pressure values (96-10000 bars) and subsurface water abundances ranging from very low (0.01%) to very high (5%) water content. Phosphine production is not favored under any plausible crustal conditions (the phosphate/phosphine fO₂ curve lies way below the most rock, the QIF buffer line).

2. 2. 3. Amount of Phosphine Produced by Volcanism

The amount of volcanism required to produce a given flux of phosphine was calculated as follows. We calculated the ratio of P(+5):P(-3) based on the f(O₂) values of six redox buffers with redox states between IW (Iron/Wustit: Fe/FeO) and MH (Magnetite/Haematite: Fe₃O₄/Fe₂O₃) buffers, including the IW and MH buffers themselves. IW and MH buffers represent the limits of oxygen fugacity commonly found in terrestrial mantle rocks. The P(+5):P(-3) ratio calculations were done for a temperature range of 700 K to 1600 K

(representing the extremes of temperatures seen in outgassing in terrestrial volcanoes), 100 to 10000 bar and 0.00015 to 0.015 rock water content. The results are shown in Figure S13a-A.

From this we can estimate the total amount of phosphorus that has to be outgassed in order to provide a flux of 4.16 kg/second across the planet (1.3×10^{11} grams per (terrestrial) year) that is needed to maintain an atmospheric concentration of ~20 ppb by the following equation:

$$P_T = 4160 \cdot \frac{P_O}{P_R},$$

where P_T = the total phosphorus outgassing needed in grams/second/planet, and P_O/P_R is the ratio of oxidized to reduced phosphorus in the outgassed phosphorus species, assuming that almost all the phosphorus is present in an oxidized form. This flux is plotted in Figure 8 of the main paper.

We relate the flux of phosphorus outgassing necessary to maintain a 20 ppb atmospheric level to terrestrial volcanic outgassing rates as follows. The rate at which phosphorus is outgassed from terrestrial volcanoes is not known, as phosphorus is produced in volcanoes as non-volatile phosphate species or as P_4O_{10} which rapidly condenses with atmospheric water to form phosphoric acid. We therefore assume that the ratio of phosphorus to sulfur production by volcanoes is the same as the ratio of phosphorus to sulfur in metamorphic rock, and estimate phosphorus ‘outgassing’ by reference to sulfur outgassing. The ratio of sulfur to phosphorus in metamorphic rock varies widely with the rock, but averages ~1.9 (Figure S13a-B). Sulfur is outgassed at a rate of approximately 285 kg/second (Halmer *et al.* 2002) on Earth, suggesting ~143 kg/second of phosphorus is outgassed on Earth.

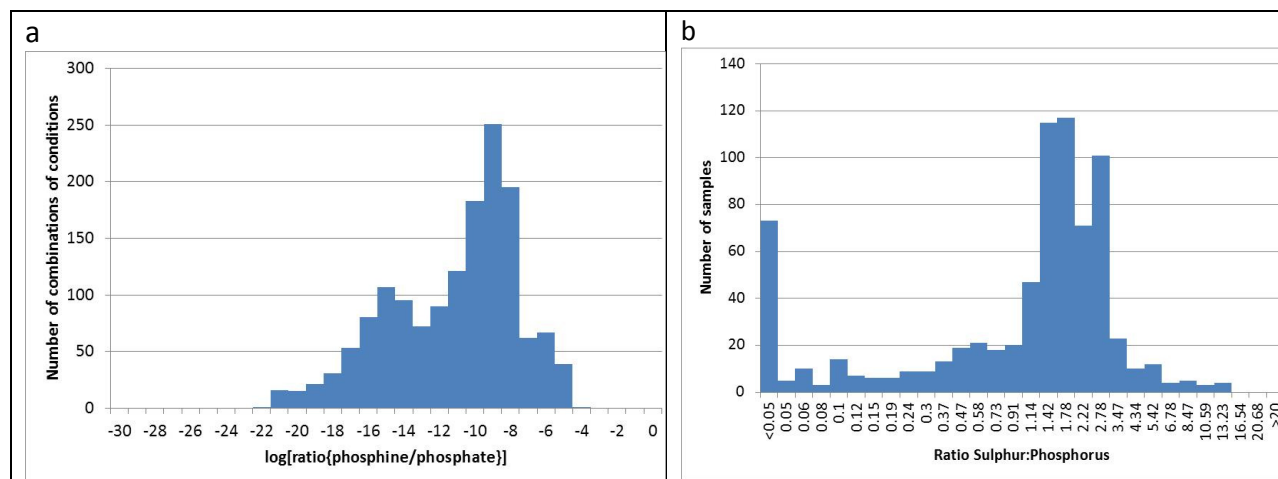


Fig. S13a. Calculation of the flux of phosphine from volcanic eruption. a) Log of ratio of $P(-3)/P(+5)$ based on fugacity calculation for a total of 1500 combinations of conditions, as described in the text. x axis: $\log_{10}(P(-3)/P(+5))$, in bins of 1 log unit. y axis: number of condition combinations producing this ratio. b) Ratio of sulfur to phosphorus in 745 igneous rock samples where both S and P concentrations were measured. x axis: sulfur/phosphorus ratio, y axis: number of samples with that ratio of S/P. Note that some samples are volcanic material from which nearly all the sulfur has been lost as sulfur gases. The average ratio S/P is 1.91, i.e. sulfur is approximately twice as abundant in these samples as phosphorus. The data were downloaded from the PetDB Database (www.earthchem.org/petdb; (Lehnert *et al.* 2000)) on 19th Sept 2019, using the following parameters: Trace elements = S AND P, igneous rock samples only, one data point per sample).

2. 3. Details on Other Potential Processes of Phosphine Formation

2. 3. 1. Formation of Phosphine by Lightning

Our assumptions are as follows. If the Vega data represents genuine atmospheric phosphorus, then the column density of phosphorus is (order of magnitude) similar to sulfuric acid (Titov *et al.* 2018). Density of cloud and haze materials in the cloud layer is $\sim 0.2 \mu\text{g}/\text{m}^3$ (assuming droplet density of 2 g/ml) (Knollenberg and Hunten 1979), of which maybe $\frac{1}{4}$ is phosphate (i.e. $\frac{1}{12}$ is phosphorus atoms). We assumed that the overall dimensions and frequency of lightning strikes are similar to those found on Earth; the average lightning bolt is 25 mm wide and 8 km long¹, i.e. $\sim 4 \text{ m}^3$; with 100 lightning strikes per second; noting that this is a matter of debate (Lorenz 2018).

We assume for simplicity that the lightning bolt leads to a complete atomization of chemicals within a droplet or within the gas inside the volume of the lightning stroke, and that subsequent recombination of the atoms into stable chemicals proceeds at random, and dependent solely on the number density of the atoms in the resulting plasma².

In principle, lightning could generate atoms in gas phase, which could then recombine to form phosphine, or if the lightning happened at an altitude where there was cloud, could recombine to make phosphite dissolved in droplets. In the second case, the droplets could then evaporate and drive disproportionation of the phosphite to generate phosphine. There are therefore four scenarios under which lightning could in principle produce phosphine (Table S9).

Name	Process	Subsequent chemistry
Gas / PH ₃	Lightning passes through atmospheric gas.	Atoms reassemble into phosphine
Gas / P ₄ O ₆		Atoms reassemble into phosphite P(+3) species dissolved in re-condensing droplets, which subsequently disproportionates to phosphine
Droplet / PH ₃	Lighting passes through droplets	Atoms reassemble into phosphine
Droplet / P ₄ O ₆		Atoms reassemble into phosphite, which subsequently disproportionates to phosphine

Table S9. Four scenarios under which lightning could produce phosphine on Venus.

We modeled all four scenarios for all the atmospheric gas partial pressures and cloud levels (and hence cloud particle compositions) described in Supplementary Section 1.3.2. and Table S5. Each set of conditions gives a mass of phosphine produced per Venusian year. The results are summarized in Figure S14.

¹ We note that there are several reports available describing lightning discharges on Earth that are unusually long (up to hundreds of kilometres) but such discharges are extremely rare (Lyons *et al.* 2020; Peterson 2019).

² This is an unrealistic but conservative assumption. Realistic kinetic model for recombination between ions in many ionization states, radicals and molecules, in a volume that is cooling at an unknown rate is not practical.

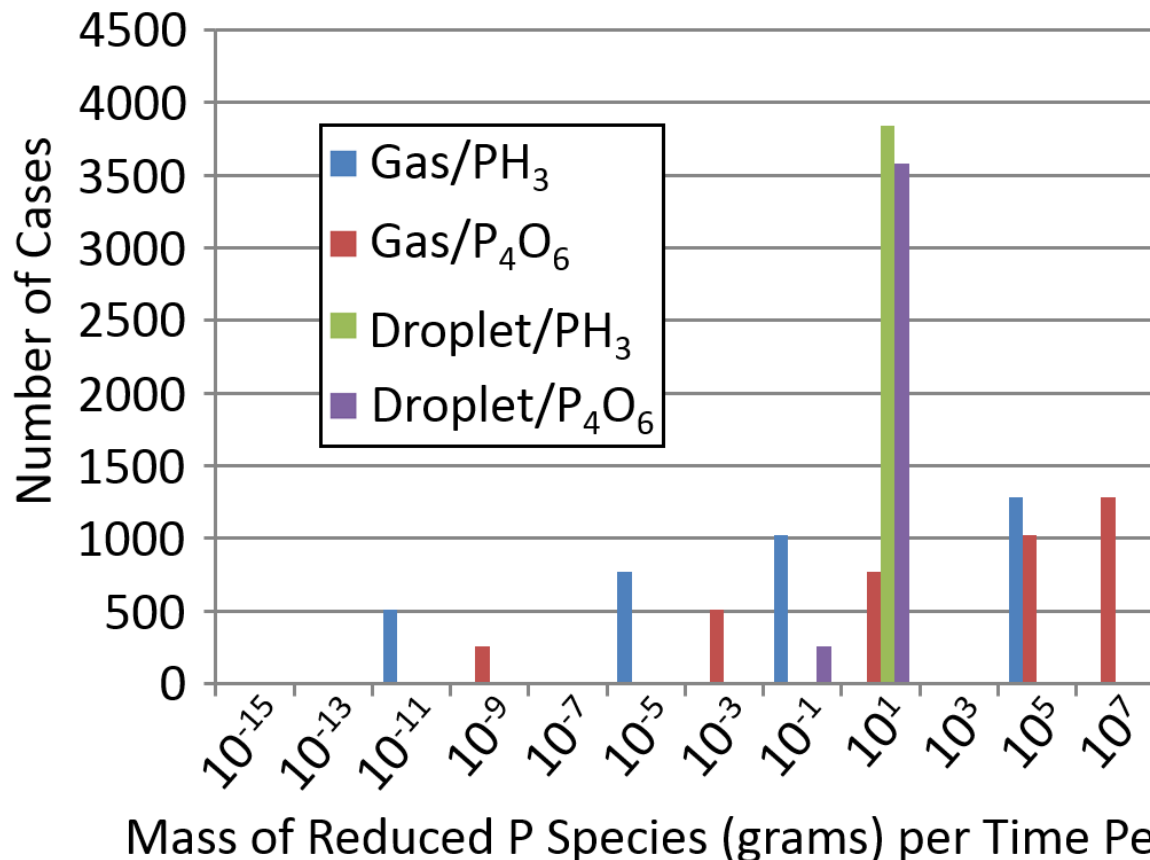


Fig. S14. Mass of phosphine produced by lightning per Venusian year. x axis: mass of phosphine produced, binned into 100-fold logarithmic bins. y axis: number of scenarios producing a given mass of phosphine. In principle, lightning could produce phosphine directly or indirectly through production of P(3+) species which subsequently disproportionate to phosphine (Table S9). In practice, none of the 3840 scenarios of different atmospheric gas concentrations and cloud base and top altitudes (see Supplementary Section 1.3.2. for details) are sufficient to produce the observable amount of phosphine. Therefore, lightning strikes on Venus are not responsible for phosphine production.

The maximum amount of phosphine produced in one Venusian year is 3.38×10^8 grams. If this accumulated in Venus' atmosphere for a full Venusian year without any destruction, it would reach a partial pressure of 0.76 parts per quadrillion, much lower than the observed phosphine concentration in the Venusian atmosphere (Greaves *et al.* 2020).

2. 3. 2. Unknown Chemistry as an Explanation

2. 3. 2. 1. Phosphine Chemistry in Concentrated Sulfuric Acid

Phosphine is readily oxidized on passing through concentrated sulfuric acid at Earth ambient temperatures. The chemistry has been known for over 140 years, as it was used as a method to remove phosphine from acetylene. Acetylene was widely used as a gas for lighting in the late 19th and early 20th century before the advent of electrification, and the gas was manufactured by

the acid hydrolysis of calcium carbide. Trace phosphide and sulfide in the carbide lead to phosphine and hydrogen sulfide in the acetylene, which caused undesirable smell in the gas and ‘haze’ of H₃PO₄ and H₂SO₄ produced on burning (Doman 1902). Passing the gas through H₂SO₄ efficiently cleared out both gases (reviewed in (Doman 1902; Leeds and Butterfield 1910)). The process fell into disuse in the West in the 1900s, replaced by purification of acetylene over chromic acid (Leeds and Butterfield 1910), and became obsolete when carbides as a source of acetylene were replaced by synthesis by partial oxidation of methane (Sachsse 1954); however the method remains in use in China (Cai *et al.* 2010; Xiao-yong 2009). Reaction temperatures are typically cited as between 0 °C and 15 °C.

There is very limited data on the kinetics of the oxidation of phosphine with sulfuric acid reaction. The citations above state that acetylene is passed up a tower down which >95% H₂SO₄ is sprayed, implying efficient removal (by rapid oxidation of phosphine to phosphoric acid) in 10s of seconds. (Dorfman *et al.* 1991) state that the reaction occurs at negligible rate at concentrations of acid below ~90% acid by weight. Such reaction behavior suggests attack on PH₃ by SO₃, which is consistent with the electrophilic attack by SO₃ on the lone pair on PH₃ (PH₃ is not significantly ionized in pure sulfuric acid, unlike NH₃ which is exclusively present as NH₄⁺), and with B3LYP *ab initio* calculations to 6-311-G level of the energy of the reaction:



(Lorenz *et al.* 1963) report that the reaction between 99% H₂SO₄ and PH₃ is at least 99% complete in 40 seconds at 60 °C , and (Perraudin 1961) reports that PH₃ is effectively cleared by bubbling through a thin layer of H₂SO₄ <~1 cm deep. (Leeds and Butterfield 1910) claim that the reaction is efficient down to -20 °C. It is therefore likely that phosphine will be oxidized efficiently by the sulfuric acid in Venus’ lower clouds. Oxidation in the upper clouds, where the concentration of sulfuric acid is below 90% and temperature below 270 K is unknown, but it is very unlikely that any process would *synthesize* phosphine under these conditions.

2. 3. 2. 2. *Production of Phosphine from Elemental Phosphorus*

Elemental phosphorus is most stable as P₄ (“White” phosphorus”) at Venus surface conditions. The standard state for elemental phosphorus - “Red” phosphorus - which is more stable at temperatures <540 K (at 1bar) is not volatile, and so would not be present in the atmosphere. Thermodynamic calculations are therefore done for P₄. However, the free energy difference between reference P and P₄ is <7 kJ per mole of phosphorus atoms at the temperatures considered in this model, and so the difference between the two allotropes will be small.

We modelled the production of phosphine from elemental phosphorus using reducing agents and hydrogen sources available in Venus' atmosphere, using the same approach as described in Supplementary Section 1.3.2. (Figure S15).

- 1) $1\frac{1}{2}\text{H}_2\text{S} + \frac{1}{4}\text{P}_4 \rightarrow \text{PH}_3 + 1\frac{1}{2}\text{S}$
- 2) $1\frac{1}{2}\text{H}_2 + \frac{1}{4}\text{P}_4 \rightarrow \text{PH}_3$
- 3) $1\frac{1}{2}\text{CO} + 1\frac{1}{2}\text{H}_2\text{O} + \frac{1}{4}\text{P}_4 \rightarrow \text{PH}_3 + 1\frac{1}{2}\text{CO}_2$
- 4) $\frac{3}{4}\text{S} + 1\frac{1}{2}\text{H}_2\text{O} + \frac{1}{4}\text{P}_4 \rightarrow \text{PH}_3 + \frac{3}{4}\text{SO}_2$
- 5) $\frac{1}{2}\text{OCS} + 1\frac{1}{2}\text{H}_2\text{O} + \frac{1}{4}\text{P}_4 \rightarrow \text{PH}_3 + \frac{1}{2}\text{SO}_2 + \frac{1}{2}\text{CO}_2$

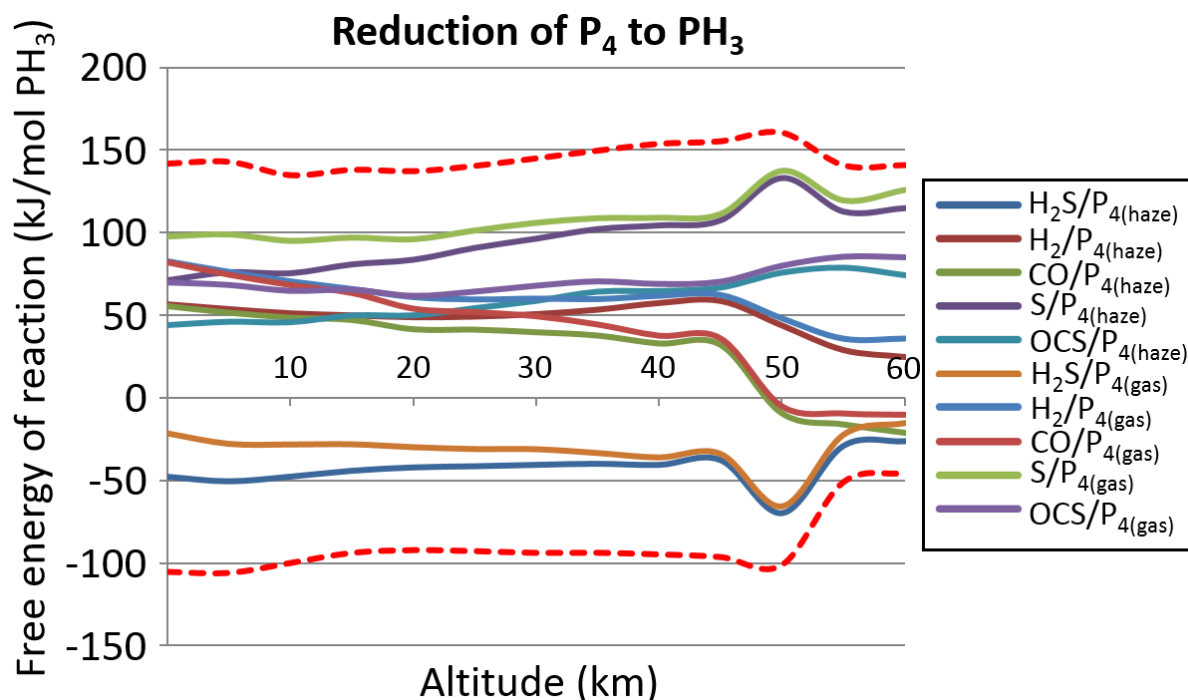


Fig. S15. Thermodynamics of phosphine production from reaction of elemental phosphorus in gas phase or as a solid ('haze') in Venus atmosphere. x axis: altitude (km), y axis: Gibbs free energy of reaction (ΔG) (kJ/mol). Dashed lines show the limits of the free energy found for any combination of gas partial pressures, for any altitude, for any reaction in a set of reactions. Only the reactions of elemental phosphorus with hydrogen sulphide may provide a source of phosphine.

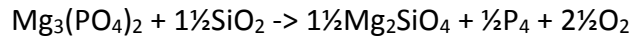
The Figure S15 shows the reaction of elemental phosphorus with hydrogen sulphide may provide a source of phosphine. Reduction of elemental phosphorus by CO and water (water to provide hydrogen atoms) is also potentially favourable at cloud level. Even with elemental phosphorus as a source of phosphorus atoms, no other reaction is favourable for making phosphine.

However, the production of elemental phosphorus it itself extremely unlikely under any plausible Venus' surface and subsurface conditions. In brief, fugacity calculations show that elemental phosphorus is no more likely to be outgassed on Venus than phosphine. Therefore, in suggesting

elemental phosphorus as a source of phosphine, we have just exchanged the difficulty of making phosphine for the equal difficulty of making elemental phosphorus.

2. 3. 2. 3. *Crustal Production of Elemental Phosphorus*

We addressed whether crustal chemistry could produce elemental phosphorus as a source of reduced phosphorus species that could subsequently be reduced to phosphine. We replicated the fugacity model shown in Supplementary Section 1.3.3., by comparing mineral oxygen fugacity buffers to the oxygen ‘fugacity’ of the following reaction:



The results are shown on Figure S16.

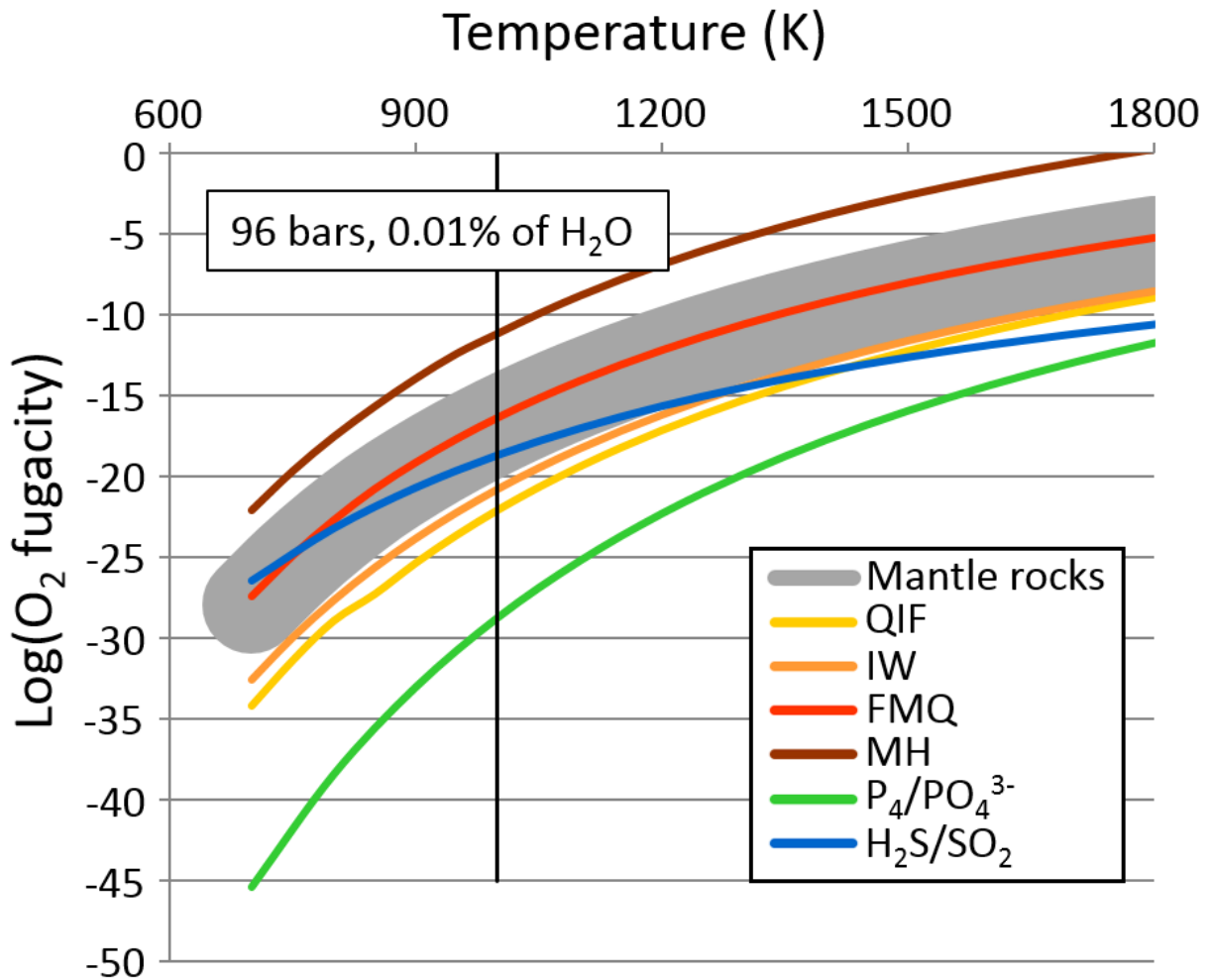


Fig. S16. Comparison of the fugacity of the phosphate/P₄ equilibrium to the fugacity of the standard mineral buffers of terrestrial rocks. x axis: log O₂ fugacity, y axis: Temperature (K). Fugacity of the production of P₄ from phosphate minerals is calculated for 96 bars and 0.01% water in the rocks. The fugacity of the phosphate/P₄

equilibrium is shown as a green line. The other curves are O_2 fugacities of standard rock buffers. The formation of elemental phosphorus is highly unlikely under Venusian conditions. Fugacity of the production of elemental phosphorus from phosphate minerals calculated for 96 bars, 0.01% water.

The results obtained for the formation of elemental phosphorus in subsurface rocks are similar to the results obtained for the possibility of the formation of phosphine (Figure S12 and Figure S13). We conclude that it is extremely unlikely that crustal rocks could produce elemental phosphorus, and as a result it is very unlikely that the observed atmospheric phosphine comes from the reduction of subsurface fraction of the elemental phosphorus.

2. 3. 2. 4. High Altitude Reduction of Calcium Phosphate

Because the free energy of calcium phosphate reduction to phosphine showed a trend that suggested further steep decline of the ΔG of formation of phosphine with altitude (Figure S17), we have calculated the theoretical free energy of phosphine formation by the reduction of calcium phosphate up to the altitude of 120 km.

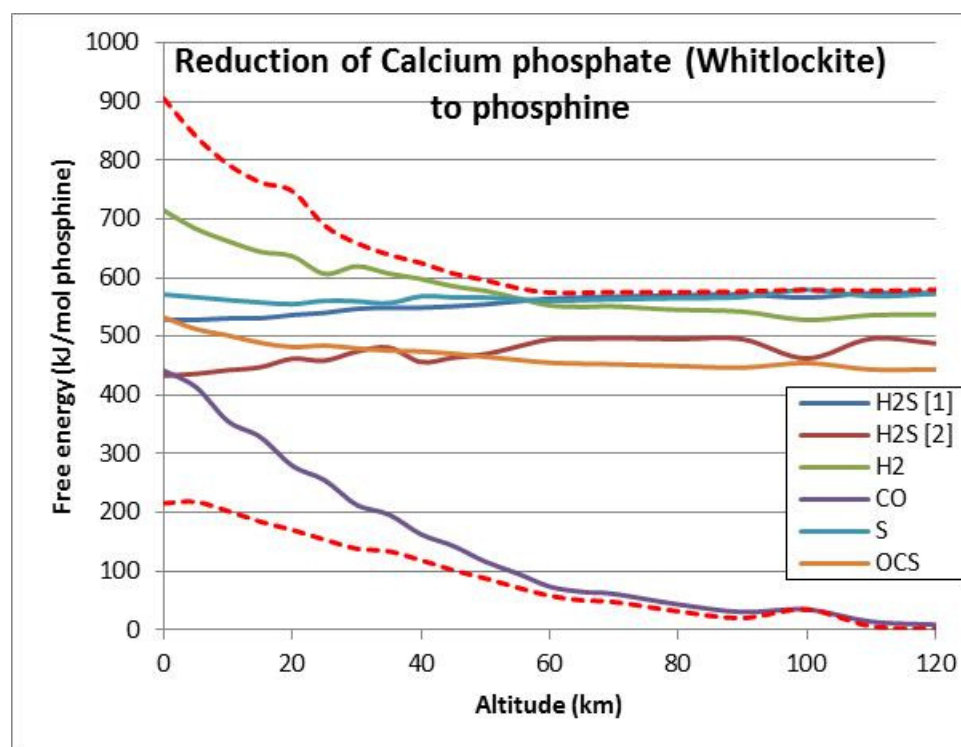


Fig. S17. The Thermodynamics of phosphine production by reduction of calcium phosphate (Whitlockite) to phosphine up to the altitude of 120 km. x axis: altitude (km), y axis: Gibbs free energy of reaction (ΔG) (kJ/mol). Dashed lines show the limits of the free energy found for any combination of gas partial pressures, for any altitude, for any reaction in a set of reactions. At 120 km the free energy of reduction of calcium phosphate to phosphine by carbon monoxide is approximately 0, however such scenario for production of phosphine is highly unlikely.

At 120 km the free energy of reduction of calcium phosphate by carbon monoxide is approximately 0, i.e. if the reduction reaction reached thermodynamic equilibrium, the atmospheric loading of phosphine would be comparable to the atmospheric loading of whitlockite. However, for this to be a source of phosphine, two implausible events have to happen:

- Whitlockite, a mineral, has to be transported to an altitude of 120 km, despite very limited vertical air flow on Venus, including being transported through the clouds without being absorbed onto cloud particles
- It must react with CO on a timescale comparable to that of the lifetime of phosphine, in an environment where the temperature is -100 °C and hence where almost all non-photochemical reactions will have a negligible rate over geological timescales, and where phosphine itself has an extremely short lifetime due to rapid photolysis by unshielded solar UV.

One could hypothesise scenarios under which this could happen (for example nanoparticles of whitlockite mixed with metallic iron/nickel could both have a long enough residence time and a high enough surface:volume ratio to reach 120 km, where the iron/nickel could catalyse reactions with carbon monoxide). However, these are *ad hoc* scenarios that are unjustified by any physical observations of the atmosphere of Venus.

2. 3. 3. Formation of Phosphine by Tribochemical Processes

An intriguing possibility for the production of phosphine from rock phosphorus is coupling of mechanical energy to phosphorus reduction in the presence of fluids, termed tribochemical synthesis. Glindemann et al (Glindemann *et al.* 2005) have explored this, and report variable conversion of rock phosphorus to PH₃, the highest values being for quartz and calcium carbonate (limestone and marble). Other rocks reported 10⁻⁶ to 10⁻⁹ conversion of phosphate to phosphine, with the exception of the pulverization of one quartz pebble. Calcium carbonate will not exist on the surface of Venus, as the CO₂ will be baked out into the atmosphere (Catling and Kasting 2017; Rasool and de Bergh 1970).

Terrestrial industry produces a large amount of crushed rock – 1.3 bln tonnes in the USA alone (Wilburn 2020), over half of it limestones and marble. However, this is probably dwarfed by the volume of rock fractured or ground up as a result of earthquakes. Marc et al have estimated the volume of landslides caused by earthquakes (Marc *et al.* 2016), which approximates exponential function of earthquake magnitude (as would be expected as magnitude is itself a log scale):

$$V = 3.81 \cdot 10^{-15} \cdot e^{4.14M} \quad (38)$$

where V is the total landslide volume in km³ and M is the Richter magnitude of the earthquake. If we apply this to all Earthquakes in 2019 that were shallower than 20 km, we estimate that those earthquakes caused ~3.10¹¹ tonnes of rock to shift in landslides (note this is a notional

figure, as many of these earthquakes were under water; however the distinction between land and water does not apply to Venus). If there were 650 ppb phosphorus in that rock (the average for metamorphic rock in PetDB Database (www.earthchem.org/petdb; (Lehnert *et al.* 2000) as described in the main text), if all of that rock was efficiently pulverized and if all underwent conversion of phosphate to phosphine with an efficiency of 10^{-6} (mid-range for Glindemann's paper, excluding limestones) then that produce 660 tonnes of phosphine per year. The flux needed to explain the phosphine on Venus is 130,000 tonnes/year. Even under these optimistic assumptions, therefore, Venus has to be ~200 times as tectonically active as Earth to sustain the observed phosphine levels.

In practice, the mechanism postulated by Glindemann et al requires very specific types of rock to be rubbed together, and requires fluid inclusions in the rock to provide hydrogen atoms for phosphine production. The former will substantially reduce the estimated production rate, and fluid inclusions will be entirely absent from the Venusian surface. The only relevant hydrogen-containing fluids that could be form on Venus would be supercritical H₂O or HCl; as these are present in the atmosphere at $3 \cdot 10^{-5}$ and 10^{-7} mole fraction respectively, their forming dense supercritical fluid phases in rocks seems unlikely. Sulfuric acid could in principle form liquid if the pressure was high enough, but as sulfuric acid efficiently and rapidly oxidizes PH₃ to phosphate, it is an unlikely fluid to participate in PH₃'s formation.

This is not to say that tribochemical production of phosphine is not significant *on Earth*, where water is abundant in surface rocks. However, we conclude that tribological phosphine production, while interesting and important chemistry, cannot explain the presence of 10-20 ppb phosphine in Venus' atmosphere. In this regard the tribochemical production of reduced phosphorus species is similar to the potential reduction of phosphate by serpentization reactions (Pasek *et al.* 2020); both are potentially important on Earth, but cannot be significant in the highly desiccated surface environment of Venus.

2. 4. Model for phosphate ion species calculation

The free energy needed to transport phosphorus species outside the cell into the cell is calculated as follows. Energy has to be input to drive the balance of ions present in the exterior milieu into that found inside the cell. The energy needed to change the phosphate ions from the equilibrium concentration found outside the cell to their concentration at pH=7 was subtracted from the free energy of reaction. When products are allowed to return to the external environment, energy is released as they relax to their thermodynamic minimum: this energy was added to the final energy of reaction. Thus, the overall Gibbs free energy available for the disproportionation reaction is given by:

$$\Delta G_x = \Delta G + \sum_{N=0}^3 R.T. \ln \left(\frac{P.HP_n}{HP.P_n} \right) - \sum_{n=0}^2 R.T. \ln \left(\frac{Q.HQ_n}{HQ.Q_n} \right), \quad (39)$$

where: ΔG is the free energy as calculated in Supplementary Section 1.3.1, P is the concentration of each of the phosphate ions at equilibrium at pH=7, HP is the concentration of the protonated ion at pH=7, for each 3 pairs of phosphate species corresponding to the three pKas of phosphoric acid ($H_3PO_4/H_2PO_4^-$, $H_2PO_4^-/HPO_4^{2-}$ and HPO_4^{2-}/PO_4^{3-}), and P_n and HP_n are the relative concentrations of the same ions at the pH assumed to be outside the cell. Q and HQ are the equivalent terms for phosphite. Equivalent calculations apply to the import and export of phosphite species. See Section 5.3.1. and Figure 9 of the main text for the overall process modelling.

3. Supplementary References:

- Amend J. P., and Shock E. L. (2001) Energetics of overall metabolic reactions of thermophilic and hyperthermophilic Archaea and Bacteria. *FEMS Microbiology Reviews*, 25: 175-243.
- Andreichikov B. (1998a) Chemistry of Small Components of Upper Shells of Venus. Lunar and Planetary Science Conference.
- Andreichikov B. M. (1987) Chemical composition and structure of the clouds of Venus inferred from the results of X-ray fluorescent analysis on descent probes VEGA 1 and 2. *Kosm. Issled.*, 25: 721-736.
- Andreichikov B. M. (1998b) Chemistry of Small Components of Upper Shells of Venus. Lunar and Planetary Science Conference.
- Arthur N. L., and Cooper I. A. (1997) Arrhenius parameters for the reactions of H atoms with PH₃ and AsH₃. *Journal of the Chemical Society, Faraday Transactions*, 93: 521-524.
- Ayers G. P., Gillett R. W., and Gras J. L. (1980) On the vapor pressure of sulfuric acid. *Geophysical Research Letters*, 7: 433-436.
- Bains W., Petkowski J. J., Sousa-Silva C., and Seager S. (2019) New environmental model for thermodynamic ecology of biological phosphine production. *Science of The Total Environment*, 658: 521-536.
- Ballesteros F. J., Fernandez-Soto A., and Martínez V. J. (2019) Diving into Exoplanets: Are Water Seas the Most Common? *Astrobiology*, 19: 642-654.
- Ballhaus C., Berry R. F., and Green D. H. (1990) Oxygen fugacity controls in the Earth's upper mantle. *Nature*, 348: 437-440.
- Ballistreri A., Montaudo G., Puglisi C., Scamporrino E., Vitalini D., and Calgari S. (1983) Mechanism of flame retardant action of red phosphorus in polyacrylonitrile. *Journal of Polymer Science: Polymer Chemistry Edition*, 21: 679-689.
- Barner H. E., and Scheurman R. V. (1978) Handbook of thermochemical data for compounds and aqueous species. Wiley Interscience, New York, NY, USA.
- Belyaev D. A., Montmessin F., Bertaux J.-L., Mahieux A., Fedorova A. A., Korablev O. I., Marcq E., Yung Y. L., and Zhang X. (2012) Vertical profiling of SO₂ and SO above Venus' clouds by SPICAV/SOIR solar occultations. *Icarus*, 217: 740-751.

- Bércecs A., Koentjoro O., Sterenberg B. T., Yamamoto J. H., Tse J., and Carty A. J. (2000) Electronic structures of transition metal phosphorus monoxide complexes. *Organometallics*, 19: 4336-4343.
- Bertaux J.-L., Vandaele A.-C., Korobeynikov O., Villard E., Fedorova A., Fussen D., Quémerais E., Belyaev D., Mahieux A., and Montmessin F. (2007) A warm layer in Venus' cryosphere and high-altitude measurements of HF, HCl, H₂O and HDO. *Nature*, 450: 646.
- Bierson C. J., and Zhang X. (2019) Chemical cycling in the Venusian atmosphere: A full photochemical model from the surface to 110 km. *Journal of Geophysical Research: Planets*, e2019JE006159.
- Bolshova T. A., and Korobeinichev O. P. (2006) Promotion and inhibition of a hydrogen—oxygen flame by the addition of trimethyl phosphite. *Combustion, Explosion and Shock Waves*, 42: 493-502.
- Buchan N. I., and Jasinski J. M. (1990) Calculation of unimolecular rate constants for common metalorganic vapor phase epitaxy precursors via RRKM theory. *Journal of Crystal Growth*, 106: 227-238.
- Burcat A., and Ruscic B. (2005) Third millennium ideal gas and condensed phase thermochemical database for combustion (with update from active thermochemical tables). Argonne National Lab.(ANL), Argonne, IL (United States).
- Cai S.-J., Zhang H.-q., and Kang J.-f. (2010) Compared Two Purification Process of Crude Acetylene. *Yunnan Chemical Technology*, 5.
- Cardelino B. H., Moore C. E., Cardelino C. A., McCall S. D., Frazier D. O., and Bachmann K. J. (2003) Semiclassical calculation of reaction rate constants for homolytic dissociation reactions of interest in organometallic vapor-phase epitaxy (OMVPE). *The Journal of Physical Chemistry A*, 107: 3708-3718.
- Catling D. C., and Kasting J. F. (2017) Atmospheric evolution on inhabited and lifeless worlds. Cambridge University Press.
- Chase M. W. J. (1998) NIST-JANAF Thermochemical Tables, fourth edition. *Journal of Physical and Chemical reference Data*, Monograph 9: 1 - 1951.
- Chen F., Judge D. L., Wu C. Y. R., Caldwell J., White H. P., and Wagener R. (1991) High-resolution, low-temperature photoabsorption cross sections of C₂H₂, PH₃, AsH₃, and GeH₄, with application to Saturn's atmosphere. *Journal of Geophysical Research: Planets*, 96: 17519-17527.
- Corrigan J. F., Doherty S., Taylor N. J., and Carty A. J. (1994) Phosphorus Monoxide, the Analog of NO: Generation of Coordinated PO via Hydrolysis of an Aminophosphinidene Ligand. X-ray Structure of the Anion [Ru₄(CO)₁₂(μ -3-PO)]. *Journal of the American Chemical Society*, 116: 9799-9800.
- Craig R. A., Reynolds R. T., Ragent B., Carle G. C., Woeller F., and Pollack J. B. (1983) Sulfur trioxide in the lower atmosphere of Venus? *Icarus*, 53: 1-9.
- Curdt W., Landi E., and Feldman U. (2004) The SUMER spectral atlas of solar coronal features. *Astronomy & Astrophysics*, 427: 1045-1054.
- Davidson D. F., Kohse-Höinghaus K., Chang A. Y., and Hanson R. K. (1990) A pyrolysis mechanism for ammonia. *International journal of chemical kinetics*, 22: 513-535.
- Dittrich K., and Townshend A. (1986) Analysis by emission, absorption, and fluorescence of small molecules in the visible and ultraviolet range in gaseous phase. *CRC Critical Reviews in Analytical Chemistry*, 16: 223-279.
- Doman W. (1902) The production of acetylene gas. King, London, UK.

- Dorfman Y., Yukht I., Levina L., Polimbetova G., Petrova T., and Emelyanova V. (1991) Oxidation of Ph₃ and Ash₃ through metal-complexes, free and connected oxygen. *USPEKHI KHIMII*, 60: 1190-1228.
- Fegley B. (1997) Why Pyrite Is Unstable on the Surface of Venus. *Icarus*, 128: 474-479.
- Fritz B., Lorenz K., Steinert W., and Zellner R. (1982) Laboratory kinetic investigations of the tropospheric oxidation of selected industrial emissions. *Phys. Chem. Behav. Atmos. Pollut. Proc. Eur. Symp.*
- Frost B. R. (1991) Introduction to oxygen fugacity and its petrologic significance. In: *Reviews in mineralogy vol 25. Oxide minerals: petrologic and magnetic significance*. edited by DH Lindsleys, Mineralogical Society of America, Washington, DC, USA.
- Fu M., Yu Z., Lu G., and Song X. (2013) Henry's law constant for phosphine in seawater: determination and assessment of influencing factors. *Chinese Journal of Oceanology and Limnology*, 31: 860-866.
- Gaillard F., and Scaillet B. (2009) The sulfur content of volcanic gases on Mars. *Earth and Planetary Science Letters*, 279: 34-43.
- Gerlach T. M. (1982) Interpretation of volcanic gas data from tholeiitic and Alkaline Mafic Lavas. *Bulletin Volcanologique*, 45: 235-244.
- Glindemann D., Edwards M., and Morgenstern P. (2005) Phosphine from Rocks: Mechanically Driven Phosphate Reduction? *Environmental Science & Technology*, 39: 8295-8299.
- Greaves J. S., Richards A. M. S., Bains W., Rimmer P. B., Sagawa H., Clements D. L., Seager S., Petkowski J. J., Sousa-Silva C., Ranjan S. and others. (2020) Phosphine Gas in the Cloud Decks of Venus. *Nature Astronomy*, in press.
- Greenewalt C. H. (1925) Partial Pressure of Water Out of Aqueous Solutions of Sulfuric Acid. *Industrial & Engineering Chemistry*, 17: 522-523.
- Greenwood N. N., and Earnshaw A. (2012) *Chemistry of the Elements*. Elsevier.
- Greiner W., Neise L., and Stöcker H. (2012) *Thermodynamics and statistical mechanics*. Springer Science & Business Media.
- Guthrie J. P. (1979) Tautomerization equilibria for phosphorous acid and its ethyl esters, free energies of formation of phosphorous and phosphonic acids and their ethyl esters, and p K a values for ionization of the P—H bond in phosphonic acid and phosphonic esters. *Canadian Journal of Chemistry*, 57: 236-239.
- Halmer M. M., Schmincke H. U., and Graf H. F. (2002) The annual volcanic gas input into the atmosphere, in particular into the stratosphere: a global data set for the past 100 years. *Journal of Volcanology and Geothermal Research*, 115: 511-528.
- Hamilton P. A., and Murrells T. P. (1985) Kinetics and mechanism of the reactions of PH₃ with O (3 P) and N (4 S) atoms. *Journal of the Chemical Society, Faraday Transactions 2: Molecular and Chemical Physics*, 81: 1531-1541.
- Haraguchi H., and Fuwa K. (1976) Determination of phosphorus by molecular absorption flame spectrometry using the phosphorus monoxide band. *Analytical Chemistry*, 48: 784-786.
- Hayduk W., Asatani H., and Lu B. C. Y. (1988) Solubility of sulfur dioxide in aqueous sulfuric acid solutions. *Journal of Chemical and Engineering Data*, 33: 506-509.
- Herrmann W. A. (1991) Between Stars and Metals: Phosphorus Monoxide, PO. *Angewandte Chemie International Edition in English*, 30: 818-819.
- Herschy B., Chang S. J., Blake R., Lepland A., Abbott-Lyon H., Sampson J., Atlas Z., Kee T. P., and Pasek M. A. (2018) Archean phosphorus liberation induced by iron redox geochemistry. *Nature communications*, 9: 1346.

- Hinshelwood C. N., and Topley B. (1924) XLVII.—The unimolecular decomposition of phosphine. *Journal of the Chemical Society, Transactions*, 125: 393-406.
- Hoffman J., Hodges R., McElroy M., Donahue T., and Kolpin M. (1979) Composition and structure of the Venus atmosphere: Results from Pioneer Venus. *Science*, 205: 49-52.
- Hoge H. J., and Lassiter J. W. (1951) Critical temperatures, pressures, and volumes of hydrogen, deuterium, and hydrogen deuteride. *Journal of Research of the National Bureau of Standards*, 47: 75.
- Hoshyaripour G., Hort M., and Langmann B. (2012) How does the hot core of a volcanic plume control the sulfur speciation in volcanic emission? *Geochemistry, Geophysics, Geosystems*, 13.
- Hu R., Seager S., and Bains W. (2012) Photochemistry in terrestrial exoplanet atmospheres. I. Photochemistry model and benchmark cases. *The Astrophysical Journal*, 761: 166.
- Huestis D. L., and Berkowitz J. (2010) Critical evaluation of the photoabsorption cross section of CO₂ from 0.125 to 201.6 nm at room temperature.
- Iyer R. S., Rogers P. J., and Rowland F. S. (1983) Thermal rate constant for addition of chlorine atoms to ethylene. *The Journal of Physical Chemistry*, 87: 3799-3801.
- Johnson M. J. A., Odom A. L., and Cummins C. C. (1997) Phosphorus monoxide as a terminal ligand. *Chemical Communications*: 1523-1524.
- Kaye J. A., and Strobel D. F. (1984) Phosphine photochemistry in the atmosphere of Saturn. *Icarus*, 59: 314-335.
- Keating G. M., Bertaux J. L., Bougher S. W., Dickinson R. E., Cravens T. E., Nagy A. F., Hedin A. E., Krasnopolsky V. A., Nicholson Iii J. Y., and Paxton L. J. (1985) Models of Venus neutral upper atmosphere: Structure and composition. *Advances in Space Research*, 5: 117-171.
- Knollenberg R. G., and Hunten D. M. (1979) Clouds of Venus: Particle size distribution measurements. *Science*, 203: 792-795.
- Krasnopolsky V. A. (2006) Chemical composition of Venus atmosphere and clouds: Some unsolved problems. *Planetary and Space Science*, 54: 1352-1359.
- Krasnopolsky V. A. (2007) Chemical kinetic model for the lower atmosphere of Venus. *Icarus*, 191: 25-37.
- Krasnopolsky V. A. (2008) High-resolution spectroscopy of Venus: Detection of OCS, upper limit to H₂S, and latitudinal variations of CO and HF in the upper cloud layer. *Icarus*, 197: 377-385.
- Krasnopolsky V. A. (2012) A photochemical model for the Venus atmosphere at 47–112 km. *Icarus*, 218: 230-246.
- Krasnopolsky V. A. (2013) S3 and S4 abundances and improved chemical kinetic model for the lower atmosphere of Venus. *Icarus*, 225: 570-580.
- Kulmala M., and Laaksonen A. (1990) Binary nucleation of water–sulfuric acid system: Comparison of classical theories with different H₂SO₄ saturation vapor pressures. *The Journal of Chemical Physics*, 93: 696-701.
- Larsen C. A., and Stringfellow G. B. (1986) Decomposition kinetics of OMVPE precursors. *Journal of Crystal Growth*, 75: 247-254.
- Leeds F. H., and Butterfield W. J. A. (1910) Acetylene, the Principles of Its Generation and Use: A Practical Handbook on the Production, Purification, and Subsequent Treatment of Acetylene for the Development of Light, Heat, and Power. C. Griffin, London, UK.

- Lehnert K., Su Y., Langmuir C. H., Sarbas B., and Nohl U. (2000) A global geochemical database structure for rocks. *Geochemistry, Geophysics, Geosystems*, 1.
- Lehninger A. L. (2004) *Lehninger Principles of Biochemistry*: David L. Nelson, Michael M. Cox. Recording for the Blind & Dyslexic.
- Linstrom P. J., and Mallard W. G. (2001) The NIST Chemistry WebBook: A Chemical Data Resource on the Internet. *Journal of Chemical & Engineering Data*, 46: 1059-1063.
- Lorenz M. L., Lutzmann H., and Reichert M. (1963) Procédé pour l'épuration d'acétylène obtenu à partir d'hydrocarbures. edited by Mdaeed l'energies, Badische Anylin & Soda-Fabrik Aktiengesellschaft, Belgium.
- Lorenz R. D. (2018) Lightning detection on Venus: a critical review. *Progress in Earth and Planetary Science*, 5: 34.
- Lyons J. R. (2008) An estimate of the equilibrium speciation of sulfur vapor over solid sulfur and implications for planetary atmospheres. *Journal of Sulfur Chemistry*, 29: 269-279.
- Lyons W. A., Bruning E. C., Warner T. A., MacGorman D. R., Edgington S., Tillier C., and Mlynarczyk J. (2020) Megaflashes: Just How Long Can a Lightning Discharge Get? *Bulletin of the American Meteorological Society*, 101: E73-E86.
- Manatt S. L., and Lane A. L. (1993) A compilation of the absorption cross-sections of SO₂ from 106 to 403 nm. *Journal of Quantitative Spectroscopy and Radiative Transfer*, 50: 267-276.
- Marc O., Hovius N., Meunier P., Gorum T., and Uchida T. (2016) A seismologically consistent expression for the total area and volume of earthquake-triggered landsliding. *Journal of Geophysical Research: Earth Surface*, 121: 640-663.
- Marcq E., Bézard B., Drossart P., Piccioni G., Reess J. M., and Henry F. (2008) A latitudinal survey of CO, OCS, H₂O, and SO₂ in the lower atmosphere of Venus: Spectroscopic studies using VIRTIS-H. *Journal of Geophysical Research: Planets*, 113.
- Marcq E., Mills F. P., Parkinson C. D., and Vandaele A. C. (2018) Composition and chemistry of the neutral atmosphere of Venus. *Space Science Reviews*, 214: 10.
- Markham A. E., and Kobe K. A. (1941) The solubility of carbon dioxide in aqueous solutions of sulfuric and perchloric acids at 25. *Journal of the American Chemical Society*, 63: 1165-1166.
- Mayer S. E. (1969) Estimation of activation energies for nitrous oxide, carbon dioxide, nitrogen dioxide, nitric oxide, oxygen, and nitrogen reactions by a bond-energy method. *The Journal of Physical Chemistry*, 73: 3941-3946.
- Médard L. (2019) *Gas Encyclopedia Air Liquide*. Elsevier.
- Nava D. F., and Stief L. J. (1989) Temperature study of oxygen atom+ phosphine reaction rate: kinetic measurements and planetary atmospheric implications. *The Journal of Physical Chemistry*, 93: 4044-4047.
- Oyama V., Carle G., Woeller F., Pollack J., Reynolds R., and Craig R. (1980) Pioneer Venus gas chromatography of the lower atmosphere of Venus. *Journal of Geophysical Research: Space Physics*, 85: 7891-7902.
- Pasek M., Omran A., Lang C., Gull M., Abbatiello J., Feng T., and Garong L. A.-L., Heather (2020) Serpentinization as a route to liberating phosphorus on habitable worlds. *Preprint*.
- Perraudin R. (1961) Procédé et dispositif d'épuration de l'acétylène par lavage à l'acide sulfurique. edited by B d'inventions, France.
- Perrot P. (1998) *A to Z of Thermodynamics*. Oxford University Press on Demand.

- Peters E. N. (1979) Flame-retardant thermoplastics. I. Polyethylene–red phosphorus. *Journal of Applied Polymer Science*, 24: 1457-1464.
- Peterson M. (2019) Research applications for the Geostationary Lightning Mapper operational lightning flash data product. *Journal of Geophysical Research: Atmospheres*, 124: 10205-10231.
- Pratt C., and Cornley K. (2014) Essential Biochemistry, third edition. John Wiley and Sons, Hoboken, NJ, USA.
- Prescott F. (1939) Intermediate chemistry, inorganic and physical. University Tutorial Press.
- Ranjan S., and Sasselov D. D. (2017) Constraints on the early terrestrial surface UV environment relevant to prebiotic chemistry. *Astrobiology*, 17: 169-204.
- Rao T. V. R., Reddy R. R., and Rao P. S. (1981) Potential energy curves and dissociation energy of the PO molecule. *Physica B+ C*, 106: 445-451.
- Rasool S. I., and de Bergh C. (1970) The runaway greenhouse and the accumulation of CO₂ in the Venus atmosphere. *Nature*, 226: 1037-1039.
- Rimmer P. B., and Helling C. (2016) A chemical kinetics network for lightning and life in planetary atmospheres. *The Astrophysical Journal Supplement Series*, 224: 9.
- Rimmer P. B., and Helling C. (2019) Erratum: A chemical kinetics network for lightning and life in planetary atmospheres. *The Astrophysical Journal Supplement Series*, accepted.
- Rimmer P. B., and Rugheimer S. (2019) Hydrogen cyanide in nitrogen-rich atmospheres of rocky exoplanets. *Icarus*, 329: 124-131.
- Robie R. A., and Hemingway, Bruce S. . (1995) Thermodynamic Properties of Minerals and Related Substances at 298.15 K and 1 Bar (10 Pascals Pressure and at Higher Temperatures). U.S. Geological Survey, Reston, VA, USA.
- Robinson D. B., and Senturk N. H. (1979) The vapor pressure and critical properties of carbonyl sulfide. *The Journal of Chemical Thermodynamics*, 11: 461-467.
- Rock P. A. (1969) Chemical thermodynamics: principles and applications. The Macmillan Company, London, UK.
- Sachsse H. (1954) Herstellung von Acetylen durch unvollständige Verbrennung von Kohlenwasserstoffen mit Sauerstoff. *Chemie Ingenieur Technik*, 26: 245-253.
- Sander R. (2015) Compilation of Henry's law constants (version 4.0) for water as solvent. *Atmospheric Chemistry & Physics*, 15.
- Scherer O. J., Braun J., Walther P., Heckmann C., and Wolmershäuser G. (1991) Phosphorus Monoxide (PO) as Complex Ligand. *Angewandte Chemie International Edition in English*, 30: 852-854.
- Schmidt M. W., Baldrige K. K., Boatz J. A., Elbert S. T., Gordon M. S., Jensen J. H., Koseki S., Matsunaga N., Nguyen K. A., and Su S. (1993) General atomic and molecular electronic structure system. *Journal of computational chemistry*, 14: 1347-1363.
- Scoles L., Yamamoto J. H., Brissieux L., Sterenberg B. T., Udachin K. A., and Carty A. J. (2001) Synthesis and Characterization of Mixed Ruthenium/Platinum μ 4-Phosphinidene, Phosphorus Monoxide, and Related Clusters. *Inorganic chemistry*, 40: 6731-6736.
- Seager S., Bains W., and Hu R. (2013) A Biomass-based Model to Estimate the Plausibility of Exoplanet Biosignature Gases. *The Astrophysical Journal*, 775: 104.
- Seiff A., Schofield J. T., Kliore A. J., Taylor F. W., Limaye S. S., Revercomb H. E., Sromovsky L. A., Kerzhanovich V. V., Moroz V. I., and Marov M. Y. (1985) Models of the structure of the atmosphere of Venus from the surface to 100 kilometers altitude. *Advances in Space Research*, 5: 3-58.

- Shemansky D. E. (1972) CO₂ extinction coefficient 1700–3000 Å. *The Journal of Chemical Physics*, 56: 1582-1587.
- Smith E. T., and Feinberg B. A. (1990) Redox properties of several bacterial ferredoxins using square wave voltammetry. *Journal of Biological Chemistry*, 265: 14371-14376.
- Sousa-Silva C., Hesketh N., Yurchenko S. N., Hill C., and Tennyson J. (2014) High temperature partition functions and thermodynamic data for ammonia and phosphine. *Journal of Quantitative Spectroscopy and Radiative Transfer*, 142: 66-74.
- Sousa-Silva C., Seager S., Ranjan S., Petkowski J. J., Hu R., Zhan Z., and Bains W. (2020) Phosphine as a Biosignature Gas in Exoplanet Atmospheres. *Astrobiology*, 20: 235-268.
- Sousa-Silva C., Tennyson J., and Yurchenko S. N. (2016) Communication: Tunnelling splitting in the phosphine molecule. *The Journal of Chemical Physics*, 145.
- Surkov A., Andreichikov B. M., and Kalinkina O. M. (1974) Composition and structure of the cloud layer of Venus.
- Surkov Y. A., Barsukov V. L., Moskalyeva L. P., Kharyukova V. P., and Kemurdzhian A. L. (1984) New data on the composition, structure, and properties of Venus rock obtained by Venera 13 and Venera 14. *Journal of Geophysical Research: Solid Earth*, 89: B393-B402.
- Surkov Y. A., Moskalyova L. P., Kharyukova V. P., Dudin A. D., Smirnov G. G., and Zaitseva S. Y. (1986) Venus rock composition at the Vega 2 Landing Site. *Journal of Geophysical Research: Solid Earth*, 91: E215-E218.
- Taylor F. W., and Hunten D. M. (2014) Chapter 14 - Venus: Atmosphere. In: *Encyclopedia of the Solar System (Third Edition)*. edited by T Spohn, D Breuer and TV Johnsons, Elsevier, Boston, pp 305-322.
- Titov D. V., Ignatiev N. I., McGouldrick K., Wilquet V., and Wilson C. F. (2018) Clouds and hazes of Venus. *Space Sci. Rec.*, 214: 126 doi.org/10.1007/s11214-018-0552-z.
- ToolBox E. (2003) Critical Temperatures and Pressures for some Common Substances.
- Toon O. B., McKay C. P., Ackerman T. P., and Santhanam K. (1989) Rapid calculation of radiative heating rates and photodissociation rates in inhomogeneous multiple scattering atmospheres. *Journal of Geophysical Research: Atmospheres*, 94: 16287-16301.
- Toy A. D. F. (2016) *The Chemistry of Phosphorus: Pergamon Texts in Inorganic Chemistry*. Elsevier.
- Truex T. J., Hammerle R. H., and Armstrong R. A. (1977) The thermal decomposition of aluminium sulfate. *Thermochimica Acta*, 19: 301-304.
- Vandaele A. C., Korablev O., Belyaev D., Chamberlain S., Evdokimova D., Encrenaz T., Esposito L., Jessup K. L., Lefèvre F., and Limaye S. (2017) Sulfur dioxide in the Venus atmosphere: I. Vertical distribution and variability. *Icarus*, 295: 16-33.
- Vinogradov A., Surkov A., and Andreichikov B. (1970a) Research in the Composition of the Atmosphere of Venus aboard Automatic Stations "Venera-5" and "Venera-6".Soviet Physics Doklady.
- Vinogradov A., Surkov Y. A., and Andreichikov B. (1970b) Research in the Composition of the Atmosphere of Venus aboard Automatic Stations "Venera-5" and "Venera-6".Soviet Physics Doklady.
- Visconti G. (1981) Multiple Scattering and Photochemistry in Planetary Atmospheres. *Memorie della Societa Astronomica Italiana*, 52: 535.
- Visscher C., and Moses J. I. (2011) Quenching of carbon monoxide and methane in the atmospheres of cool brown dwarfs and hot Jupiters. *The Astrophysical Journal*, 738: 72.

- Whitney J. A. (1984) Fugacities of sulfurous gases in pyrrhotite-bearing silicic magmas. *American Mineralogist*, 69: 68-78.
- Wilburn D. R. (2020) National Minerals Information Center - Mineral Commodity Summaries.
- Xiao-yong Z. (2009) Process for purification of crude acetylene gas by using concentrated sulphuric acid [J]. *Polyvinyl Chloride*, 7.
- Yamamoto J., Udachin K., Enright G., and Carty A. (1998) Phosphorus monoxide as a quadruply bridging ligand: syntheses and X-ray crystal structures of Ru 5 (CO) 15 (Á 4-PF) and [H 2 NCy 2][Ru 5 (CO) 15 (Á 4-PO)]. *Chemical Communications*: 2259-2260.
- Yaws C., and Knovel. (1999) Chemical Properties Handbook: Physical, Thermodynamics, Environmental Transport, Safety & Health Related Properties for Organic &. McGraw-Hill Education.
- Yu X., Li S.-M., Liu J.-Y., Xu Z.-F., Li Z.-S., and Sun C.-C. (1999) Direct Dynamics Study on the Hydrogen Abstraction Reaction $\text{PH}_3 + \text{H} \rightarrow \text{PH}_2 + \text{H}_2$. *The Journal of Physical Chemistry A*, 103: 6402-6405.
- Zhan Z., Seager S., Petkowski J. J., Sousa-Silva C., Ranjan S., Huang J., and Bains W. (2020) Assessment of Isoprene as a Possible Biosignature Gas in Exoplanets with Anoxic Atmospheres. *Astrobiology*, in review.
- Zhang Q., Wang H., Dalla Lana I. G., and Chuang K. T. (1998) Solubility of sulfur dioxide in sulfuric acid of high concentration. *Industrial & engineering chemistry research*, 37: 1167-1172.
- Zhang X., Liang M. C., Mills F. P., Belyaev D. A., and Yung Y. L. (2012) Sulfur chemistry in the middle atmosphere of Venus. *Icarus*, 217: 714-739.